IN SILICO IDENTIFICATION OF NOVEL NATURAL INHIBITORS OF CARBOHYDRATE METABOLIC PATHWAY IN CANCER CELLS

Project report
submitted to the

Department of Biochemistry and Microbial Sciences

Central University of Punjab

For the degree of

M.Sc Life Sciences with specialization in Biochemistry

Submitted by

Swastika Dash

(Registration No: 16mslsbc14)

M.Sc. Life Sciences with Specialization in Biochemistry

Under the Supervision of

Dr. Shashank K.

Department of Biochemistry and Microbial Sciences
Central University of Punjab
Bathinda, 151001
INDIA

May, 2018

DECLARATION

I declare that the project entitled "***In silico* identification of novel natural inhibitors of carbohydrate metabolic pathway in cancer cells**", has been prepared by me under the guidance of Dr. Shashank Kumar, Assistant Professor, Department of Biochemistry and Microbial Sciences, Central University of Punjab. No part of project has formed the basis for the award of any degree or fellowship previously.

(Swastika Dash)
M.Sc. Life Sciences with specialization in Biochemistry
Department of Biochemistry and Microbial Sciences,
School of Basic and Applied Sciences,
Central University of Punjab,
Bathinda- 151001.

Date:

CERTIFICATE

I certify that Swastika Dash has prepared her Project entitled "***In silico* identification of novel natural inhibitors of carbohydrate metabolic pathway in cancer cells**", for the award of M.Sc. Life Sciences with specialization in Biochemistry degree of Central University of Punjab, under my guidance. She carried out this work at the Department of Biochemistry and Microbial Sciences, school of Basic and Applied Sciences, Central University of Punjab.

Dr. Shashank Kumar
Assistant Professor
Department of Biochemistry and Microbial Sciences
School of Basic and Applied Sciences
Central University of Punjab,
Bathinda-151001

Date:

ABSTRACT

***In silico* identification of novel natural inhibitors of carbohydrate metabolic pathway in cancer cells**

Name of the student: Swastika Dash
Registration number: 16mslsbc14
Degree for which submitted: Masters of Science
Supervisor: Dr. Shashank Kumar
Department: Biochemistry and microbial sciences
School: Basic and Applied Sciences

Keywords: Anticancer potential, Glycolysis, *in silico,* Methylated flavonoids, Carbohydrate metabolism

Carbohydrate metabolism in cancer cells is linked to the 'Warburg Effect' which states that, under aerobic conditions, cancer cells metabolize approximately ten fold more glucose to lactate in a given time than normal cells; typically altered glycolytic pathway regulation. This has made the blocking of glycolytic pathway enzymes, a fascinating strategy to find treatment for cancer. This project addresses in a comprehensive manner the main glycolytic enzymes accounting for high-rate glycolysis in cancer cells. In addition, highlights of inhibitors that can be used to target the particular enzymes to decrease proliferation have also been done. Furthermore, besides the known inhibitors, receptor-based molecular docking of certain methylated flavonoids was performed with the proteins (isozymes of carbohydrate metabolic pathway enzymes) to find the lead inhibitors. The proteins used in the study are GLUT1 (4PYP), Hexokinase2 (2NZT), Phosphofructokinase2 (2AXN), Pyruvate kinaseM2 (3GQY), Lactate dehydrogenase A (4AJP) and Enolase2 (5IDZ). The dock scores were in the range of -5.88 to -9.68 against different target proteins. The methylated flavonoids 2-(3,4-dihydroxyphenyl)-3,5-dihydroxy-7-methoxy-4H-chromen-4-one, 5,7-dihydroxy-2-(3-hydroxy-4-methoxyphenyl)-6,8-dimethoxy-4H-chromen-4-one, 2-(3,4-dimethylphenyl)-5,7-dimethyl-4H-chromen-4-one and 6-hydroxy-3,5,7,8-tetramethoxy-2-(3,4,5-trimethoxyphenyl)-4H-chromen-4-one showed better dock scores for the target proteins in comparison to the standard inhibitors. Thus these methylated flavonoids might be considered promising leads for further development of glycolytic pathway inhibitors in cancer cells.

Swastika Dash Dr. Shashank Kumar

ACKNOWLEDGEMENT

Firstly I extend immense gratitude to my revered seminar advisor Dr. Shashank Kumar, Assistant Professor, Department of Biochemistry and Microbial Sciences, for instilling in me the confidence and drive for doing an arduous task and having faith in my abilities to accomplish any assignment which I set out to do. I am also thankful to him for being a guardian, a friend as well as an erudite scientist to troubleshoot the problems encountered during the scientific report presentation preparation..

I wish to thank Mr. Prem Prakash Kushwaha (Ph.D. scholar), Santosh K. Maurya, Atul Singh and my classmates for their kind cooperation and support.

At last but not the least, I am thankful to every individual who has helped and inspired me during my seminar preparation and has wished for my bright future.

Swastika Dash
Date

TABLE OF CONTENTS

LIST OF TABLES

LIST OF FIGURES

LIST OF ABBREVIATIONS

Abbreviations	Expansion
ADME/T	Absorption, Distribution, Metabolism, Excretion and Toxicity
ADT	Auto Dock Tool
AT	Ames Test
CADD	Computer-Aided Drug Design
CHC	Alpha-cyano-4-hydroxy-cinnamate
DMSO	Dimethyl sulfoxide
DPPH	1, 1Diphenyl-2-Picryl Hydrazyl
ENO	Enolase
FBP	Fructose-2,6-bisphosphatases
GBM	Glioblastoma
GLUT1	Glucose transporter 1
HER2	Human Epidermal growth factor receptor-2
HIF-1	Hypoxia inducible factor-1
HK2	Hexokinase2
LDHA	Lactate dehydrogenase A
MCT1-4	Monocarboxylate transporters 1-4
MTT	3-(4,5- dimethylthiazol-2-yl)-2,5-diphenyltetrazolium bromide
OXPHO	Oxidative Phosphorylation
PDB	Protein Data Bank
PFK	6-phosphofructo-2-kinase
PFKFB3	Phosphofructokinase2
PKM2	Pyruvate KinaseM2


1
• INTRODUCTION

1.1 Introduction

The formation, breakdown and inter-conversion of carbohydrates in living organisms are known as carbohydrate metabolism. Since ages, carbohydrates have played a significant role in being the most essential component of the body; by providing the requisite energy for different metabolic purposes. Digestion breaks down the ingested complex carbohydrates to form simpler quintessential products such as glucose, fructose and galactose. Ultimately, glucose serves to be the major product of carbohydrate breakdown which channelizes through various pathways to provide energy to the cells or gets stored as glycogen in the mammalian body. In cancer cells, carbohydrate metabolism is linked to the 'Warburg Effect' which states that, under aerobic conditions, cancer cells metabolize approximately ten folds more glucose to lactate in a given time than normal cells; typically altered glycolytic pathway regulation. This has made the blocking of glycolytic pathway enzymes, a fascinating strategy to find treatment for cancer (Chen *et al.,* 2014). Lots of experimental studies and research has been carried out to develop new anti-cancer drugs for prevention and treatment of various cancers. Recurrence of tumors and side effects of the chemotherapeutic drugs is a major issue of concern. Chemotherapeutic drugs have adverse effects on immune system and health. Moreover, tumor cells may also induce drug resistance (Song *et al.,* 2014). Therefore, development of new reliable natural anti-cancer drug is necessary to cure various kinds of cancer. Since time immemorial, various phytochemicals have actively been used by people to treat many kinds of diseases. The major reason being these phytochemicals are easily available and have no/very poor side effects. Natural products have thus played a very crucial role in drug discovery and have led to a revolution in pharmacology and medicine (Lahlou, 2013). Thus new approaches should be done in identifying the natural products as potent inhibitors of the glycolytic pathway enzymes that lead to proliferation in cancer cells providing a cure to this devastating disease.

1.2 Knowledge gap

Natural products have been used for centuries as remedies against various diseases and ailments. Yet, there has been very few studies done on the targeting of glycolytic

enzymes responsible for cancer cell proliferation by natural product inhibitors for the treatment of cancer. Furthermore, identification of new natural inhibitors of glycolysis pathway in cancer cells and there *in silico* scientific screening and validation has been yet to be studied.

1.3 Hypothesis

Since very few studies have been reported on targeting of major glycolytic enzymes involved in carcinogenesis, identification of new novel natural inhibitors of glycolytic pathway in cancer cells has yet to be done. The present study has been designed to identify and screen the active phytochemicals against carbohydrate metabolic pathway in cancer using *in silico* techniques.

1.4 Objective

In silico anticancer potential screening of natural phytochemicals against carbohydrate metabolic pathway in cancer cells.

2.1 Carbohydrate metabolism

Carbohydrate metabolism in the body leads to the emergence of glucose to be the major catabolic product. To be precise, the way in of glucose into the cells is basically mediated by facilitated diffusion through a family of hexose transporters termed as GLUT (1-4) transporters. The glucose that enters undergoes various enzymatic reactions to produce pyruvate as the major product while storing energy released during this process as ATP and NADH by the process of glycolysis. This glycolysis occurs mainly in the cytosol of the cell. The pyruvate thus produced, under anaerobic conditions gets converted into lactate and production of further energy. While in the presence of oxygen, the pyruvate is converted to acetyl-CoA molecules. These acetyl-CoA molecules then enter the Citric Acid cycle (TCA cycle or Kreb's cycle) where large (most) of the ATP molecules are generated through a number of enzymatic reactions (Lodish, 2000). Ultimately, the NADH and CO_2 produced by TCA cycle is channelized to the oxidative phosphorylation (electron transport) pathway which involves various enzymes and uses the chemical energy to produce ATP through the involvement of ATP synthase. This occurs mainly in the mitochondria. The pentose phosphate pathway is an alternative method of oxidizing glucose where the intermediate of glycolytic pathway (Glucose-6-phosphate) serves as the precursor. This is divided into oxidative and non-oxidative phases and leads to the release of NADPH and pentose (5-Carbon sugars) as well as ribose-5-phosphate (major precursor of nucleotide metabolism).

2.2 Cancer cell metabolism

Carbohydrate metabolism in normal cells and cancer cells has shown remarkable differences to be studied upon, in general. In normal cells, where glucose metabolism takes place through glycolysis under anaerobic conditions; in cancer cells, glucose metabolism is marked by accelerated aerobic glycolysis. The discovery of high rates of aerobic glycolysis in cancer cells by Otto Warburg in late 1920s led to the assumption that respiration, through the process of oxidative phosphorylation (OXPHO) is impaired or damaged in cancer cells. This phenomenon was termed to be 'Warburg effect' (Hay, 2016). Since cancer cells need to produce enough energy to survive when supplies and waste disposals are limited and to divert metabolic

intermediates from energy production to the biosynthetic pathways supporting cell proliferation; enhanced aerobic glycolysis takes place to fuel sufficient energy to the tumor cells. There are various changes occurring in glucose metabolism in cancer cells, mainly in the glycolytic pathway, through the involvement of a number of committed steps in the pathway.

2.3 Natural anticancer products

Natural products have been a great source for treatment of many types of cancer. They provide a considerable protection from many types of cancers as well as other diseases. The antioxidant medicinal plants are a good source for protection against cancer. Thus, consuming antioxidant fruits, vegetables and herbs etc. can have numerous protective effects (Bhanot *et al.,* 2011).

2.3.1 History of natural anticancer products

The concept of natural products has its roots back in 19th century. Classical examples of drug compounds discovered this way is morphine, the active agent in Opium, and digoxin, a heart stimulant originating from flower *Digitalis lanata* (Lahlou, 2013). Historically natural products have been a rich source of compounds that have a great importance in medicine, pharmacy and biology. A number of important new commercial drugs have been obtained from natural sources (Gordaliza, 2007). Drugs of natural origin can be classified as original natural products, products derived semi-synthetically from natural products or synthetic products based on natural product models.

Natural products have a dramatic impact on area of cancer. From 155 anticancer drugs developed since 1940s, 47% being either a natural product or a direct derivation itself (Ribnicky *et al.*, 2008). The knowledge associated with traditional medicine and use of medicinal plants as potential medicines has led to isolation of many natural products that have become well-known pharmaceuticals today. Widely used breast cancer drug Paclitaxel, isolated from the bark of *Taxus brevifolia,* first collected by United States Department of Agriculture (USDA) in 1962 is a great example of natural anticancer drug.

2.3.2 Importance and advantages of natural anticancer products

Due to development of resistance to chemotherapeutic drugs, search for new anticancer drugs and therapies is still a priority goal of cancer therapy (Song *et al*., 2014). Natural products have been considered to be the best source of drugs for past many years as these have no or very poor side-effects and easy availability. Moreover, natural products have structural and chemical diversity. Therefore these are an excellent source of active therapeutic agents.

2.3.3 Currently used natural anticancer products

Plants are useful source of approved anticancer products. Phloretin, a natural flavonoid is a competitive inhibitor of GLUT and has been studied to retard tumor growth. Silybin, an additional natural flavonoid has recently been revealed as a GLUT inhibitor and is undergoing clinical trials for prostate cancer (Porporato *et al.*, 2011). Recently, one of the studies reported that a natural compound namely oleanolic acid (OA), found widely in plants which shows its excellent anti-cancer properties by constraining aerobic glycolysis process by shifting PKM2 to PKM1. Natural products, such as Shikonin and its analog alkannin, belonging to a family of necroptotic inducers, displayed potent and promising selective inhibition of PKM2 by not inhibiting PKM1 and PKL (Dong *et al.,* 2016). Gossypol (AT-101), a natural product found in cottonseed, is a non-selective inhibitor of LDH that blocks the binding of NADH (Doherty *et al.*, 2013). Another compound was identified which constraints both LDH isoform (LDHA and LDHB), initiates apoptosis of hepatocellular carcinoma cell lines and destructs proliferation of breast cancer cells at rather high concentration, namely galloflavin.

2.4 Inhibitors of glucose transporters (GLUT1)

GLUT1 belongs to the GLUT family of transporters required for glucose shuttling across membranes. They have a high affinity for glucose and thus ensure sufficient glucose uptake by the cells (Shibuya *et al.*, 2015). Usually, there are 14 glucose transporters isoforms, with different affinities for glucose. But GLUT1 tends to be overexpressed in many cancers because of their nature of irreversibility and high affinity for glucose. Overexpression of GLUT1 in various types of cancer has provided

a strong cause for the anticancer use of GLUT inhibitors. Studies have led to the finding of 2-Deoxyglucose (2-DG) as a GLUT inhibitor and as an anti-cancer drug. Although individually its efficacy has failed to give results, it has proven efficacy in normalizing human osteosarcoma and non-small cell lung cancers to adriamycin and paclitaxel. A natural flavonoid and a competitive GLUT inhibitor, Phloretin has also been studied to retard tumor and cancer cell growth. Silybin, an additional natural flavonoid has recently been revealed as a GLUT inhibitor and is undergoing clinical trials for prostate cancer. The compound Cytochalasin B and Forskolin (naturally-occurring) which binds at the GLUT1 sugar export site or close to it are well known bound inhibitors of human GLUT1. Cytochalasin B is a mycotoxin that is cell-permeable and displays a macrocyclic ring structure (Kapoor *et al.*, 2016). Two more inhibitors are also studied that are, glucose transporter-inhibitor 1 (GLUT-i1) and glucose transporter-inhibitor 2 (GLUT-i2) based on a phenylalanine-amide core scaffold.

A novel small molecule, WZB117, has been studied to kill lung and breast cancer cells by inhibiting GLUT1-mediated glucose transport (Ojelabi *et al*., 2016). WZB117 inhibits uptake of the non-metabolizable sugar, 3-o-methylglucose by RBCs and is a competitive inhibitor of GLUT1-mediated zero-trans sugar uptake and exchange transport but is a non-competitive inhibitor of zero-trans exit. This molecule binds at or near the exofacial sugar-binding site of GLUT1. Further, a small molecule inhibitor, Fasentin has been studied to inhibit the intracellular domain of GLUT1 and thereby restricting glucose uptake by GLUT1. Thus, the inhibition of function or expression of GLUT1 can be considered a way of exclusively targeting cancer cells that rely upon a high rate of uptake of glucose for anaerobic glycolysis.

2.5 Inhibitors of hexokinase 2

Hexokinase-2 belongs to the hexokinase family of enzymes that control the first rate-limiting step of glycolysis. They perform the phosphorylation of glucose to Glucose-6-Phosphate which involves the transfer of phosphate from ATP. The phosphorylated form of glucose, i.e. Glucose-6-phosphate gets entrapped inside the cell and fuels glycolysis as well as pentose phosphate pathway (Porporato *et al*., 2011). Usually,

there are four main hexokinases isoforms in mammalian cells- HK1, HK2, HK3 and HK4. All are high-affinity hexokinases, but HK1 and HK2 have the unique ability to bind to mitochondria in a voltage-dependent anion channel (VDAC)- dependent manner. HK2 is a HIF-1(Hypoxia-Inducible Factor-1) - target gene product and exists bound to the outer mitochondrial membrane with VDAC channel as compared to other isoforms. This particular presence of HK2-VDAC interaction provides preferential access to ATP (permeating VDAC). This also prevents the negative feed-back inhibition by glucose-6-phosphate, which makes sure enough glucose is utilized by tumor cells expressing mitochondria-bound HK2 (Mathupala *et al*.,2006). The interaction of HK2 and VDAC further interferes with the binding of pro-apoptotic proteins to VDAC which would otherwise have had triggered apoptosis. Thus, HK2 binding to VDAC offers both metabolic advantages as well as protection against apoptosis. The overexpression of HK2 has been found in many cancer types compared with normal tissues and cells (Wang *et al*., 2016).

Since HK2 has been widely characterized to upregulate glycolysis and a repressor of apoptosis in numerous types of cancers; efforts have been made to study its specific inhibitors and target for anti-cancer drug discovery. Lonidamine has been studied widely as a specific inhibitor of mitochondria-bound hexokinase (Lin *et al*., 2016). The current leading compound is 3-Bromopyruvate (3-BP), an alkylating agent reacting with cysteine residues in proteins. It is thus considered to be an HK inhibitor and exerts antitumor activities (including metastatic suppression) in quite a lot of types of cancers. But, it may cause unavoidable side-effects since it may affect multiple enzymes and is unstable. It also exhibits restriction of glycolysis at a high concentration only (Zhang *et al*., 2014). Metformin, a commonly used anti-diabetic drug and 2- deoxyglucose are also reported to be potent HK2 inhibitors. A decarboxylase inhibitor (FDA-approved) that is usually used for the treatment of Parkinson’s disease, Benserazide, is also reported to hold back tumor growth by inhibiting Hexokinase2. It has been found in studies that the glucose-binding pocket of Benserazide is occupied by its pyrogallol moiety through H-bond interactions and adopted a similar conformation of the substrate glucose and thus competitively inhibits it. The identification of Benserazide as an HK2 inhibitor will definitely pave the

way for the development of more Benz analogs as novel antitumor agents (Li *et al*., 2017). Also, the azole derivative analogs such as Clotrimazole and Bifonazole that perform by interfering with HK-VDAC binding that releases the enzyme from mitochondria to cytosol can be used as an inhibitor of HK activity. Thus, to suppress glycolysis in cancer cells either direct inhibition of HK2 can be done or disrupting the HK-VDAC interaction that can induce apoptosis.

2.6 Inhibitors of phosphofructokinase 2 (PFKFB3)

Fructose-2,6-bisphosphate is an important regulatory point of glycolysis acting as an allosteric activator of PFK1, one of the rate-controlling enzymes of glycolysis. Fructose-2,6-bisphosphate (F-2,6-BP) is produced from fructose-6-phosphate by a family of homodimeric enzymes known as 6-phosphofructo-2-kinase/fructose-2,6-bisphosphatases (PFKFB) (Porpora *et al*., 2011). PFKFBs are bifunctional enzymes which means that they can catalyze either the ATP-dependent phosphorylation of F6P to F2,6BP (PFK2 activity) or the de-phosphorylation of F2,6BP to F6P (FBPase activity). The various isoforms of PFKFB comprise of four members i.e, PFKFB1, PFKFB2, PFKFB3 and PFKFB4. PFKFB1, PFKFB2, PFKFB4 show the same amount of PFK2 and FBPase activity whereas PFKFB3 has high PFK2 activity and almost negligible FBPase activity. PFKFB3 gene is a target of HIF-1 (Hypoxia-Inducible Factor-1) and thus is seen as a major induction in hypoxia. Hypoxic stimulation of PFK2 activity of PFKFB3 is henceforth exaggerated through phosphorylation of a serine residue at position 462 of human sequence, a process involving AMP-activated protein kinase. Thus, PFKFB3 is considered to be highly expressed in many human tumors and sustains high-rate glycolysis (Hay, 2016). Till now, 3-(3-pyridinyl)-1-(4-pyridinyl)-2-propen-1-one (3PO) has been studied to be the only specific inhibitor of PFKFB3. It has been studied and found to decrease the concentration of Fructose-2,6-bisphosphate in tumor cells, leading to less glucose uptake and suppression of growth of cancer cells. However, there are clinical trials going on where there have been studies where, treatment with lapatinib, an FDA-approved HER2 inhibitor (Human Epidermal growth factor receptor-2), also decreased PFKFB3 expression and thus glucose metabolism in $HER2^{+}$ cells (O'Neal *et al*., 2016). Studies have also

been done to find PFK15 (1-(4-pyridinyl)-3-(2-quinolinyl)-2-propen-1-one), as an inhibitor of PFKFB3, against gastric cancer. Results showed that PFK15 retarded the proliferation leading to cell cycle arrest by blocking signaling pathways. Thus, PFK15 has been established to be a promising anti-cancer drug by targeting aerobic glycolysis (Zhu *et al*., 2016).

2.7 Inhibitors of pyruvate kinase M2

Pyruvate kinase (PK) is an enzyme of the glycolytic pathway which catalyzes a rate-limiting step of glycolysis. The de-phosphorylation of phosphoenolpyruvate (PEP) into pyruvate to produce ATP is accomplished by this enzyme (Porpora *et al*., 2011). There are four pyruvate kinase isoforms in mammalian cells- PKM1, PKM2, PKR and PKL which are encoded by two separate genes. The same gene, PKLR, encodes PKR and PKL through the use of alternative promoters. PKR expression is restricted to red blood cells, whereas PKL is expressed at elevated levels in the liver and to some extent in the kidney. PKM1 and PKM2 are encoded by another gene, PKM, through alternative splicing. Selection of isozymes causes the uncontrolled proliferation observed in cancer. PKM2 re-expression and down-regulation of PKM1 is associated with tumorigenesis. The active pyruvate kinases are tetramers. Whereas PKM1 is a constitutively active tetramer, the tetrameric active form of PKM2 is allosterically regulated by various metabolites. High-yield ATP production is provided by the tetrameric configuration, whereas it's dimeric conformation allows the intermediates of glycolysis to be channelized towards biosynthesis. The tetrameric form is elevated by the accumulation of the glycolytic intermediate F-1,6-BP and by the biosynthetic byproduct serine. The phosphorylation of tyrosine 105 in response to several oncogenic tyrosine kinases further accelerates the formation of dimers. The transfer of a non-ATP-producing phosphate to a histidine residue of phosphoglycerate mutase plays a critical role in controlling the accumulation of PEP. Most cancer cells express PKM2, thereby achieving a fine balance between promoting ATP production or cell proliferation. Moreover, the glycolysis and tumor angiogenesis is further promoted by PKM2 cooperation with HIF-1 that transactivates the associated genes. (Hay, 2016).

Since a major role is played by PKM2 in cancer cell metabolism and proliferation, development of a potent anticancer drug that targets PKM2 may be of great significance. Inhibitors of PKM2 are based on the fact that proliferating cells are highly dependent on energy and lessening the activity of PKM2 would inhibit energy regeneration (Wong *et al*., 2013). Natural products, such as Shikonin and its analog alkannin, belonging to a family of necroptotic inducers, displayed potent and promising selective inhibition of PKM2 by not inhibiting PKM1 and PKL. RNA interference targeting PKM2 has also been studied to induce growth and caspase-dependent apoptosis in numerous cancer cell lines. Also, the peptide aptamers, which inhibit PKM2 and not the homologous PKM1, has been seen to induce a significant decrease in cell proliferation and size under conditions where glucose metabolism is disrupted. An enormous library of diverse compounds was screened to ultimately identify two small molecule inhibitors (water-soluble) which have potential to inhibit PKM2 versus PKM1 selectivity. Both molecules were reported to presumably block the allosteric F-1,6-BP-binding site of PKM2 absent in PKM1. Numerous PKM2 inhibitors have been established, comprising TT-232, VK3, VK5 and Compound 3. Compound 3 possess the ability to cause PKL inhibition, whereas VK3 and VK5 selectively inhibit PKM2 to reduce glycolysis in cancer cells (Heiden *et al*., 2011). Recently, one of the studies reported that a natural compound namely oleanolic acid (OA), found widely in plants which shows its excellent anti-cancer properties by constraining aerobic glycolysis process by shifting PKM2 to PKM1. Besides energy, cells having proliferative potential, strictly depend on the cell building blocks synthesis that is favored by less active dimeric PKM2. Thus, tetrameric form of PKM2 activation (highly active) may also inhibit cell proliferation because of the total deficiency of precursors for the synthesis of cell building blocks. Two representative compounds, namely- thieno(3,2b)pyrrole (3,2d) pyridazinone and substituted N,N-diarylsulfonamide, were found to be potent activators of PKM2. Both the compounds behave as a cell-permeable analogs. These compounds also resemble the Fructose bisphosphate-allosteric activator of PKM2. Activation of PKM2 regulates both metabolism of cancer cell (*in vitro*) and tumor growth (xenograft). Another study showed that 2-oxo-N-aryl-1,2,3,4-tetrahydroquinoline-6-sulfonamides also activated

PKM2 for the reduction of aerobic glycolysis. Altogether, various studies signify that PKM2 is an effective target for curative approaches. However, the only problem lies in the existence of PKM2 in normal cells also and the metabolic escape it undergoes. (Dong *et al*., 2016). Nonetheless, the curative activation of PKM2 seems promising in restricting the metabolism of proliferative cells in cancer.

2.8 Inhibitors of lactate dehydrogenase A (LDHA)

Pyruvate is at the central point between different metabolic pathways. It is the product of glycolysis, the product of oxidation of malate in proliferating cells, the main component of the Kreb's cycle, the alanine precursor in a reversible transamination reaction (nitrogen donated by glutamate) and the substrate producing lactate by redox reaction. The latter reaction that involves the simultaneous reduction of pyruvate and the oxidation of NADH into NAD^+, allows the sufficient availability of the NAD^+ pool necessary for self-sufficiency of glycolysis. NAD^+ is definitely mandatory for the oxidative phosphorylation of glyceraldehyde-3-phosphate into 1,3-diphosphoglycerate by GAPDH. Reduction of pyruvate into lactate also allows glycolytic cells to maintain the levels of pyruvate low enough to avoid cell death (Porporato *et al*., 2011). This reversible reaction is catalyzed by the LDH family of tetrameric enzymes. Lactate Dehydrogenases are encoded by four separate genes (LDHA, LDHB, LDHC and LDHD). The two highly expressed isozymes, LDHA and LDHB can form either homo-tetramers or hetero-tetramers. LDHA has a higher affinity for pyruvate and LDHB has a higher affinity for lactate; LDHA favors the forward reaction and LDHB favors the reverse reaction. Thus, LDHA is the predominantly expressed LDH in cancer cells (Hay, 2016).

By restoring the NAD^+ pool required for the GAPDH reaction, LDHA plays an essential role in the accentuation of high-rate glycolysis and is therefore recognized as a therapeutic target for cancer. Inhibition of LDHA expression by using RNA interference impairs tumor initiation, maintenance and progression. 3-dihydroxy-6-methyl-7-(phenylmethyl)-4-propylnaphthalene-1-carboxylic acid (FX11), a selective inhibitor (competitive in nature) has been recognized through screening a varied number of compounds obtained from gossypol, a natural compound and a known

malarial LDH inhibitor. FX11 induced oxidative stress and cell senescence *in vitro*, which led to progression inhibition of human lymphoma and pancreatic cancer xenografts *in vivo*. Recently, N-Hydroxy-2-carboxy-substituted indole compounds have been recognized as LDHA specific inhibitors (Miao *et al*., 2013). Gossypol (AT-101), a natural product found in cottonseed, is a non-selective inhibitor of LDH that blocks the binding of NADH. However, gossypol also inhibits GAPDH, which is an NAD^+-dependent enzyme, and thus its antitumor activity may also include the inhibition of GAPDH. Another compound was identified which constraints both LDH isoforms (LDHA and LDHB), initiates apoptosis of hepatocellular carcinoma cell lines and destructs proliferation of breast cancer cells at rather high concentration, namely galloflavin. Other potent and selective LDHA inhibitor include GSK 2837808A (3-[{3-(cyclopropylamino)sulfonyl-7(2,4-dimethoxy-5-pyrimidinyl)-4-quinolinyl]amino)-5-(3,5-difluorophenoxy) benzoic acid and NHI-2 (methyl 1-hydroxy-6-phenyl-4-(trifluoromethyl)-1H-indole-2 carboxylate. The former inhibits the lactate production in selected cancer cell lines, reduces glucose uptake and enhances mitochondrial oxygen consumption in carcinoma cells whereas the later inhibits cell growth and lactate production in HeLa cells (Doherty *et al*., 2013). Also, oxamate (sodium oxamate), an inhibitor of LDHA, has been identified to be a potential anticancer agent. Oxamate treatment of cells has shown to induce protective autophagy in gastric cancer cell lines. Inhibition of LDH by oxamate also caused G2/M cell cycle arrest via downregulation of the CDK1/cyclin B1 pathway and supported apoptosis through augmentation of mitochondrial ROS generation (Zhao *et al*., 2015).

2.9 Inhibitors of monocarboxylate transporter (MCT1-4)

The LDHA reaction yields lactate and protons (from NADH). To avoid the death of cells and acidification, several systems have been developed that can combat these situations. These systems are called Monocarboxylate transporter (MCT). These are transmembrane proteins (12 span) with N-terminus and C-terminus in the cytosolic domain and are proton-coupled. There are in total 14 subtypes of MCTs but not all of these are currently characterized. There are various isoforms of the transporter namely, MCT1, MCT2, MCT3 and MCT4 which are passive lactate-proton

symporters. Among these, MCT4 has the lowest-affinity for lactate and is coded by a HIF-1 target gene. That is why it is modified for the lactic acid export from glycolytic cancer cells and plays an important role in the regulation of pH inside the cells. On the other hand, MCT1 has an intermediate affinity for lactate and is universally expressed in healthy and cancer tissues. In tumor, it facilitates uptake by oxidative tumor cells in a pathway involving lactate oxidation into pyruvate which helps in the maintenance of the TCA cycle (Gurrapu *et al*., 2015). Thus, high expression of MCT1 and MCT4 is related to proliferation and invasion of cancer cells.

Cochaperone immunoglobulin-family single-membrane pass proteins are required for the transfer of MCT to the surface of the cell membrane is considered to be quite an exploitable feature of these transporters. MCT1, MCT3 and MCT4 bind to CD147 for expression on the cell surface whereas MCT2 binds to embigin. The expression of a CD147 thus also requires an MCT protein that stabilizes the binding. The opportunity to simultaneously target tumor metabolism and angiogenesis within the same molecule is offered by MCT1 inhibitors. The development of several small-molecule inhibitors by genetic knock-down studies has established the importance of targeting lactate transporters in cancer therapeutics. Knockdown of MCT1 or inhibition of MCTs with the small molecule Alpha-cyano-4-hydroxy-cinnamate (CHC) impairs tumor cell proliferation, migration and survival. Further, it also impairs tumorigenic potential of Glioblastoma (GBM) cells in intracranial xenografts. It is supposedly a specific MCT1 inhibitor. AR-C117977, an additional MCT inhibitor has been found to have properties that suppress the immune system which will significantly prolong skin graft and heart allograft survival in mice (Kennedy *et al*., 2010). Recently a small molecule inhibitor of MCT1 has been studied known as AZD3965. It is an explicit MCT1 inhibitor and is able to restrict transport of lactate both into and out of the cell. The greater effect, however, has been seen on the uptake of lactate. It was also able to produce statistically significant inhibition of cancer cell growth. AZD3965 would be particularly helpful at killing the hypoxic areas of the tumor, as these are the areas that would lack glucose when the aerobic fraction is unable to use lactate as a metabolic substrate (Bola *et al*., 2014). A small molecule, AR-C117977, has also been developed as a specific MCT1 inhibitor for mild immunosuppression.

Targeting CD147 is also an attractive antitumor strategy for they are essential for the stabilization and localization of MCTs to the cell membrane. One approach involves the generation of humanized anti-CD147 antibodies that can induce antibody-dependent-cell-mediated cytotoxicity (ADCC). Such antibodies may also be utilized to deliver the drugs to CD147/MCT expressing cancer cells, which will destroy the cancer cells irrespective of their MCT expression status. The organomercurial reagent p-chloromercuribenzene sulfonate (pCBMS) inhibits the activity of MCT1 and MCT4 by disrupting their association with CD147 (Kennedy *et al*., 2010). Thus, developing more such potent inhibitors that possess the ability to inhibit Monocarboxylate transporters and the associated CD147 is the need of the hour will add to the anti-cancer armament.

2.10 Inhibitors of enolase

Enolase is the enzyme that is involved in the conversion reaction of dehydration of 2-phosphoglycerate to phosphoenolpyruvate in the final step of glycolysis. There are three types of enolase isoenzymes in mammals: alpha-enolase (ENO1) present in almost all mature tissues; beta-enolase (ENO3) existing primarily in muscle tissues and gamma-enolase (ENO2) mainly in nervous and neuroendocrine tissues (Capello *et al*., 2017). ENO1 is also identified as 2-phospho-D-glycerate hydrolase and is a metalloenzyme that requires Mg^{2+} ion as a metal activator. This enzyme is considered to be a multifunctional enzyme because of its varied roles such as being a glycolytic enzyme as well as a plasminogen receptor in which it mediates the activation of plasmin and ECM degradation (Ramos *et al*., 2012). Thus, it plays a crucial role in cancer proliferation, metastasis and invasion. In tumor cells, ENO1 is over-expressed and supports the Warburg effect.

Since ENO1 overexpression and post-translational modifications (acetylation and methylation) is prominent in cancer cells, it could be of diagnostic and prognostic value in many cancer types. ENO1's biochemical, proteomics and immunological characterization and its capability to activate a strong specific humoral and cellular immune response, makes this enzyme a promising anti-tumor target. Studies have revealed many potential inhibitors of enolase enzyme. The discovery of 'ENOblock', a

small-molecule inhibitor has been made which is the first non-substrate analog of the enzyme. It directly binds to ENO1 and inhibits its activity and can also inhibit cancer cell metastasis in vivo. Thus it is capable of being used in biological assays (Lung *et al*., 2017). The use of phosphonoacetohydroxamic acid (phAH) was done to target the translational ability of ENO1. It is a pan-enolase transition-state analog inhibitor for various cancer types. It inhibits both the enolase enzymatic activity and proliferation of cancer cells. Another inhibitor has been studied which an antibiotic is called SF2312. It is produced by the actinomycete *Micromonospora* and is active against a range of bacteria. It is the first reported phosphonate natural product inhibitor of enolase. It is an effective inhibitor of enolase with mixed competitive and non-competitive kinetics (Leonard *et al*., 2016). For most enolases, fluoride acts as an inhibitor and binds to enolase at the active center of the enzyme, forming a complex. This complex then blocks the binding of substrates to the enzyme, thereby exerting an inhibitory effect. The inhibition is mostly of competitive type (Qin *et al*., 2006). Other chemical inhibitors of enolase include D-tartonate and 3-aminoenolpyruvate-2-phosphate. Thus, altogether the inhibition of ENO1 acts as a potential anticancer target since it represses glycolytic pathway. All the above mentioned ENO1 inhibitors are very promising candidate compounds for pharmacokinetic and pharmacodynamic studies to assess their potential as anticancer drugs.

2.11 Computer-based drug designing

Most of the cancer drugs are small molecules designed to bind, interact and modulate the biological activity of the receptors. Computer-aided drug designing (CADD) is being exploited to identify hits, pick leads and optimize drug leads by studying their physicochemical, pharmaceutical and ADME\T (absorption, distribution, metabolism, excretion and toxicity) properties (Kumar, 2016). The objective of CADD is to augment the set of molecules with prudent active, drug-like properties and abolish compounds with undesirable properties such as inactive, reactive, toxic, poor ADME/T. The ADEM/T property of compound gives some important *in silico* prediction of the lead compound that includes bio-availability, blood-brain barrier crossing and inhibition of K^+ ion channels etc. *In silico* screening approach is the leading technique for preliminary identification of natural products as inhibitors of

targets protein and predicting their biological binding mode. In other words, *in silico* modeling is used considerably to minimize time and resource requirements of chemical synthesis and biological *in vitro* and *in vivo* testing (Kumar, 2016).

3.1 *In silico* anticancer potential screening

3.1.1 Protein preparation

The crystal structure of proteins GLUT1 (4PYP), Hexokinase2 (2NZT), PFKFB3 (2AXN), Pyruvate kinaseM2 (3GQY), Lactate dehydrogenase A (4AJP) and Enolase2 (5IDZ) were retrieved from the PDB (Protein Data Bank). All the heteroatom was removed leaving only the residues of the receptor. Preparation of the target protein with ADT involved the addition of polar hydrogen to the macromolecule, an essential step to correct the calculation of partial charge. Finally, a Gasteiger charge was calculated for each atom of the macromolecule in the target in Auto Dock 4.2. The energy minimization of protein structure was done by steepest decent method.

3.1.2 Ligand preparation

Literature-based phytochemicals were used as ligand for molecular docking (Figure 1). The 3D or 2D structures of phytochemicals were drawn using the Marvin Sketch software and respective reported standard inhibitors of particular protein were retrieved from NCBI PubChem in .sdf format. Open Babel molecule format converter was used for conversion of 2D to 3D conformation, Marvin Sketch software performed the conversion from .sdf to .pdb (for docking) file. Ligand's energy was minimized by applying mmff94 force field and conjugate gradients optimization algorithm using PyRx-Python prescription 0.8 for 200 steps.

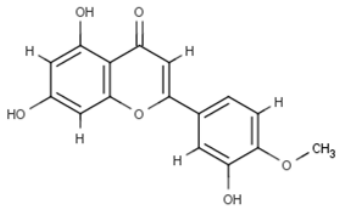

(1)

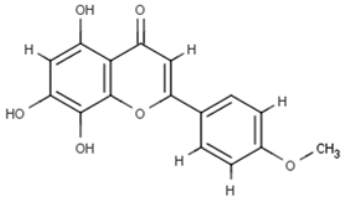

(2)

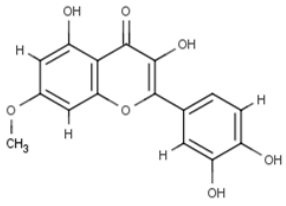

(3)

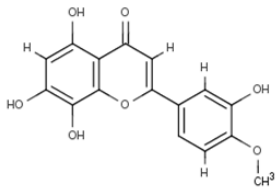

(4)

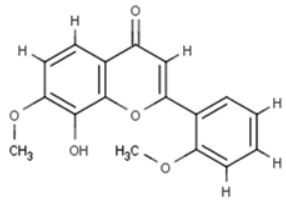

(5)

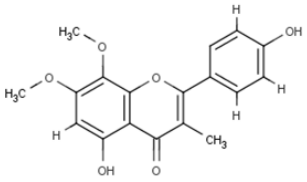

(6)

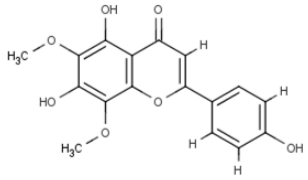

(7)

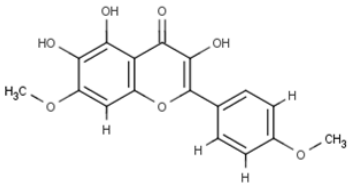

(8)

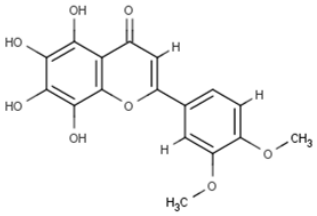

(9)

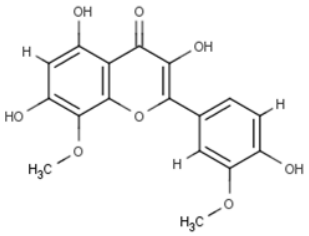

(10)

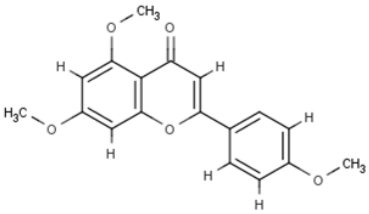

(11)

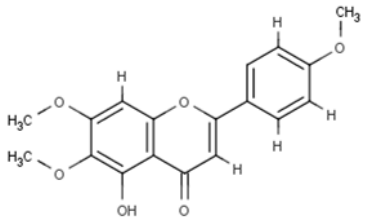

(12)

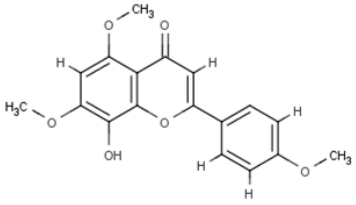

(13)

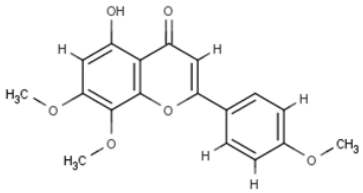

(14)

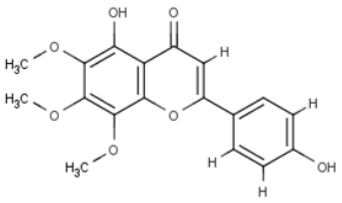

(15)

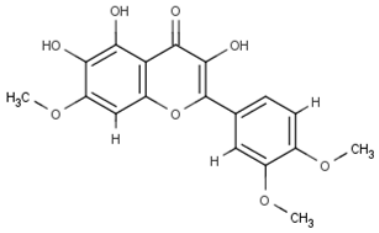

(16)

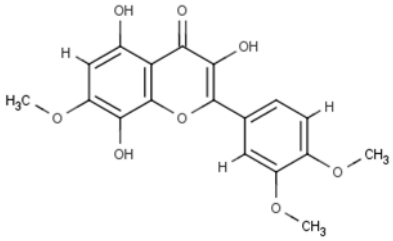

(17)

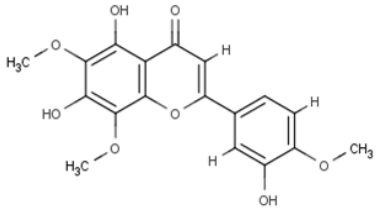

(18)

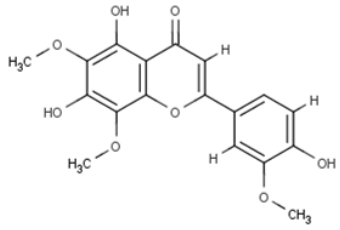

(19)

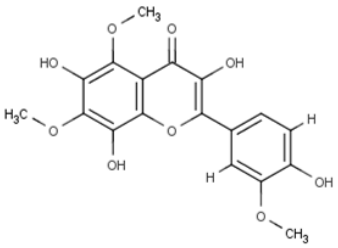

(20)

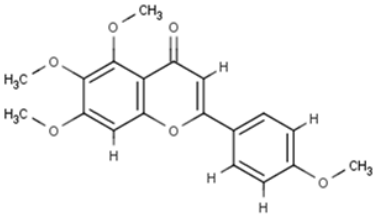

(21)

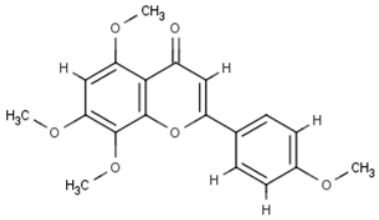

(22)

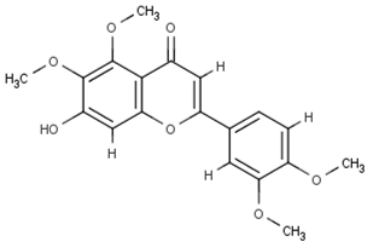

(23)

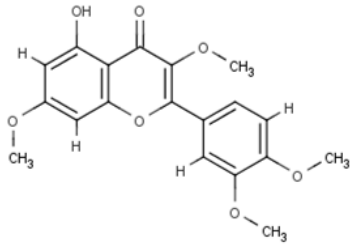

(24)

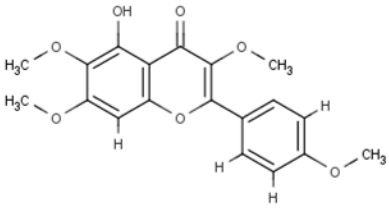

(25)

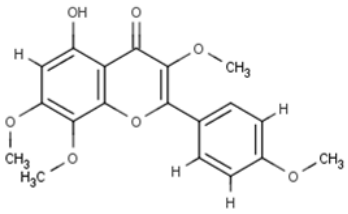

(26)

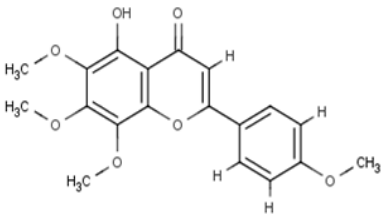

(27)

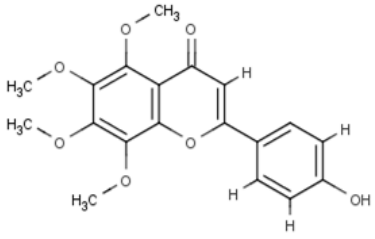

(28)

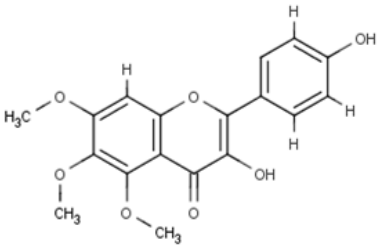

(29)

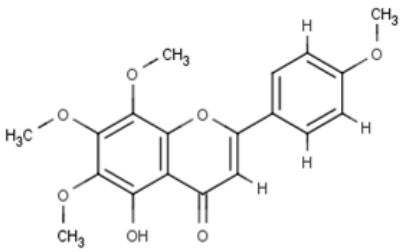

(30)

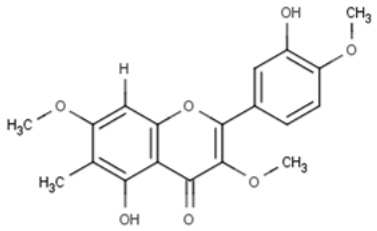

(31)

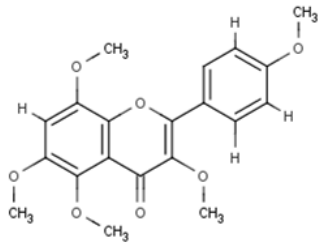

(32)

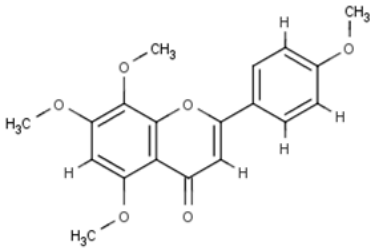

(33)

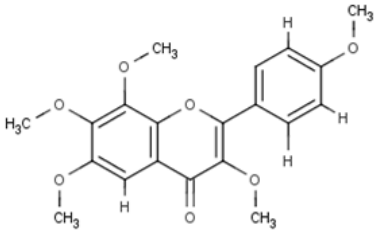

(34)

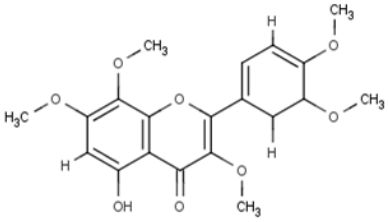

(35)

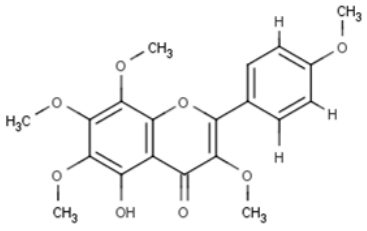

(36)

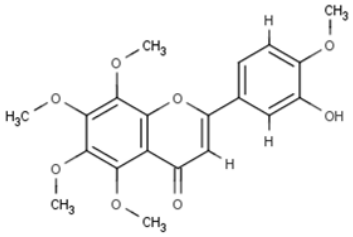

(37)

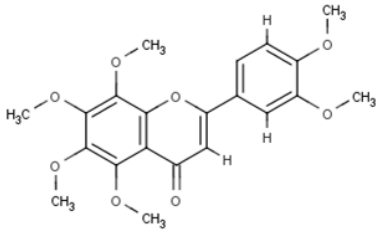

(38)

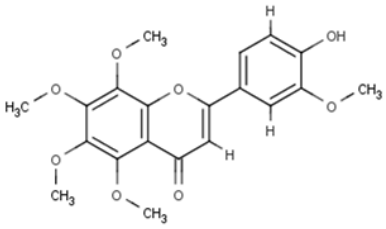

(39)

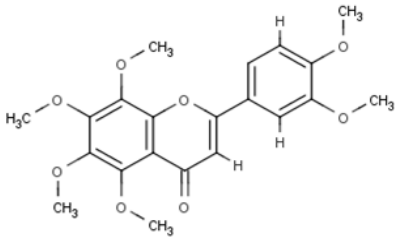

(40)

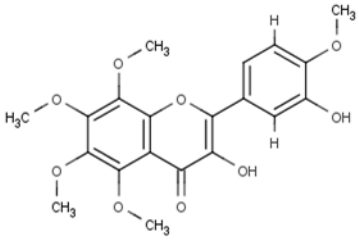

(41)

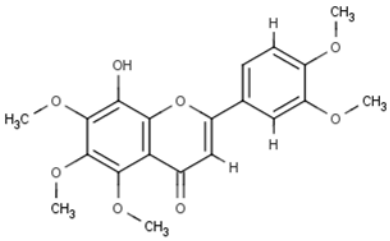

(42)

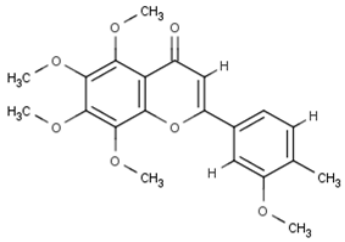

(43)

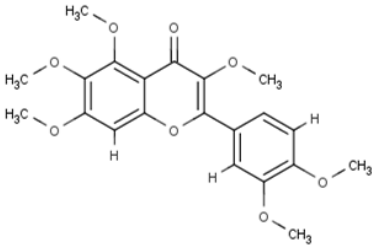

(44)

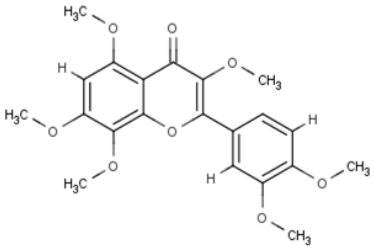

(45)

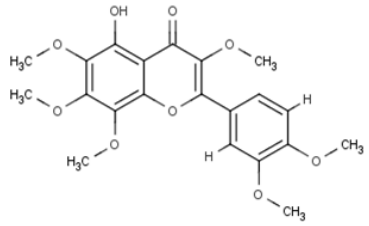

(46)

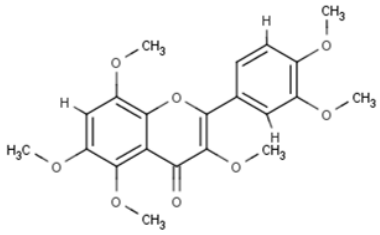

(47)

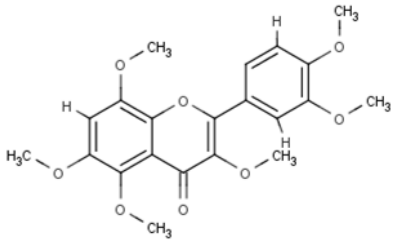

(48)

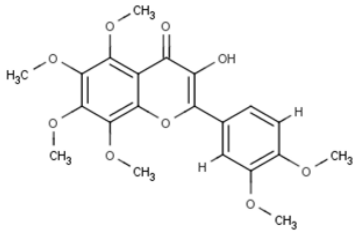

(49)

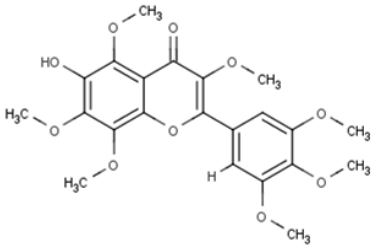

(50)

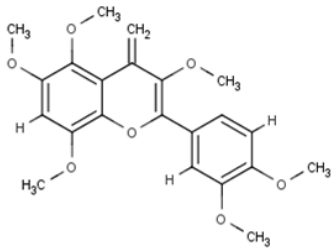

(51)

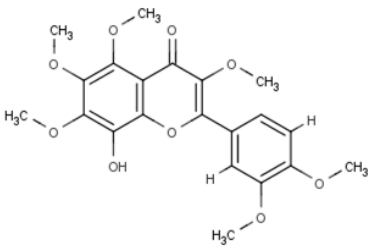

(52)

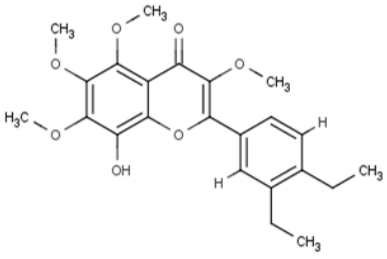

(53)

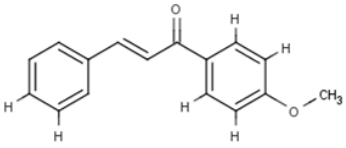

(54)

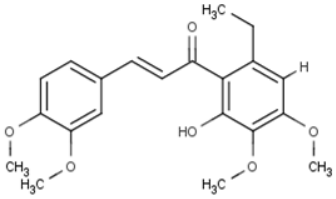

(55)

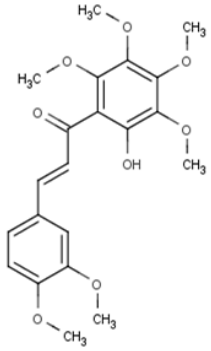

(56)

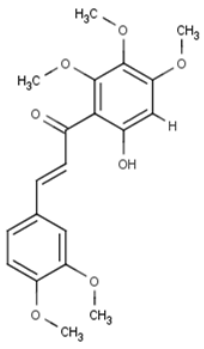

(57)

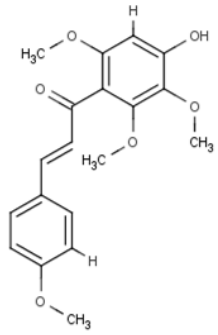

(58)

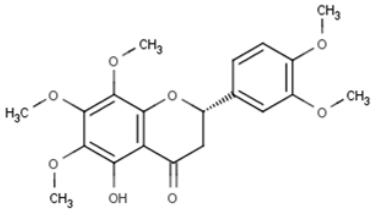

(59)

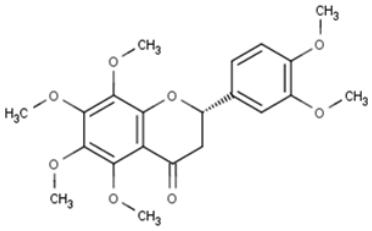

(60)

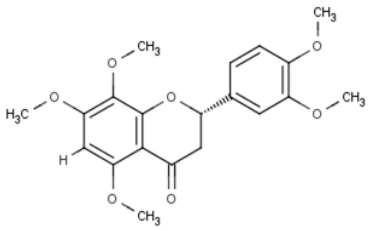

(61)

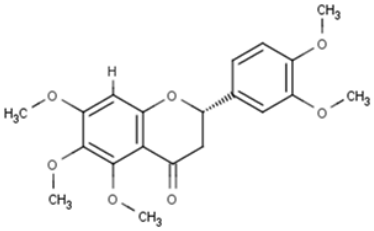

(62)

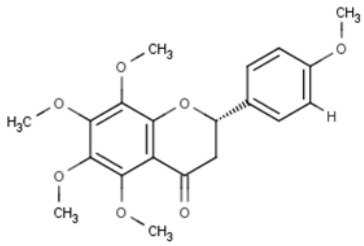

(63)

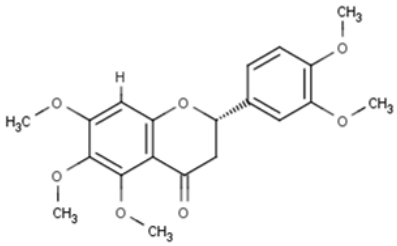

(64)

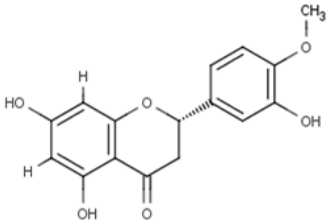

(65)

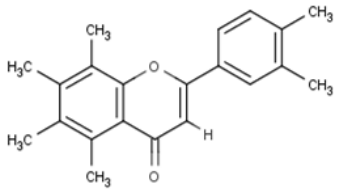

(66)

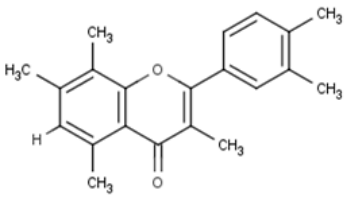

(67)

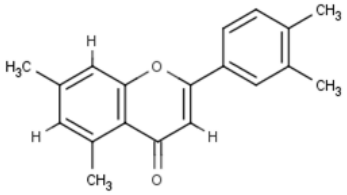

(68)

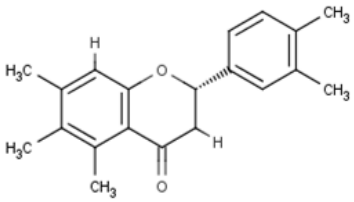

(69)

Figure 3.1: Structure of methylated flavonoids

(1) 5, 7-dihydroxy-2-(3-hydroxy-4-methoxyphenyl)-4H-chromen-4-one; **(2)** 5,7,8-trihydroxy-2-(4-methoxyphenyl)-4H-chromen-4-one; **(3)** 2-(3,4-dihydroxyphenyl)-3,5-dihydroxy-7-methoxy-4H-chromen-4-one; **(4)** 2-(3,4-dihydroxyphenyl)-3,5-dihydroxy-7-methoxy-4H-chromen-4-one; **(5)** 8-hydroxy-7-methoxy-2-(2-methoxyphenyl)-4H-chromen-4-one; **(6)** 5-hydroxy-2-(4-hydroxyphenyl)-7,8-dimethoxy-3-methyl-4H-chromen-4-one; **(7)** 5-hydroxy-2-(4-hydroxyphenyl)-7,8-dimethoxy-3-methyl-4H-chromen-4-one; **(8)** 3,5,6-trihydroxy-7-methoxy-2-(4-methoxyphenyl)-4H-chromen-4-one; **(9)** 2-(3,4-dimethoxyphenyl)-5,6,7,8-tetrahydroxy-4H-chromen-4-one; **(10)** 3,5,7-trihydroxy-2-(4-hydroxy-3-methoxyphenyl)-8-methoxy-4H-chromen-4-one; **(11)** 5,7-dimethoxy-2-(4-methoxyphenyl)-4H-chromen-4-one; **(12)** 5-hydroxy-6,7-dimethoxy-2-(4-methoxyphenyl)-4H-chromen-4-one; **(13)** 8-hydroxy-5,7-dimethoxy-2-(4-methoxyphenyl)-4H-chromen-4-one; **(14)** 5-hydroxy-7,8-dimethoxy-2-(4-methoxyphenyl)-4H-chromen-4-one; **(15)** 5-hydroxy-2-(4-hydroxyphenyl)-6,7,8-trimethoxy-4H-chromen-4-one; **(16)** 2-(3,4-dimethoxyphenyl)-3,5,6-tihydroxy-7-methoxy-4H-chromen-4-one; **(17)** 2-(3,4-dimethoxyphenyl)-3,5,8-trihydroxy-7-methoxy-4H-chromen-4-one -4-one; **(18)** 5,7-dihydroxy-2-(3-hydroxy-4-methoxyphenyl)-6,8-dimethoxy-4H-chromen-4-one; **(19)** 5,7-dihydroxy-2-(4-hydroxy-3-methoxyphenyl)-6,8-dimethoxy-4H-chromen-4-one; **(20)** 3,6,8-trihydroxy-2-(4-hydroxy-3-methoxyphenyl)-5,7-dimethoxy-4H-chromen-4-one; **(21)** 5,6,7-trimethoxy-2-(4-methoxyphenyl)-4H-chromen-4-one; **(22)** 5,7,8-trimethoxy-2-(4-methoxyphenyl)-4H-chromen-4-one; **(23)** 2-(3,4-dimethoxyphenyl)-7-hydroxy-5,6-dimethoxy-4H-chromen-4-one; **(24)** 2-(3,4-dimethoxyphenyl)-7-hydroxy-5,6-dimethoxy-4H-chromen-4-one; **(25)** 3-hydroxy-2-(4-hydroxyphenyl)-5,6,7-trimethoxy-4H-chromen-4-one; **(26)** 5-hydroxy-3,7,8-trimethoxy-2-(4-methoxyphenyl)-4H-chromen-4-one; **(27)** 5-hydroxy-6,7,8-trimethoxy-2-(4-methoxyphenyl)-4H-chromen-4-one; **(28)** 2-(4-hydroxyphenyl)-5,6,7,8-tetramethoxy-4H-chromen-4-one; **(29)** 3-hydroxy-2-(4-hydroxyphenyl)-5,6,7-trimethoxy-4H-chromen-4-one; **(30)** 5-hydroxy-6,7,8-trimethoxy-2-(4-methoxyphenyl)-4H-chromen-4-one; **(31)** 5-hydroxy-2-(3-hydroxy-4-methoxyphenyl)-3,7-dimethoxy-6-methyl-4H-chromen-4-one; **(32)** 3,5,6,8-tetramethoxy-2-(4-methoxyphenyl)-4H-chromen-4-one; **(33)** 5,7,8-trimethoxy-2-(4-methoxyphenyl)-4H-chromen-4-one; **(34)** 3,6,7,8-tetramethoxy-2-(4-methoxyphenyl)-4H-chromen-4-one; **(35)** 2-(3,4-dimethoxyphenyl)-5-hydroxy-3,7,8-trimethoxy-4H-chromen-4-one; **(36)** 5-hydroxy-3,6,7,8-tetramethoxy-2-(4-methoxyphenyl)-4H-chromen-4-one; **(37)** 2-(3-hydroxy-4-methoxyphenyl)-5,6,7,8-tetramethoxy-4H-chromen-4-one; **(38)** 2-(3,4-dimethoxyphenyl)-5,6,7,8-tetramethoxy-4H-chromen-4-one hydrate; **(39)** 2-(4-hydroxy-3-methoxyphenyl)-5,6,7,8-tetramethoxy-4H-chromen-4-one; **(40)** 2-(3,4-dimethoxyphenyl)-5,6,7,8-tetramethoxy-4H-chromen-4-one; **(41)** 3-hydroxy-2-(3-hydroxy-4-methoxyphenyl)-5,6,7,8-tetramethoxy-4H-chromen-4-one; **(42)** 2-(3,4-dimethoxyphenyl)-8-hydroxy-5,6,7-trimethoxy-4H-chromen-4-one; (43) 5,6,7,8-tetramethoxy-2-(3-methoxy-4-methylphenyl)-4H-chromen-4-one; **(44)** 2-(3,4-dimethoxyphenyl)-3,5,6,7-tetramethoxy-4H-chromen-4-one; **(45)** 2-(3,4-dimethoxyphenyl)-3,5,7,8-tetramethoxy-4H-chromen-4-one; **(46)** 2-(3,4-dimethoxyphenyl)-5-hydroxy-3,6,7,8-tetramethoxy-4H-chromen-4-one; **(47)** 2-(3,4-dimethoxyphenyl)-3,5,6,8-tetramethoxy-4H-chromen-4-one; **(48)** 2-(2,5-

dimethoxyphenyl)-3,6,7,8-tetramethoxy-4H-chromen-4-one; **(49)** 2-(3,4-dimethoxyphenyl)-3-hydroxy-5,6,7,8-tetramethoxy-4H-chromen-4-one; **(50)** 6-hydroxy-3,5,7,8-tetramethoxy-2-(3,4,5-trimethoxyphenyl)-4H-chromen-4-one; **(51)** 2-(3,4-dimethoxyphenyl)-3,5,6,8-tetramethoxy-4-methylidene-4H-chromene; **(52)** 2-(3,4-dimethoxyphenyl)-8-hydroxy-3,5,6,7-tetramethoxy-4H-chromen-4-one; **(53)** 2-(3,4-diethylphenyl)-8-hydroxy-3,5,6,7-tetramethoxy-4H-chromen-4-one; **(54)** (2E)-1-(4-methoxyphenyl)-3-phenylprop-2-en-1-one; **(55)** (2E)-3-(3,4-dimethoxyphenyl)-1-(6-ethyl-2-hydroxy-3,4-dimethoxyphenyl)prop-2-en-1-one; **(56)** (2E)-3-(3,4-dimethoxyphenyl)-1-(2-hydroxy-3,4,6-trimethoxyphenyl)prop-2-en-1-one; **(57)** (2E)-3-(3,4-dimethoxyphenyl)-1-(6-hydroxy-2,3,4-trimethoxyphenyl)prop-2-en-1-one; **(58)** 2E)-1-(4-hydroxy-2,3,6-trimethoxyphenyl)-3-(4-methoxyphenyl)prop-2-en-1-one; **(59)** (2S)-2-(3,4-dimethoxyphenyl)-5-hydroxy-6,7,8-trimethoxy-3,4-dihydro-2H-1-benzopyran-4-one; **(60)** (2S)-2-(3,4-dimethoxyphenyl)-5,6,7,8-tetramethoxy-3,4-dihydro-2H-1-benzopyran-4-one; **(61)** (2S)-2-(3,4-dimethoxyphenyl)-5,6,7-trimethoxy-3,4-dihydro-2H-1-benzopyran-4-one; **(62)** (2S)-2-(3,4-dimethoxyphenyl)-5,7,8-trimethoxy-3,4dihydro-2H-1-benzopyran-4-one; **(63)** (2S)-5,6,7,8-tetramethoxy-2-(4-methoxyphenyl)-3,4-dihydro-2H-1-benzopyran-4-one; **(64)** (2S)-2-(3,4-dimethoxyphenyl)-5,6,7-trimethoxy-3,4-dihydro-2H-1-benzopyran-4-one; **(65)** (2S)-5,7-dihydroxy-2-(3-hydroxy-4-methoxyphenyl)-3,4-dihydro-2H-1-benzopyran-4-one; **(66)** 2-(3,4-dimethylphenyl)-5,6,7,8-tetramethyl-4H-chromen-4-one; **(67)** 2-(3,4-dimethylphenyl)-3,5,7,8-tetramethyl-4H-chromen-4-one; **(68)** 2-(3,4-dimethylphenyl)-5,7-dimethyl-4H-chromen-4-one; **(69)** (2S)-2-(3,4-dimethylphenyl)-5,6,7-trimethyl-3,4-dihydro-2H-1-benzopyran-4-one

Source: Wen, L., Jiang, Y., Yang, J., Zhao, Y., Tian, M., Yang, B. (2017). Structure, bioactivity, and synthesis of methylated flavonoids. *Annals of the New York Academy of Sciences* **1398(1):**1-10

3.1.3 Molecular docking simulation

Virtual molecular screening is the process by which small-molecule libraries are docked to a macromolecule to hit upon lead compounds with desired biological function. Crystal structure of target enzyme GLUT1 (4PYP), Hexokinase2 (2NZT), PFKFB3 (2AXN), Pyruvate kinaseM2 (3GQY), Lactate Dehydrogenase A (4AJP) and Enolase2 (5IDZ) were obtained from the RCSB Protein Data Bank. The preparation of the target enzyme with the Auto Dock Tools involved the addition of hydrogen atoms to the target enzyme which is a necessary step for the computation of partial atomic charges. Docking of the ligands and proteins was done by the PyRx software. PyRx is open version software with an incisive user interface that runs on almost all major operating systems. Each of these compounds was docked into target proteins accordingly with positions, orientations and conformations of the ligand in the receptor binding site, and the docking structure possessing the lowest energy was preferred.

For docking experiments, the proteins and the ligands were loaded into Auto Dock Tools 4.2 (ADT). Gestgeiger partial charges assigned after merging nonpolar hydrogen and torsions applied to the ligands by rotating all rotatable bonds. Docking calculations were carried out on the protein models. Polar hydrogen atoms and solvation parameters were added with the help of Auto Dock tools. Docking was performed with the targeted proteins interface by keeping the X, Y and Z dimensions and the center grid box values. The grid box includes the entire binding site of the proteins interface and provides enough space for the ligands translational and rotational walk. Then, the PyRx-Python prescription 0.8 is used for visualization of the interaction pattern in the protein-ligand complex.

Table 3.1: Centre grid box values for the targeted proteins

Protein	X-axis	Y-axis	Z-axis
GLUT1	586.58	-29.13	208.13
Hexokinase2	-23.5	-55.28	33.71
Phosphofructokinase	-5.24	49.32	-1.45
Pyruvate kinase M2	9.99	3.35	13.5
Lactate dehydrogenaseA	4.96	9.52	17.9
Enolase2	74.81	220.21	-92.61

3.2 *In vitro* antioxidant activity assay

The free radical scavenging activity of the compound 003 was measured *in vitro* by 2,2-diphenyl-1-picrylhydrazyl (DPPH) assay. The appropriate concentration of DPPH solution was prepared in methanol followed by addition of 1mL of the test sample (003) at different concentrations. Different concentrations of the test sample were prepared in distilled water. The dye solution was prepared by dissolving 7mg of DPPH in 200ml of methanol. The content was mixed and allowed to stand for 30minutes and measured by recording the absorbance at 517nm. The lower absorbance of the reaction mixture indicated higher free radical activity. The percentage scavenging activities (% Inhibition) at different concentrations of the phytochemicals was calculated using the following formula:

(%)I=[(Ac−As)/Ac] ×100

where *I* is inhibition and A_C and A_S are the absorbance values of the control and the sample, respectively. Three replicates were made for each sample and results were expressed as mean ± SD (Kumar *et.al*, 2014).

3.3 *In vitro* cell proliferation assay

In vitro anticancer potential of the sample (Compound A) against colon cancer cell lines (HT29) was performed using MTT [3-(4,5- dimethylthiazol-2-yl)-2,5-diphenyltetrazolium bromide] (Kumar *et. al*, 2013). Cell suspension (100μL) was incubated for 24 hours followed by addition of 100μL compound A (100μg/well) and further was incubated for 72 hours. MTT solution (10μL) was added to each of the 96 wells, and then plates were wrapped with aluminum foil and incubated at 37◦ C for 4 hours which led to the formation of MTT-formazon crystals. Absorbance was measured by ELISA reader at 540nm. Controls and samples were assayed in triplicate. The results were shown as mean ± SD. The percentage viability of the sample was calculated by the following formulae:

(%) I=[(Ac−As)/Ac] ×100 where *I* is inhibition and A_C and A_S are the absorbance values of the control and the sample, respectively.

3.4 Antibacterial assay: Disk diffusion method

The antimicrobial activity of compound A against bacterial species such as *E.coli* was determined using Kirby-Bauer disk diffusion method (Bauer *et. al*, 1966). The inoculum suspension of bacterial strains was swabbed on the entire surface of LB agar. Sterile 6 mm diameter paper discs (Himedia) saturated with 20µL of phytochemicals (drug) prepared in DMSO (containing 2 mg extract/disc) were aseptically placed on the upper layer of the inoculated agar surfaces and plates were incubated at 37°C for 24 hours. Antibacterial activity was determined by measuring diameter of the zone of inhibition (ZOI) surrounding discs. Standard antibiotic discs of penicillin (10 µg/disc) and norfloxacin (10 µg/disc) were used as positive control. Discs containing 20 µL DMSO were used as a negative control. Antimicrobial assay was performed in triplicate and results were reported as average of three replicates

4.1 *In silico* anticancer potential of phytochemicals

4.1.1 Ligand-protein binding analysis

The ligands were docked at the heterodimer interfaces of proteins to predict the binding interactions. The result of molecular docking study is summarized in the following table (Table 2). The ligands such as 5,7-dihydroxy-2-(3-hydroxy-4-methoxyphenyl)-4H-chromen-4-one; 5,7,8-trihydroxy-2-(4-methoxyphenyl)-4H-chromen-4-one; 2-(3,4-dihydroxyphenyl)-3,5-dihydroxy-7-methoxy-4H-chromen-4-one; 2-(3,4-dihydroxyphenyl)-3,5-dihydroxy-7-methoxy-4H-chromen-4-one; 8-hydroxy-7-methoxy-2-(2-methoxyphenyl)-4H-chromen-4-one; 5-hydroxy-2-(4-hydroxyphenyl)-7,8-dimethoxy-3-methyl-4H-chromen-4-one; 5-hydroxy-2-(4-hydroxyphenyl)-7,8-dimethoxy-3-methyl-4H-chromen-4-one; 3,5,6-trihydroxy-7-methoxy-2-(4-methoxyphenyl)-4H-chromen-4-one; 2-(3,4-dimethoxyphenyl)-5,6,7,8-tetrahydroxy-4H-chromen-4-one; 3,5,7-trihydroxy-2-(4-hydroxy-3-methoxyphenyl)-8-methoxy-4H-chromen-4-one; 5,7-dimethoxy-2-(4-methoxyphenyl)-4H-chromen-4-one; 5-hydroxy-6,7-dimethoxy-2-(4-methoxyphenyl)-4H-chromen-4-one; 8-hydroxy-5,7-dimethoxy-2-(4-methoxyphenyl)-4H-chromen-4-one; 5-hydroxy-7,8-dimethoxy-2-(4-methoxyphenyl)-4H-chromen-4-one; 5-hydroxy-2-(4-hydroxyphenyl)-6,7,8-trimethoxy-4H-chromen-4-one; 2-(3,4-dimethoxyphenyl)-3,5,6-trihydroxy-7-methoxy-4H-chromen-4-one; 2-(3,4-dimethoxyphenyl)-3,5,8-trihydroxy-7-methoxy-4H-chromen-4-one; 5,7-dihydroxy-2-(3-hydroxy-4-methoxyphenyl)-6,8-dimethoxy-4H-chromen-4-one; 5,7-dihydroxy-2-(4-hydroxy-3-methoxyphenyl)-6,8-dimethoxy-4H-chromen-4-one; 3,6,8-trihydroxy-2-(4-hydroxy-3-methoxyphenyl)-5,7-dimethoxy-4H-chromen-4-one; 5,6,7-trimethoxy-2-(4-methoxyphenyl)-4H-chromen-4-one; 5,7,8-trimethoxy-2-(4-methoxyphenyl)-4H-chromen-4-one; 2-(3,4-dimethoxyphenyl)-7-hydroxy-5,6-dimethoxy-4H-chromen-4-one; 2-(3,4-dimethoxyphenyl)-7-hydroxy-5,6-dimethoxy-4H-chromen-4-one; 3-hydroxy-2-(4-hydroxyphenyl)-5,6,7-trimethoxy-4H-chromen-4-one; 5-hydroxy-3,7,8-trimethoxy-2-(4-methoxyphenyl)-4H-chromen-4-one; 5-hydroxy-6,7,8-trimethoxy-2-(4-methoxyphenyl)-4H-chromen-4-one; 2-(4-hydroxyphenyl)-5,6,7,8-tetramethoxy-4H-chromen-4-one; 3-hydroxy-2-(4-hydroxyphenyl)-5,6,7-trimethoxy-4H-chromen-4-one; 5-hydroxy-6,7,8-trimethoxy-2-(4-methoxyphenyl)-4H-chromen-4-one; 5-hydroxy-2-(3-hydroxy-4,5-dimethoxyphenyl)-3,7-dimethoxy-4H-chromen-4-

one; 3,5,6,8-tetramethoxy-2-(4-methoxyphenyl)-4H-chromen-4-one; 5,7,8-trimethoxy-2-(4-methoxyphenyl)-4H-chromen-4-one; 3,6,7,8-tetramethoxy-2-(4-methoxyphenyl)-4H-chromen-4-one; 2-(3,4-dimethoxyphenyl)-5-hydroxy-3,7,8-trimethoxy-4H-chromen-4-one; 5-hydroxy-3,6,7,8-tetramethoxy-2-(4-methoxyphenyl)-4H-chromen-4-one; 2-(3-hydroxy-4-methoxyphenyl)-5,6,7,8-tetramethoxy-4H-chromen-4-one; 2-(3,4-dimethoxyphenyl)-5,6,7,8-tetramethoxy-4H-chromen-4-one hydrate; 2-(4-hydroxy-3-methoxyphenyl)-5,6,7,8-tetramethoxy-4H-chromen-4-one; 2-(3,4-dimethoxyphenyl)-5,6,7,8-tetramethoxy-4H-chromen-4-one; 3-hydroxy-2-(3-hydroxy-4-methoxyphenyl)-5,6,7,8-tetramethoxy-4H-chromen-4-one; 2-(3,4-dimethoxyphenyl)-8-hydroxy-5,6,7-trimethoxy-4H-chromen-4-one; 5,6,7,8-tetramethoxy-2-(3-methoxy-4-methylphenyl)-4H-chromen-4-one; 2-(3,4-dimethoxyphenyl)-3,5,6,7-tetramethoxy-4H-chromen-4-one; 2-(3,4-dimethoxyphenyl)-3,5,7,8-tetramethoxy-4H-chromen-4-one; 2-(3,4-dimethoxyphenyl)-5-hydroxy-3,6,7,8-tetramethoxy-4H-chromen-4-one; 2-(3,4-dimethoxyphenyl)-3,5,6,8-tetramethoxy-4H-chromen-4-one; 2-(2,5-dimethoxyphenyl)-3,6,7,8-tetramethoxy-4H-chromen-4-one; 2-(3,4-dimethoxyphenyl)-3-hydroxy-5,6,7,8-tetramethoxy-4H-chromen-4-one; 6-hydroxy-3,5,7,8-tetramethoxy-2-(3,4,5-trimethoxyphenyl)-4H-chromen-4-one; 2-(3,4-dimethoxyphenyl)-3,5,6,8-tetramethoxy-4-methylidene-4H-chromene; 2-(3,4-dimethoxyphenyl)-8-hydroxy-3,5,6,7-tetramethoxy-4H-chromen-4-one; 2-(3,4-diethylphenyl)-8-hydroxy-3,5,6,7-tetramethoxy-4H-chromen-4-one; (2E)-1-(4-methoxyphenyl)-3-phenylprop-2-en-1-one; (2E)-3-(3,4-dimethoxyphenyl)-1-(6-ethyl-2-hydroxy-3,4-dimethoxyphenyl)prop-2-en-1-one; (2E)-3-(3,4-dimethoxyphenyl)-1-(2-hydroxy-3,4,6-trimethoxyphenyl)prop-2-en-1-one; (2E)-3-(3,4-dimethoxyphenyl)-1-(6-hydroxy-2,3,4-trimethoxyphenyl)prop-2-en-1-one; (2E)-1-(4-hydroxy-2,3,6-trimethoxyphenyl)-3-(4-methoxyphenyl)prop-2-en-1-one; (2S)-2-(3,4-dimethoxyphenyl)-5-hydroxy-6,7,8-trimethoxy-3,4-dihydro-2H-1-benzopyran-4-one; (2S)-2-(3,4-dimethoxyphenyl)-5,6,7,8-tetramethoxy-3,4-dihydro-2H-1-benzopyran-4-one; (2S)-2-(3,4-dimethoxyphenyl)-5,6,7-trimethoxy-3,4-dihydro-2H-1-benzopyran-4-one; (2S)-2-(3,4-dimethoxyphenyl)-5,7,8-trimethoxy-3,4dihydro-2H-1-benzopyran-4-one; (2S)-5,6,7,8-tetramethoxy-2-(4-methoxyphenyl)-3,4-dihydro-2H-1-benzopyran-4-one; (2S)-2-(3,4-dimethoxyphenyl)-5,6,7-trimethoxy-3,4-dihydro-2H-1-benzopyran-4-one; (2S)-5,7-dihydroxy-2-(3-hydroxy-4-methoxyphenyl)-3,4-

dihydro-2H-1-benzopyran-4-one; 2-(3,4-dimethylphenyl)-5,6,7,8-tetramethyl-4H-chromen-4-one; 2-(3,4-dimethylphenyl)-3,5,7,8-tetramethyl-4H-chromen-4-one; 2-(3,4-dimethylphenyl)-5,7-dimethyl-4H-chromen-4-one; (2S)-2-(3,4-dimethylphenyl)-5,6,7-trimethyl-3,4-dihydro-2H-1-benzopyran-4-one were docked with targeted proteins to predict the binding score. The table (Table 2) summarizes the results of molecular docking studies comprising lowest binding energy and proteins residues involved in hydrogen bonding with screened ligands (selected standard inhibitors and phytochemicals). Further, the ligands having the lowest binding energy were predicted. Comparative study for the mean of the lowest binding energy of all ligands indicated that out of 69 phytochemicals only 2-(3,4-dihydroxyphenyl)-3,5-dihydroxy-7-methoxy-4H-chromen-4-one, 5,7-dihydroxy-2-(3-hydroxy-4-methoxyphenyl)-6,8-dimethoxy-4H-chromen-4-one and 2-(3,4-dimethylphenyl)-5,7-dimethyl-4H-chromen-4-one have the highest affinity for proteins such as GLUT1 (4PYP), Hexokinase2 (2NZT), PFKFB3 (2AXN), Pyruvate kinaseM2 (3GQY), Lactate DehydrogenaseA (4AJP) and Enolase2 (5IDZ) due to their lowest binding energy. Further the molecule 2-(3,4-dihydroxyphenyl)-3,5-dihydroxy-7-methoxy-4H-chromen-4-one has the highest affinity for Phosphofructokinase2 (PFKFB3) and GLUT1 with a docking score as -7.14 and -9.68 respectively. The phytochemical 5,7-dihydroxy-2-(3-hydroxy-4-methoxyphenyl)-6,8-dimethoxy-4H-chromen-4-one has shown maximum affinity for both Hexokinase2 and Pyruvate kinase M2 with a docking score of -7.07 and -9.55 respectively. The molecule 2-(3,4-dimethylphenyl)-5,7-dimethyl-4H-chromen-4-one with a docking score of -7.14 possess highest affinity for Lactate dehydrogenaseA protein.

Table 4.1: Comparative table of binding affinity of ligands with targeted proteins

S.No	PCID	Name	A	B	C	D	E	F
1	25142799	PFK15	-3.19					
2	2327	Benserazide		-7.81				
3	5208	Shikonin			-7.11			

4	3503	Gossypol			-7.5		
5	5311281	Cytochalasin B				-4.24	
6	52913330	SF2312					-6.3

S.No	Methylated compounds	A	B	C	D	E	F
1.	5,7-dihydroxy-2-(3-hydroxy-4-methoxyphenyl)-4H-chromen-4-one	-5.66	-4.91	-8.27	-4.5	-7.4	-1.4
2.	5,7,8-trihydroxy-2-(4 methoxyphenyl)-4H-chromen-4-one	-6.96	-5.99	-8.3	-5.41	-8.97	-0.09
3.	2-(3,4-dihydroxyphenyl)-3,5-dihydroxy-7-methoxy-4H-chromen-4-one	-6.22	-5.3	-9.19	-4.39	-8.59	-0.14
4.	2-(3,4-dihydroxyphenyl)-3,5-dihydroxy-7-methoxy-4H-chromen-4-one	-7.14	-6.32	-8.76	-5.15	-9.68	-0.66
5.	8-hydroxy-7-methoxy-2-(2-methoxyphenyl)-4H-chromen-4-one	-6.96	-4.55	-8.7	-6.21	-7.43	-5.63
6.	5-hydroxy-2-(4-hydroxyphenyl)-7,8-dimethoxy-3-methyl-4H-chromen-4-one	-3.16	-4.24	-8.26	-4.36	-6.79	-2.94
7.	5-hydroxy-2-(4-hydroxyphenyl)-7,8-dimethoxy-3-methyl-4H-chromen-4-one	-4.85	-5.64	-9.15	-4.5	-6.69	0.43
8.	3,5,6-trihydroxy-7-methoxy-2-(4-methoxyphenyl)-4H-chromen-4-one	-5.94	-6.31	-8.44	-4.82	-8.1	0.19
9.	2-(3,4-dimethoxyphenyl)-5,6,7,8-tetrahydroxy-4H-chromen-4-one	-6.71	-6.81	-9.15	-4.69	-8.6	0.44
10.	3,5,7-trihydroxy-2-(4-hydroxy-3-methoxyphenyl)-8-	-6.77	-6.88	-9.1	-4.42	-9.09	-2.11

	methoxy-4H-chromen-4-one						
11.	5,7-dimethoxy-2-(4 methoxyphenyl)-4H-chromen-4-one	-3.9	-3.52	-7.36	-4.37	-6.66	-3.59
12.	5-hydroxy-6,7-dimethoxy-2-(4-methoxyphenyl)-4H-chromen-4-one	-4.64	-4.51	-6.66	-5.54	-6.85	-3.51
13.	8-hydroxy-5,7-dimethoxy-2-(4-methoxyphenyl)-4H-chromen-4-one	-4.07	-4	-6.38	-3.13	-7.11	-8.3
14.	5-hydroxy-7,8-dimethoxy-2-(4-methoxyphenyl)-4H-chromen-4-one	-3.55	-3.64	-6.69	-4.13	-6.48	-0.91
15.	5-hydroxy-2-(4-hydroxyphenyl)-6,7,8-trimethoxy-4H-chromen-4-one	-3.67	-4.61	-8.63	-4.31	-7.63	-3.48
16.	2-(3,4-dimethoxyphenyl)-3,5,6-trihydroxy-7-methoxy-4H-chromen-4-one	-6.02	-6.51	-8.46	-5.91	-8.59	1.99
17.	2-(3,4-dimethoxyphenyl)-3,5,8-trihydroxy-7-methoxy-4H-chromen-4-one	-6.92	-5.66	-7.63	-5.04	-7.86	-7.8
18.	5,7-dihydroxy-2-(3-hydroxy-4-methoxyphenyl)-6,8-dimethoxy-4H-chromen-4-one	-5.17	-7.07	-9.55	-3.86	-7.88	-8.6
19.	5,7-dihydroxy-2-(4-hydroxy-3-methoxyphenyl)-6,8-dimethoxy-4H-chromen-4-one	-5.68	-5.91	-9.48	-4.43	-7.65	-7.5
20.	3,6,8-trihydroxy-2-(4-hydroxy-3-methoxyphenyl)-5,7-dimethoxy-4H-chromen-4-one	-6.68	-5.53	-9.3	-4.74	-8.14	3.87
21.	5,6,7-trimethoxy-2-(4-methoxyphenyl)-4H-chromen-4-one	-3.47	-1.94	-7.31	-3.34	-6.16	-7.8
22.	5,7,8-trimethoxy-2-(4-methoxyphenyl)-4H-chromen-4-one	-2.13	-3.41	-8.56	-3.34	-5.76	-7.6

23.	2-(3,4-dimethoxyphenyl)-7-hydroxy-5,6-dimethoxy-4H-chromen-4-one	-4.68	-4.28	-7.06	-4.86	-6.78	-7.2
24.	2-(3,4-dimethoxyphenyl)-7-hydroxy-5,6-dimethoxy-4H-chromen-4-one	-3.94	-4.21	-7.31	-3.52	-6.72	-1.11
25.	3-hydroxy-2-(4-hydroxyphenyl)-5,6,7-trimethoxy-4H-chromen-4-one	-4.84	-3.54	-6.7	-4.4	-7.12	-6.2
26.	5-hydroxy-3,7,8-trimethoxy-2-(4-methoxyphenyl)-4H-chromen-4-one	-3.82	-3.9	-7.6	-4.45	-6.8	-1.79
27.	5-hydroxy-6,7,8-trimethoxy-2-(4-methoxyphenyl)-4H-chromen-4-one	-3.65	-2.71	-7.28	-5.05	-7.4	-3.48
28.	2-(4-hydroxyphenyl)-5,6,7,8-tetramethoxy-4H-chromen-4-one	-3.21	-3.17	-7.55	-4.75	-6.56	-2.55
29.	3-hydroxy-2-(4-hydroxyphenyl)-5,6,7-trimethoxy-4H-chromen-4-one	-5.3	-4.49	-6.4	-4.54	-7.75	2.23
30.	5-hydroxy-6,7,8-trimethoxy-2-(4-methoxyphenyl)-4H-chromen-4-one	-2.71	-4.8	-7.17	-5.18	-6.57	-3.27
31.	5-hydroxy-2-(3-hydroxy-4,5-dimethoxyphenyl)-3,7-dimethoxy-4H-chromen-4-one	-6.44	-5.14	-8.3	-4.53	-7.52	1.59
32.	3,5,6,8-tetramethoxy-2-(4-methoxyphenyl)-4H-chromen-4-one	-0.27	-2.83	-6.19	-5.34	-6.16	-2.1
33.	5,7,8-trimethoxy-2-(4-methoxyphenyl)-4H-chromen-4-one	-3.2	-3.68	-8.33	-4.14	-6.23	0.84
34.	3,6,7,8-tetramethoxy-2-(4-methoxyphenyl)-4H-chromen-4-one	-3.19	-2.12	-6.07	-3.98	-5.07	-1.35
35.	2-(3,4-dimethoxyphenyl)-5-hydroxy-3,7,8-trimethoxy-4H-chromen-4-one	-3.65	-4.21	-6.9	-4.13	-6.97	-0.28

36.	5-hydroxy-3,6,7,8-tetramethoxy-2-(4-methoxyphenyl)-4H-chromen-4-one	-2.74	-3.2	-7.24	-4.78	-6.65	0.08
37.	2-(3-hydroxy-4-methoxyphenyl)-5,6,7,8-tetramethoxy-4H-chromen-4-one	-3.68	-1.49	-6.98	-4.16	-7.02	2.8
38.	2-(3,4-dimethoxyphenyl)-5,6,7,8-tetramethoxy-4H-chromen-4-one hydrate	-3.73	-3.55	-6.89	-5	-6.48	-1.41
39.	2-(4-hydroxy-3-methoxyphenyl)-5,6,7,8-tetramethoxy-4H-chromen-4-one	-4.83	-4.14	-6.61	-4.79	-7.87	-1.67
40.	2-(3,4-dimethoxyphenyl)-5,6,7,8-tetramethoxy-4H-chromen-4-one	-2.75	-3.44	-6.61	-5.42	-6.75	-2.33
41.	3-hydroxy-2-(3-hydroxy-4-methoxyphenyl)-5,6,7,8-tetramethoxy-4H-chromen-4-one	-3.74	-2.84	-8.36	-4.8	-7.35	0.84
42.	2-(3,4-dimethoxyphenyl)-8-hydroxy-5,6,7-trimethoxy-4H-chromen-4-one	-5.18	-2.99	-7.07	-4.05	-6.52	-2.13
43.	5,6,7,8-tetramethoxy-2-(3-methoxy-4-methylphenyl)-4H-chromen-4-one	-2.54	-3.64	-6.63	-3.92	-6.69	-1.66
44.	2-(3,4-dimethoxyphenyl)-3,5,6,7-tetramethoxy-4H-chromen-4-one	-5.17	-1.97	-6.13	-4.39	-6.48	-0.93
45.	2-(3,4-dimethoxyphenyl)-3,5,7,8-tetramethoxy-4H-chromen-4-one	-1.23	-3.6	-7.24	-4.8	-6.54	-2.46
46.	2-(3,4-dimethoxyphenyl)-5-hydroxy-3,6,7,8-tetramethoxy-4H-chromen-4-one	-3.14	-4.79	-7.15	-4.8	-6.98	-3.25
47.	2-(3,4-dimethoxyphenyl)-3,5,6,8-tetramethoxy-4H-chromen-4-one	-3.76	-2.84	-6.31	-4.48	-6.19	-1.6
48.	2-(2,5-dimethoxyphenyl)-3,6,7,8-tetramethoxy-4H-chromen-4-one	-3.12	-3.18	-9.09	-3.97	-5.41	0.47
49.	2-(3,4-dimethoxyphenyl)-3-hydroxy-5,6,7,8-	-3.2	-4.26	-6.96	-6.94	-6.73	-4.11

	tetramethoxy-4H-chromen-4-one						
50.	6-hydroxy-3,5,7,8-tetramethoxy-2-(3,4,5-trimethoxyphenyl)-4H-chromen-4-one	-3.93	-4.23	-6.68	-5.53	-7.5	-5.88
51.	2-(3,4-dimethoxyphenyl)-3,5,6,8-tetramethoxy-4-methylidene-4H-chromene	-1.85	-2.89	-6.23	-5.77	-5.72	-5.11
52.	2-(3,4-dimethoxyphenyl)-8-hydroxy-3,5,6,7-tetramethoxy-4H-chromen-4-one	-5.27	-3.64	-6.94	-5.22	-6.91	-3.4
53.	2-(3,4-diethylphenyl)-8-hydroxy-3,5,6,7-tetramethoxy-4H-chromen-4-one	-4.46	-3.64	-7.84	-6.15	-7.05	-3.93
54.	(2E)-1-(4-methoxyphenyl)-3-phenylprop-2-en-1-one	-3.12	-1.96	-7.6	-5.18	-6.78	-3.4
55.	(2E)-3-(3,4-dimethoxyphenyl)-1-(6-ethyl-2-hydroxy-3,4-dimethoxyphenyl)prop-2-en-1-one	-4.48	-4.27	-8.73	-5.65	-7.39	-1.84
56.	(2E)-3-(3,4-dimethoxyphenyl)-1-(2-hydroxy-3,4,6-trimethoxyphenyl)prop-2-en-1-one	-4.22	-3.16	-7.1	-4.66	-7.67	-2.63
57.	(2E)-3-(3,4-dimethoxyphenyl)-1-(6-hydroxy-2,3,4-trimethoxyphenyl)prop-2-en-1-one	-6.08	-4.95	-8.21	-5.13	-7.41	-3.43
58.	(2E)-1-(4-hydroxy-2,3,6-trimethoxyphenyl)-3-(4-methoxyphenyl)prop-2-en-1-one	-4.41	-4.25	-7.61	-4.74	-6.84	0.09
59.	(2S)-2-(3,4-dimethoxyphenyl)-5-hydroxy-6,7,8-trimethoxy-3,4-dihydro-2H-1-benzopyran-4-one	-4.31	-3.96	-7.2	-5.05	-7.31	-0.26
60.	(2S)-2-(3,4-dimethoxyphenyl)-5,6,7,8-tetramethoxy-3,4-dihydro-	-5.71	-2.14	-6.68	-6.15	-5.68	-4.05

61.	2H-1-benzopyran-4-one (2S)-2-(3,4-dimethoxyphenyl)-5,6,7-trimethoxy-3,4-dihydro-2H-1-benzopyran-4-one	-3.72	-2.64	-4.52	-7.04	-6.63	-4.87
62.	(2S)-2-(3,4-dimethoxyphenyl)-5,7,8-trimethoxy-3,4dihydro-2H-1-benzopyran-4-one	-3.42	-3.02	-5.04	-6.42	-6.76	-3.12
63.	(2S)-5,6,7,8-tetramethoxy-2-(4-methoxyphenyl)-3,4-dihydro-2H-1-benzopyran-4-one	-2.83	-2.83	-5.21	-5.9	-5.59	-5.58
64.	(2S)-2-(3,4-dimethoxyphenyl)-5,6,7-trimethoxy-3,4-dihydro-2H-1-benzopyran-4-one	-3.79	-2.05	-6.93	-5.07	-6.48	-2.64
65.	(2S)-5,7-dihydroxy-2-(3-hydroxy-4-methoxyphenyl)-3,4-dihydro-2H-1-benzopyran-4-one	-5.87	-5.59	-8.77	-5.48	-7.16	-3.77
66.	2-(3,4-dimethylphenyl)-5,6,7,8-tetramethyl-4H-chromen-4-one	-1.76	-2.69	-7.19	-6.69	-7.32	-5.86
67.	2-(3,4-dimethylphenyl)-3,5,7,8-tetramethyl-4H-chromen-4-one	-2.28	-2.25	-7.42	-6.62	-6.75	-5.2
68.	2-(3,4-dimethylphenyl)-5,7-dimethyl-4H-chromen-4-one	-3.05	-3	-7.46	-7.14	-6.32	-5.29
69.	(2S)-2-(3,4-dimethylphenyl)-5,6,7-trimethyl-3,4-dihydro-2H-1-benzopyran-4-one	-2.06	-2.8	-6.84	-6.47	-6.62	-4.7

A= Phosphofructokinase2 (2axn), B= Hexokinase2 (2nzt), C=Pyruvate kinase M2 (3gqy), D=Lactate dehydrogenase A (4ajp), E= GLUT1 (4pyp) and F= Enolase (5idz), PubChem ID (PCID)

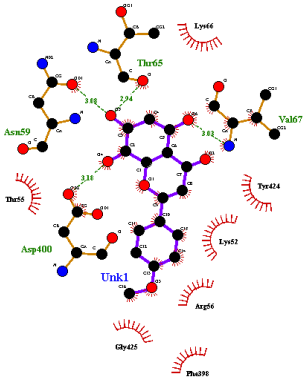
Lys66
Thr65
Asn59
Val67
Thr56
Tyr424
Lys52
Asp400
Unk1
Arg56
Gly425
Pha398

(1)

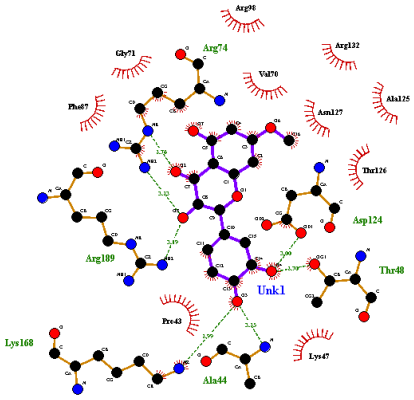
Arg98
Gly71
Arg74
Arg132
Val70
Phe67
Ala125
Asn127
Thr126
Asp124
Arg189
Thr48
Unk1
Pro43
Lys168
Lys47
Ala44

(2)

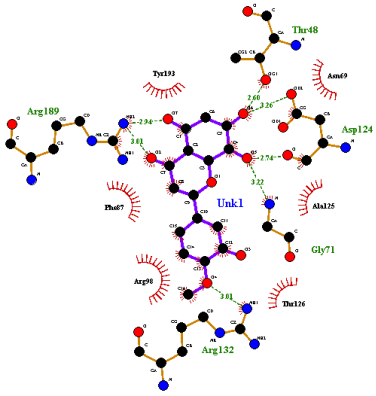
Thr48
Tyr193
Asn69
Arg189
Asp124
Unk1
Phe67
Ala125
Gly71
Arg98
Thr126
Arg132

(3)

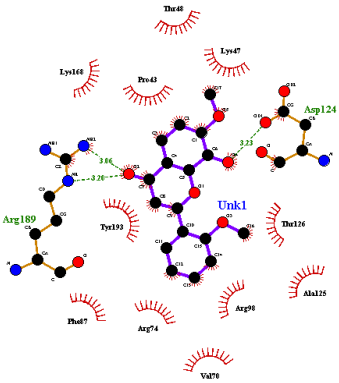
Thr48
Lys47
Lys168
Pro43
Asp124
Unk1
Arg189
Tyr193
Thr126
Phe67
Arg74
Arg98
Ala125
Val70

(4)

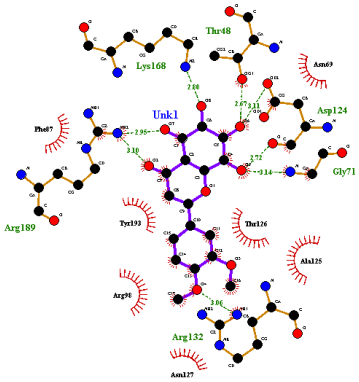
Thr48
Lys168
Asn69
Unk1
Asp124
Phe67
Gly71
Arg189
Tyr193
Thr126
Ala125
Arg98
Arg132
Asn127

(5)

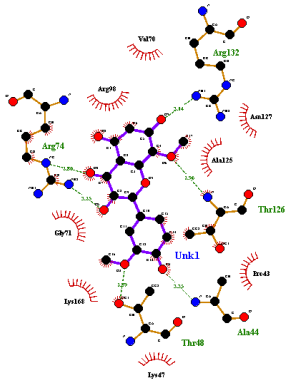
Val70
Arg132
Arg98
Asn127
Arg74
Ala125
Thr126
Gly71
Unk1
Pro43
Lys168
Ala44
Thr48
Lys47

(6)

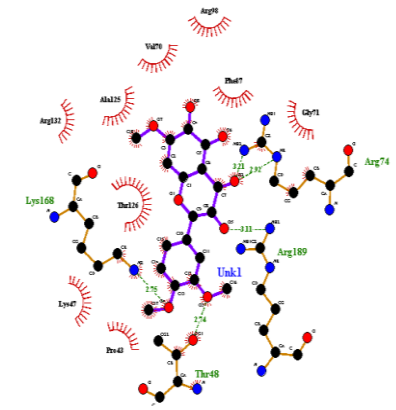
Arg96
Val70
Phe67
Ala125
Arg132
Gly71
Arg74
Lys168
Thr126
Arg189
Unk1
Lys47
Pro43
Thr48

(7)

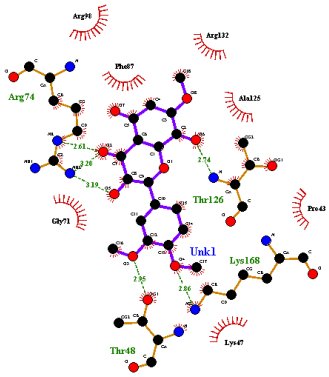
Arg96
Arg132
Phe67
Arg74
Ala125
Thr126
Gly71
Pro43
Unk1
Lys168
Thr48
Lys47

(8)

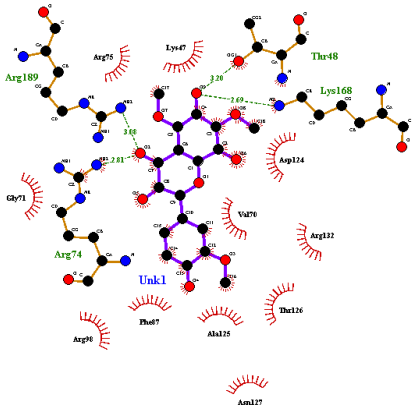
Arg189
Arg75
Lys47
Thr48
Lys168
Asp124
Gly71
Val70
Arg132
Arg74
Unk1
Thr126
Phe67
Ala125
Arg96
Asn127

(9)

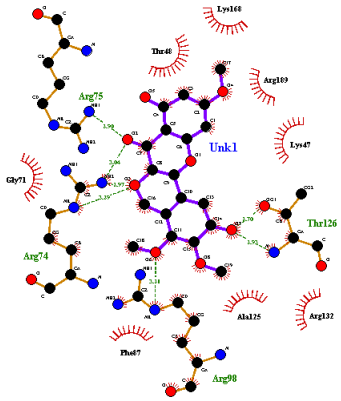
Lys168
Thr48
Arg189
Arg75
Unk1
Lys47
Gly71
Thr126
Arg74
Ala125
Arg132
Phe67
Arg98

(10)

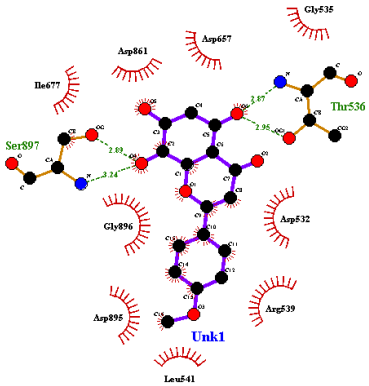
Gly535
Asp657
Asp861
Ile677
Thr536
Ser897
Gly896
Arg532
Asp895
Arg539
Unk1
Leu541

(11)

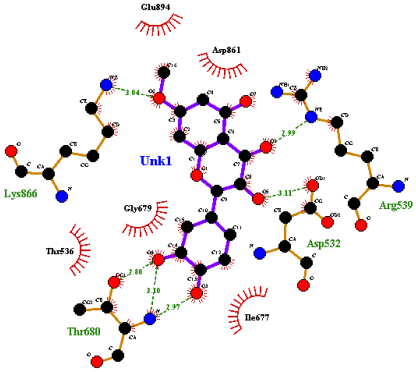
Glu894
Asp861
Unk1
Lys866
Arg539
Gly679
Asp532
Thr536
Thr680
Ile677

(12)

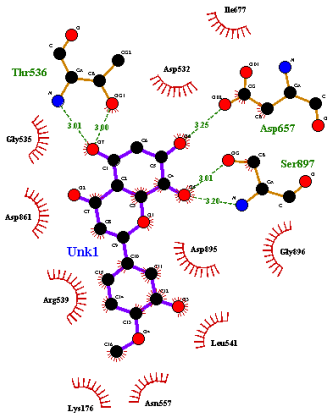

(13)

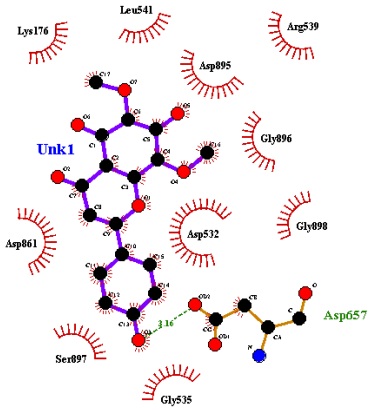

(14)

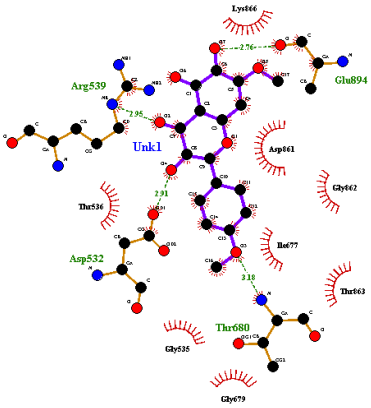

(15)

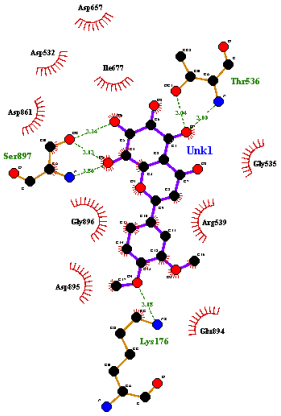

(16)

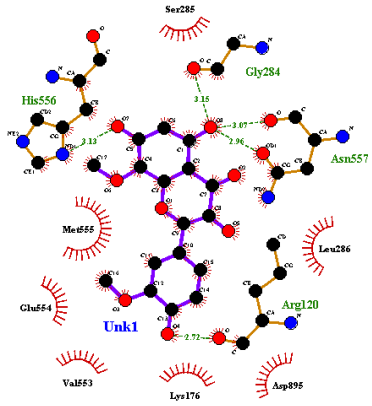

(17)

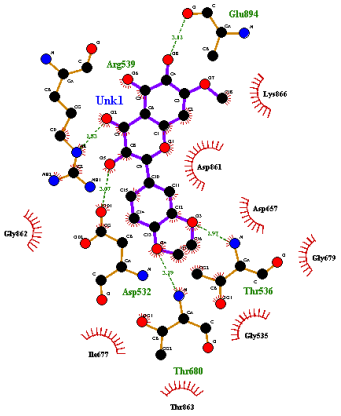

(18)

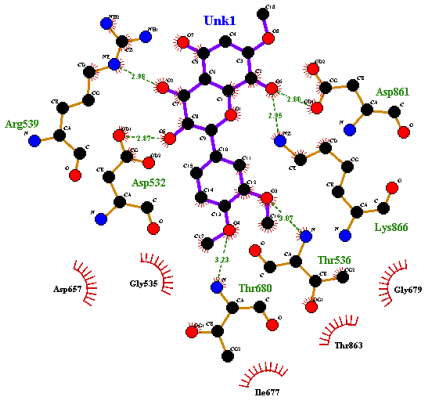

(19)

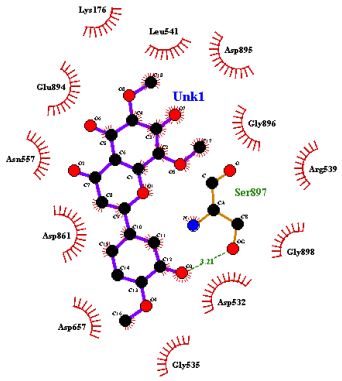

(20)

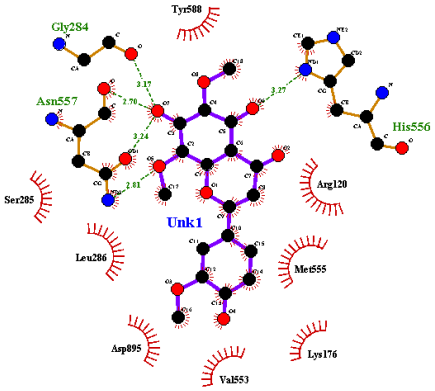

(21)

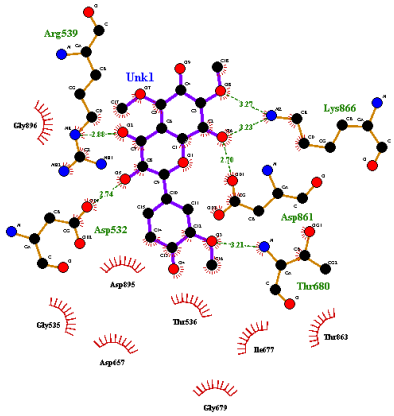

(22)

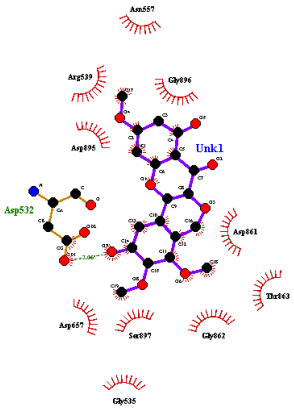

(23)

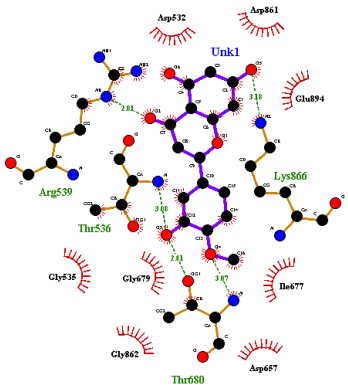

(24)

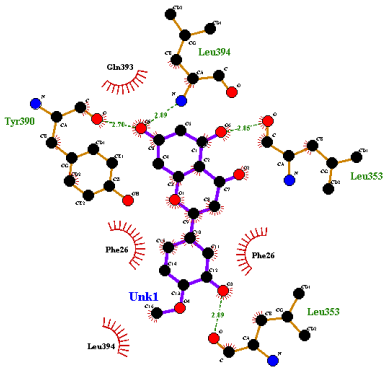

(25)

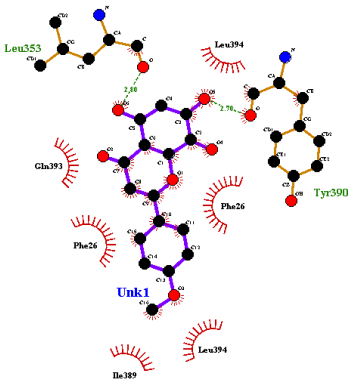

(26)

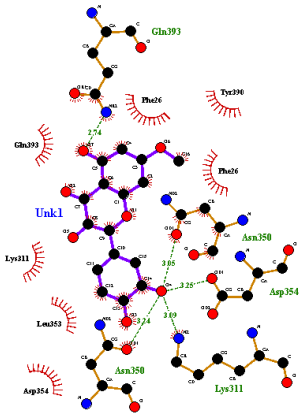

(27)

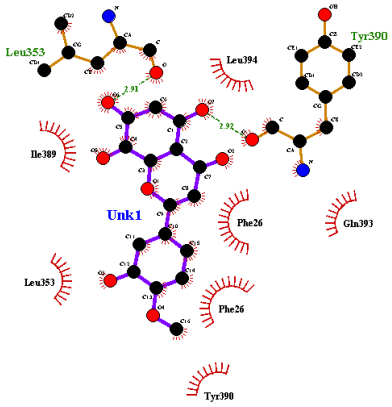

(28)

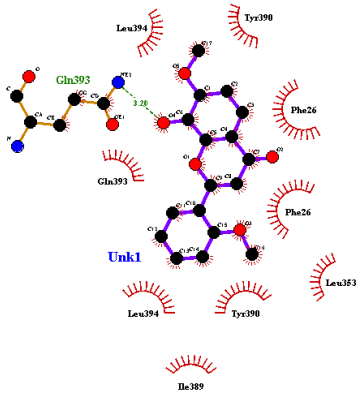

(29)

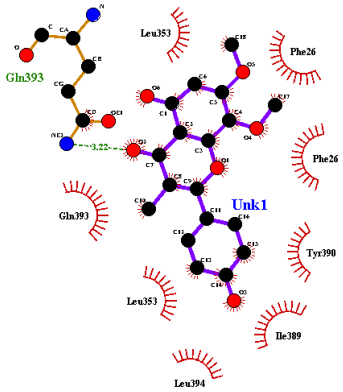

(30)

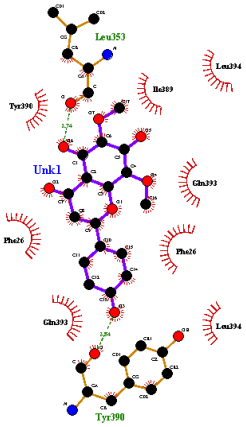

(31)

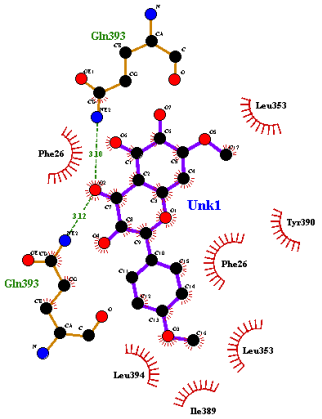

(32)

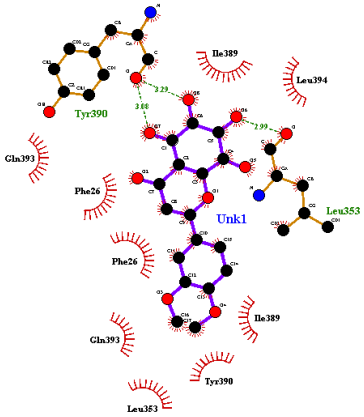

(33)

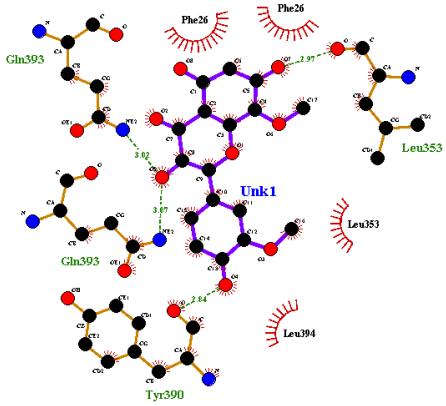

(34)

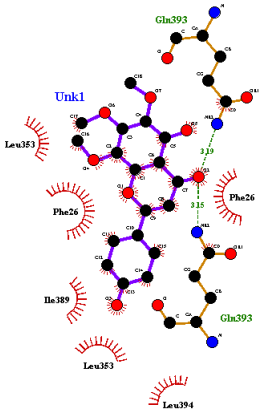

(35)

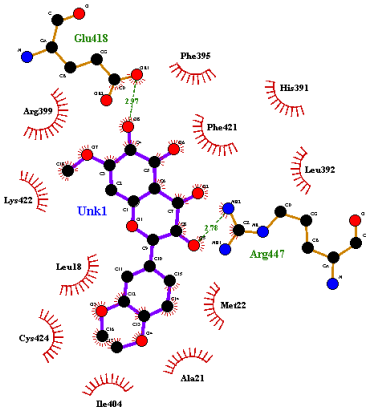

(36)

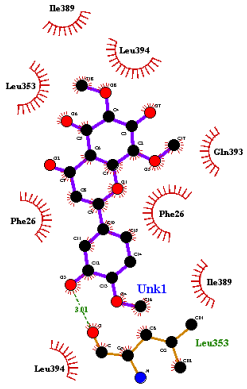

(37)

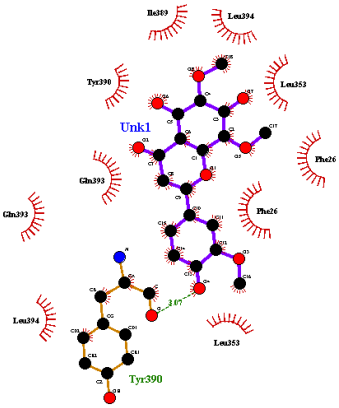

(38)

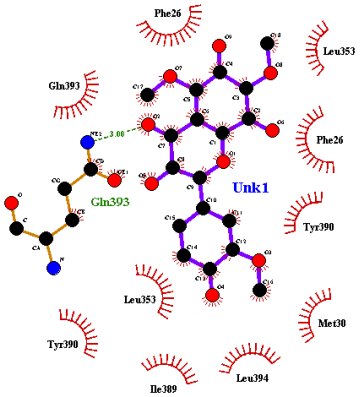

(39)

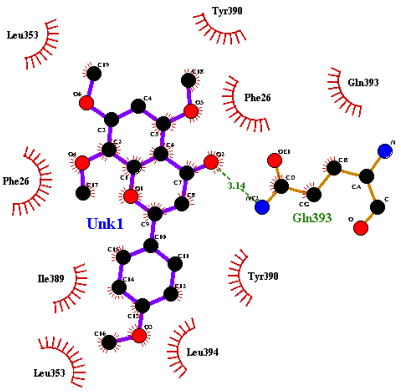

(40)

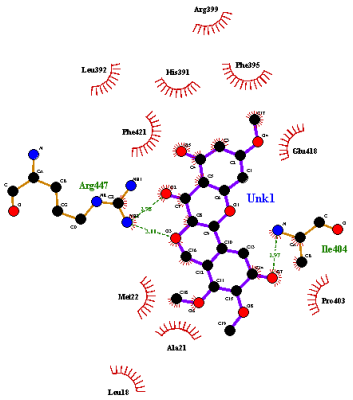

(41)

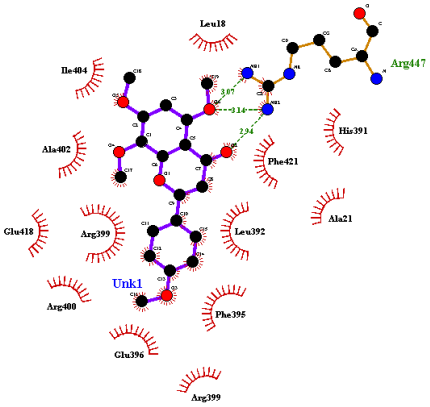

(42)

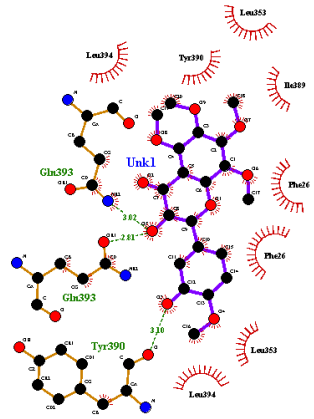

(43)

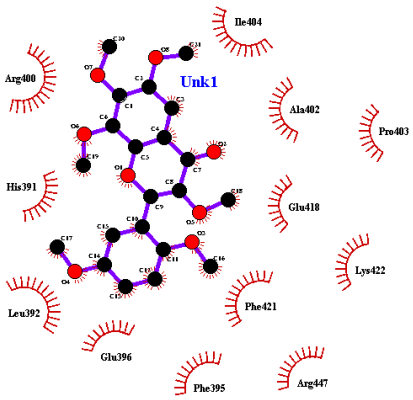

(44)

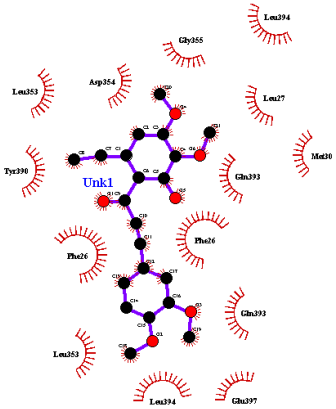

(45)

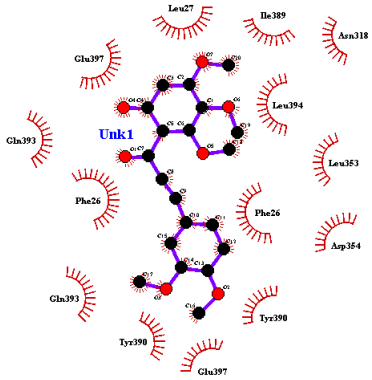

(46)

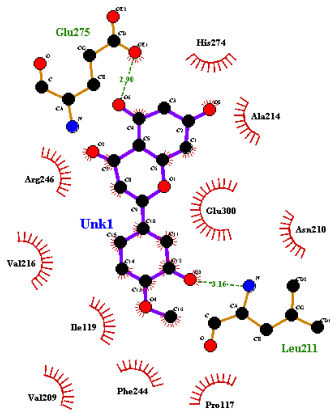

(47)

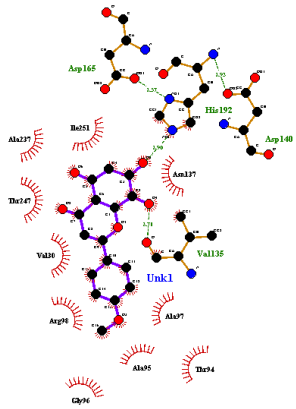

(48)

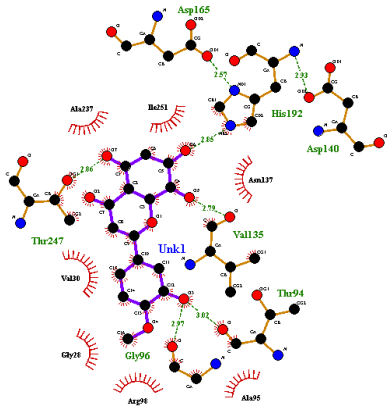

(49)

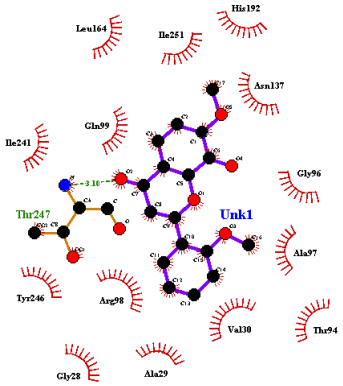

(50)

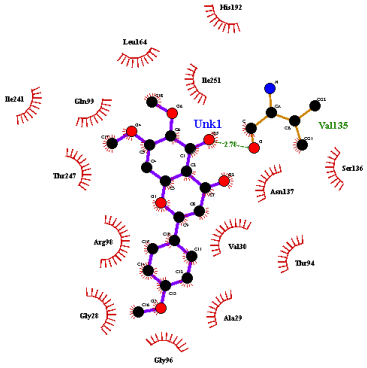

(51)

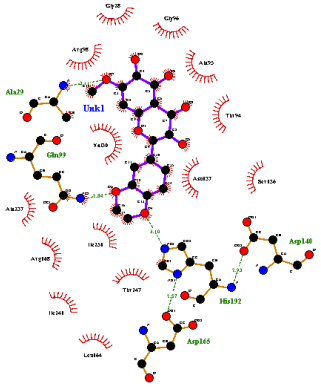

(52)

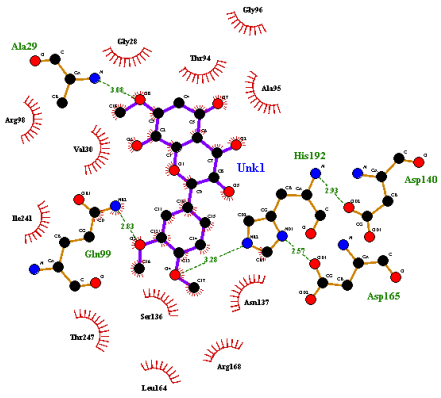

(53)

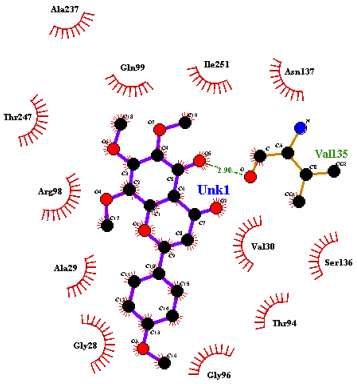

(54)

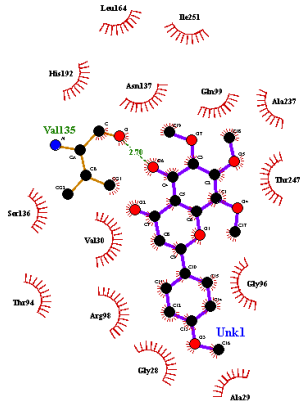

(55)

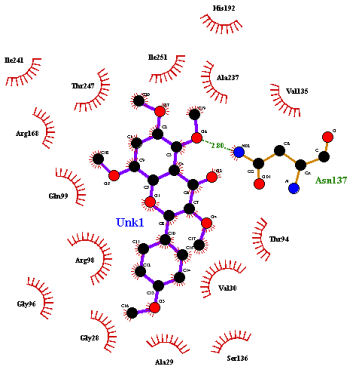

(56)

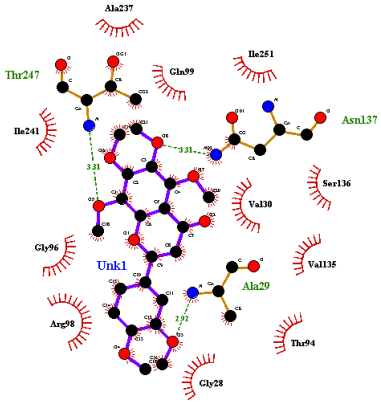

(57)

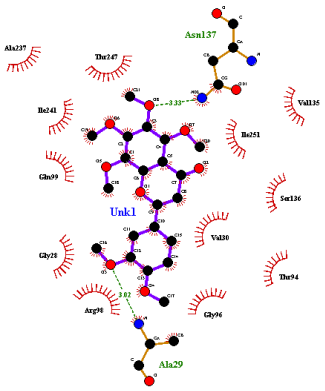

(58)

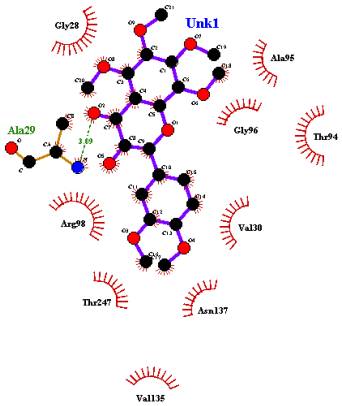

(59)

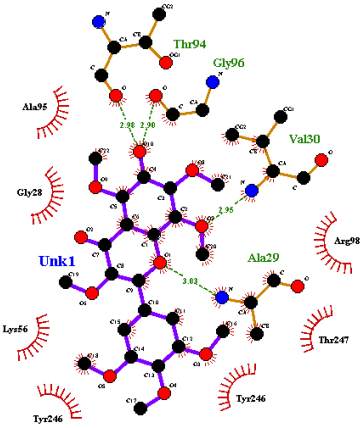

(60)

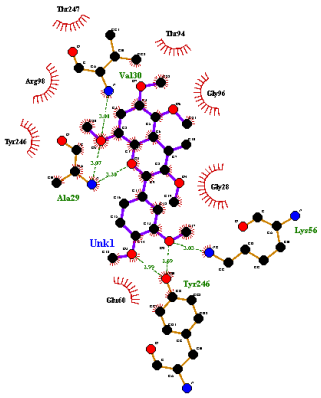

(61)

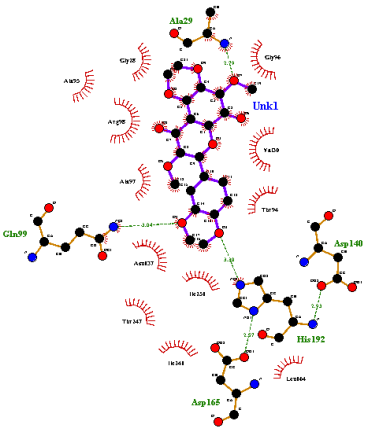

(62)

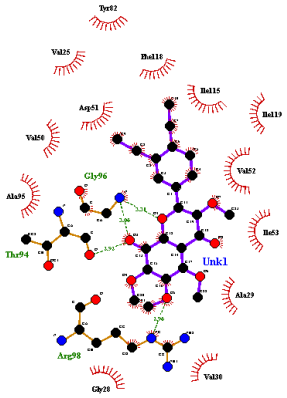

(63)

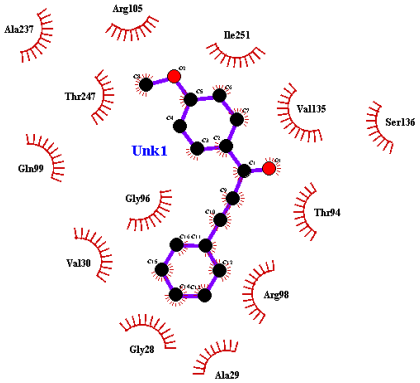

(64)

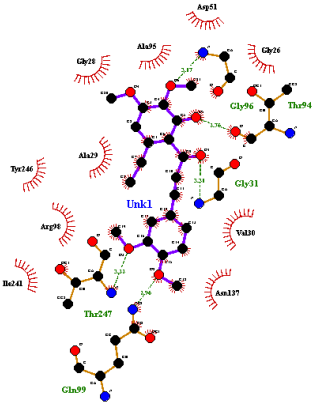

(65)

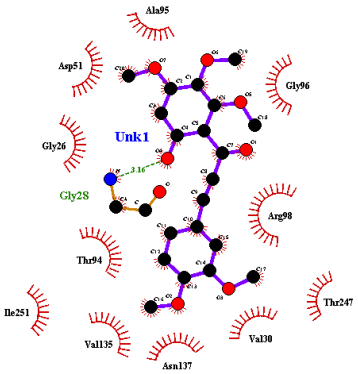

(66)

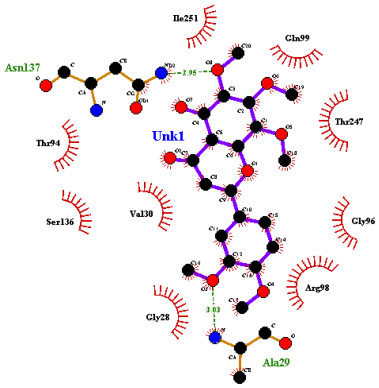

(67)

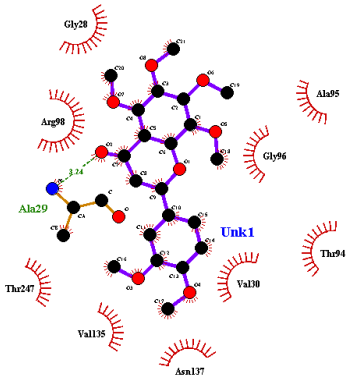

(68)

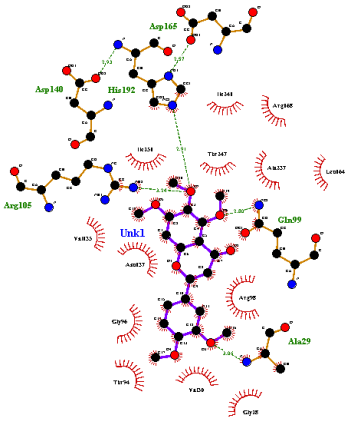

(69)

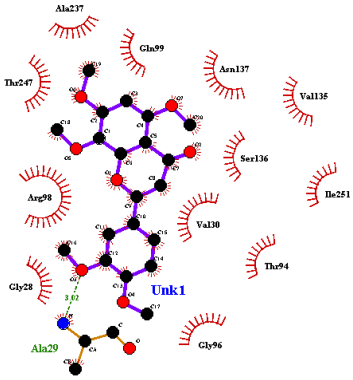

(70)

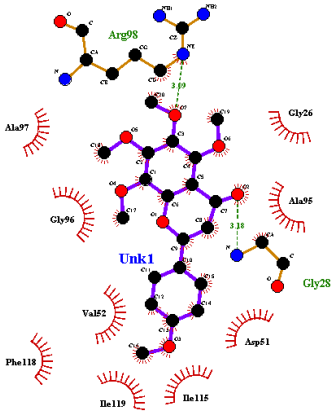

(71)

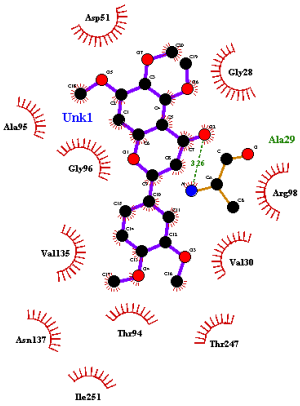

(72)

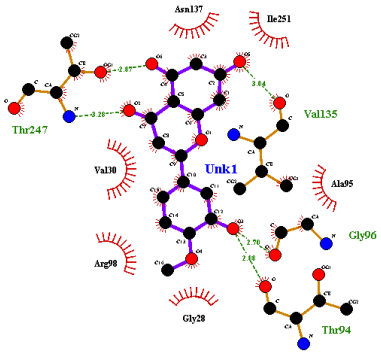

(73)

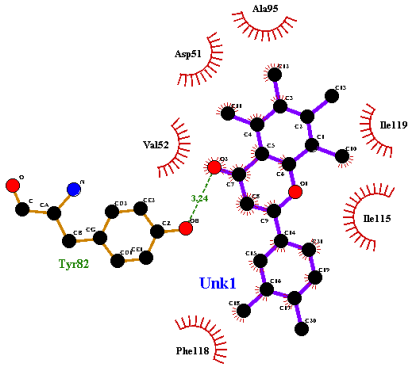

(74)

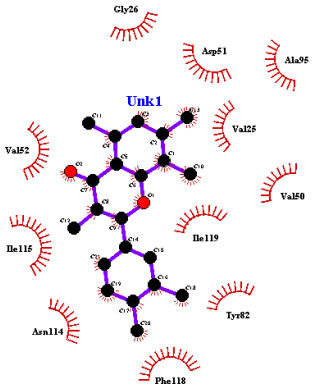

(75)

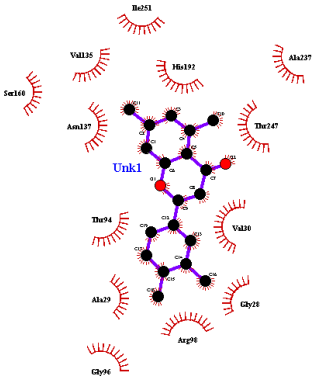

(76)

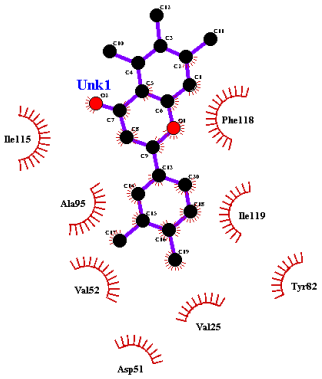

(77)

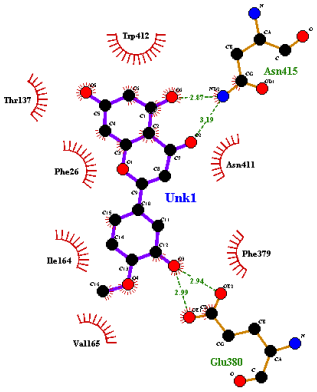

(78)

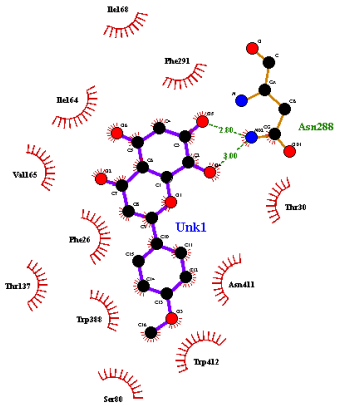

(79)

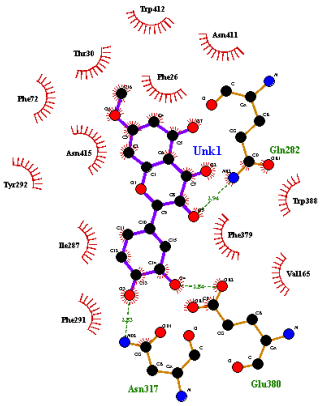

(80)

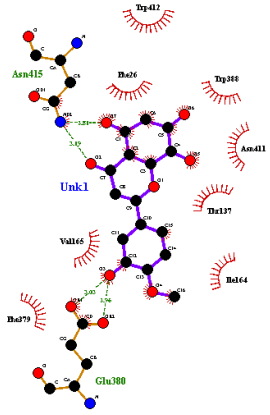

(81)

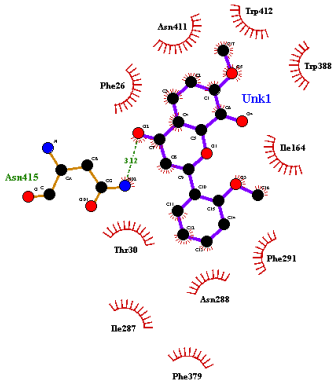

(82)

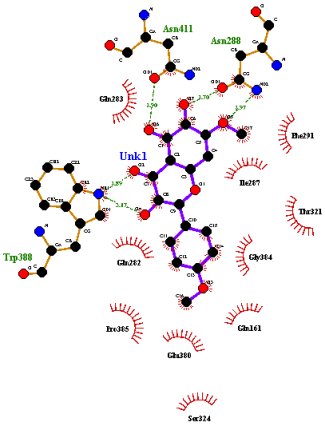

(83)

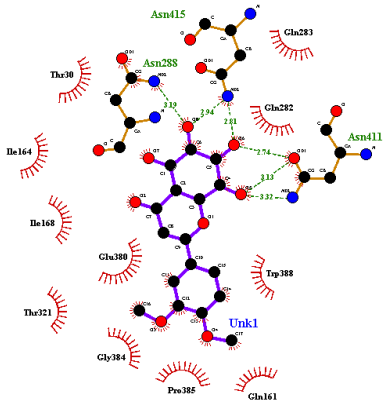

(84)

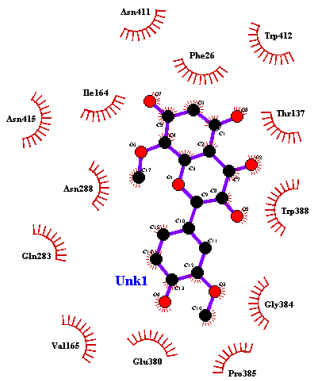

(85)

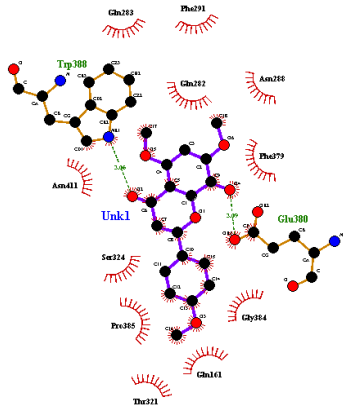

(86)

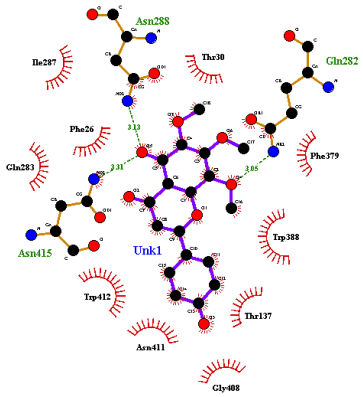

(87)

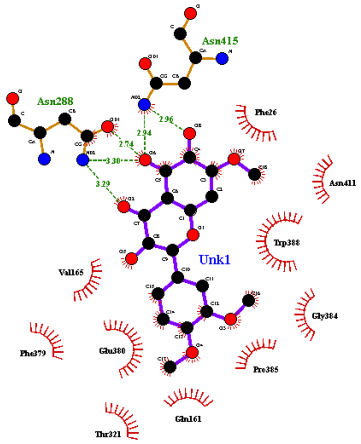

(88)

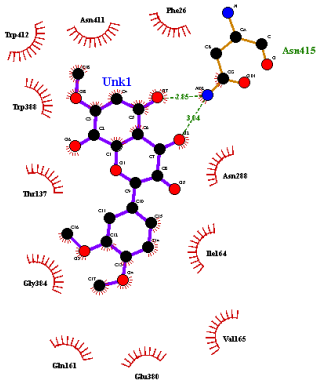

(89)

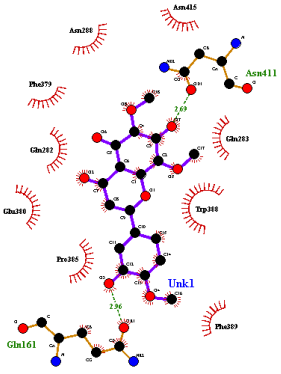

(90)

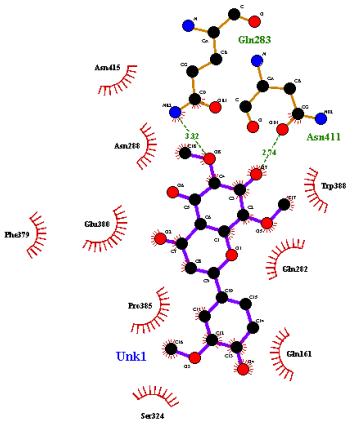

(91)

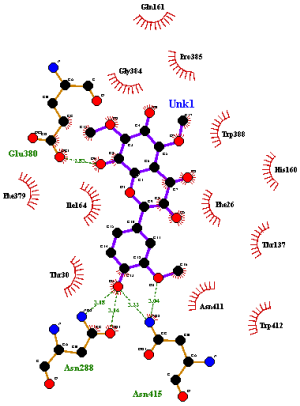

(92)

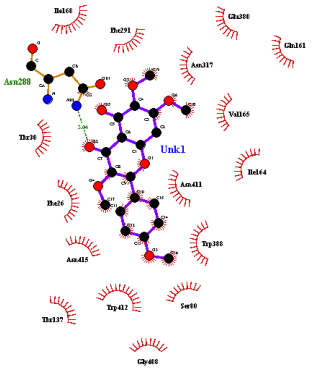

(93)

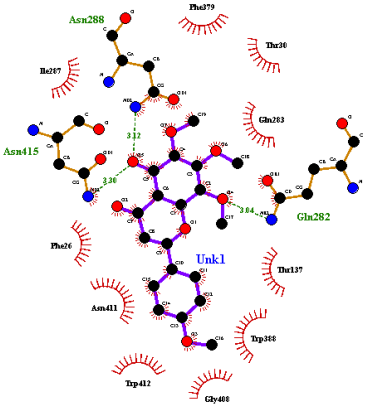

(94)

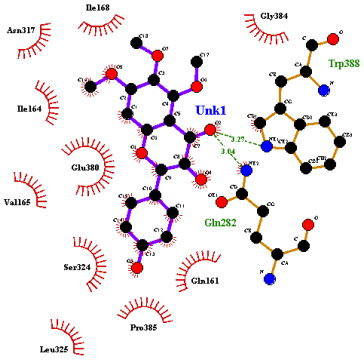

(95)

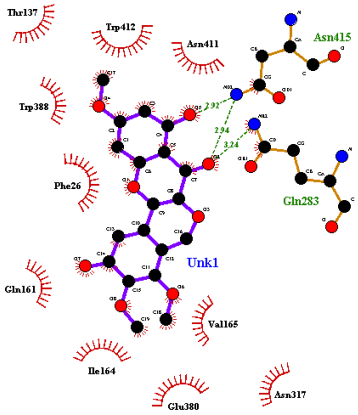

(96)

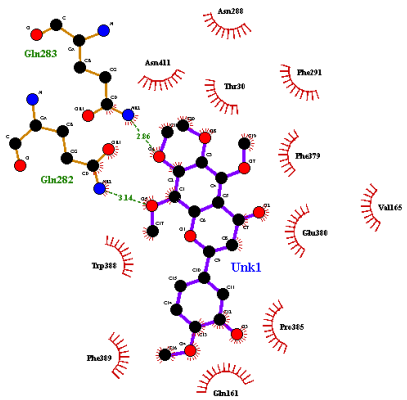

(97)

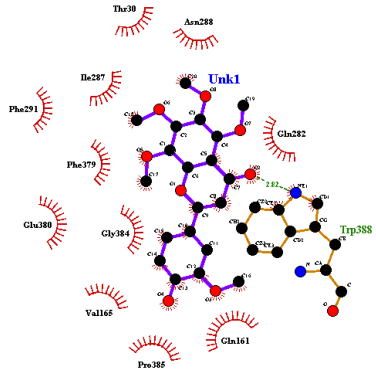

(98)

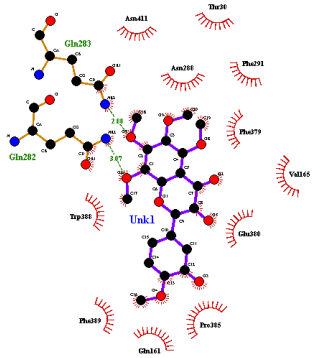

(99)

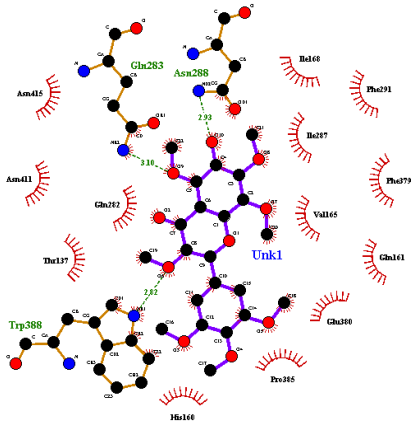

(100)

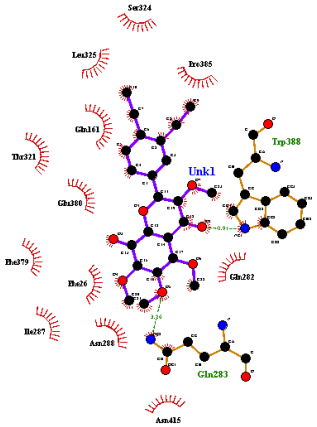

(101)

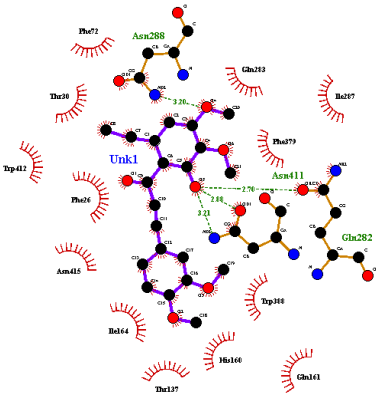

(102)

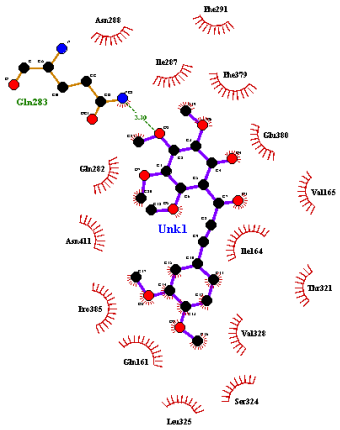

(103)

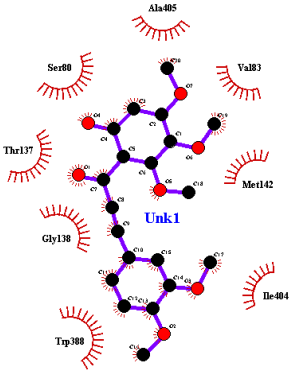

(104)

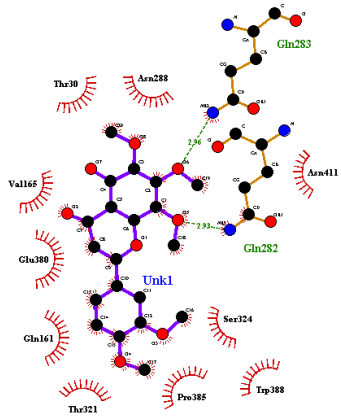

(105)

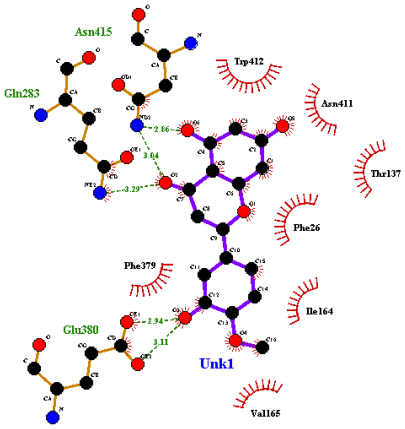

(106)

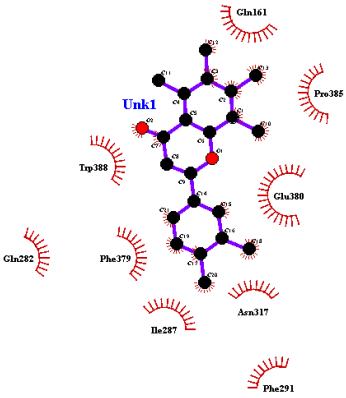

(107)

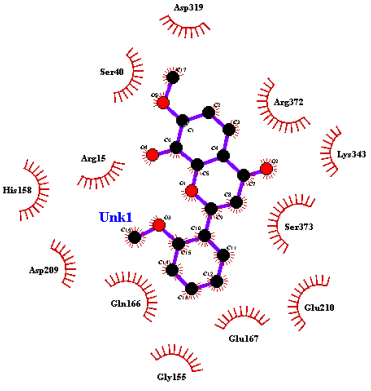

(108)

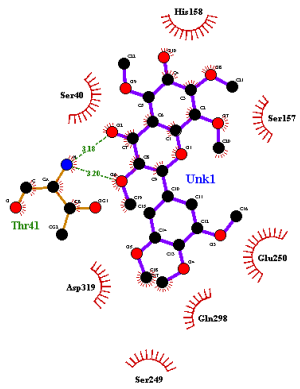

(109)

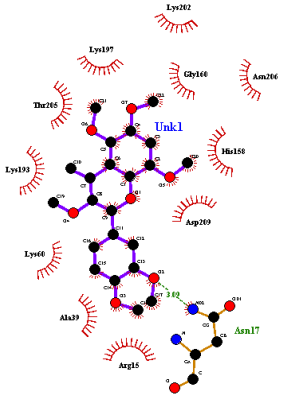

(110)

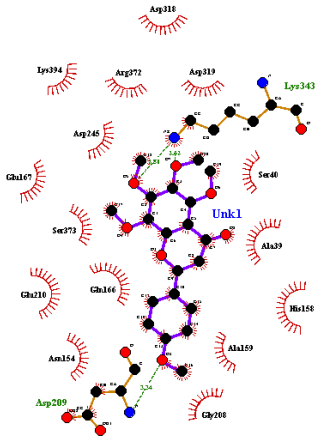

(111)

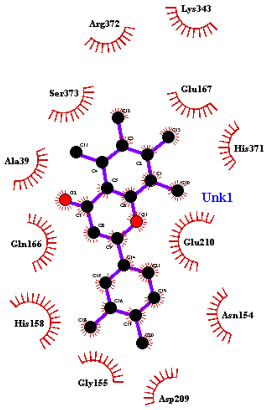

(112)

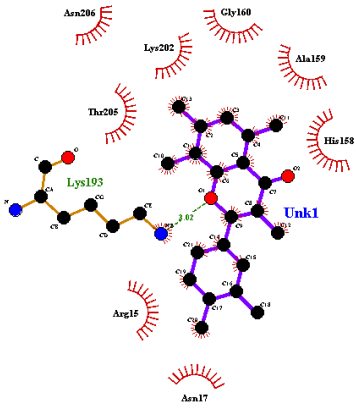

(113)

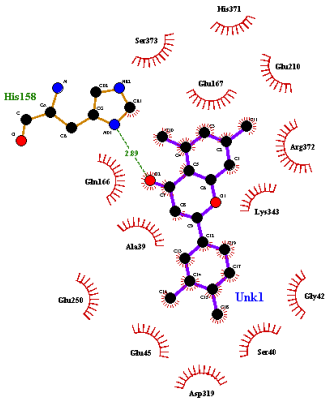

(114)

Figure 4.1: Ligplot showing amino acids of target protein involved in interaction with ligand. The Ligplot+(v.1.4.5) presents interaction profile of lead phytochemicals

and the interface between heterodimers of signaling proteins with lowest binding energy compared to known inhibitors. The amino acid residues involved in the hydrogen bonding as well as hydrophobic interactions are shown in the figure as well as listed below.

(1) Phosphofructokinase2 and ligand 2; **(2)** Phosphofructokinase2 and ligand 3; **(3)** Phosphofructokinase2 and ligand 4; **(4)** Phosphofructokinase2 and ligand 5**; (5)** Phosphofructokinase2 and ligand 9; **(6)** Phosphofructokinase2 and ligand 10; **(7)** Phosphofructokinase2 and ligand 16; **(8)** Phosphofructokinase2 and ligand 17; **(9)** Phosphofructokinase2 and ligand 20; **(10)** Phosphofructokinase2 and ligand 31; **(11)** Hexokinase2 and ligand 2; **(12)** Hexokinase2 and ligand 3; **(13)** Hexokinase2 and ligand 4; **(14)** Hexokinase2 and ligand 7; **(15)** Hexokinase2 and ligand 8; **(16)** Hexokinase2 and ligand 9; **(17)** Hexokinase2 and ligand 10; **(18)** Hexokinase2 and ligand 16; **(19)** Hexokinase2 and ligand 17; **(20)** Hexokinase2 and ligand 18; **(21)** Hexokinase2 and ligand 19; **(22)** Hexokinase2 and ligand 20; **(23)** Hexokinase2 and ligand 31; **(24)** Hexokinase2 and ligand 65; **(25)** Pyruvate kinaseM2 and ligand 1; **(26)** Pyruvate kinaseM2 and ligand 2; **(27)** Pyruvate kinaseM2 and ligand 3; **(28)** Pyruvate kinaseM2 and ligand 4; **(29)** Pyruvate kinase M2 and ligand 5; **(30)** Pyruvate kinaseM2 and ligand 6; **(31)** Pyruvate kinaseM2 and ligand 7; **(32)** Pyruvate kinaseM2 and ligand 8; **(33)** Pyruvate kinaseM2 and ligand 9; **(34)** Pyruvate kinaseM2 and ligand 10; **(35)** Pyruvate kinase M2 and ligand 15; **(36)** Pyruvate kinaseM2 and ligand 16; **(37)** Pyruvate kinaseM2 and ligand 18; **(38)** Pyruvate kinaseM2 and ligand 19; **(39)** Pyruvate kinaseM2 and ligand 20; **(40)** Pyruvate kinaseM2 and ligand 22; **(41)** Pyruvate kinaseM2 and ligand 31; **(42)** Pyruvate kinaseM2 and ligand 33; **(43)** Pyruvate kinaseM2 and ligand 41; **(44)** Pyruvate kinaseM2 and ligand 48; **(45)** Pyruvate kinaseM2 and ligand 55; **(46)** Pyruvate kinaseM2 and ligand 57; **(47)** Pyruvate kinaseM2 and ligand 65; **(48)** Lactate dehydrogenase A and ligand 2; **(49)** Lactate dehydrogenase A and ligand 4; **(50)** Lactate dehydrogenase A and ligand 5; **(51)** Lactate dehydrogenase A and ligand 12; **(52)** Lactate dehydrogenase A and ligand 16; **(53)** Lactate dehydrogenase A and ligand 17; **(54)** Lactate dehydrogenase A and ligand 27; **(55)** Lactate dehydrogenase A and ligand 30; **(56)** Lactate dehydrogenase A and ligand 32; **(57)** Lactate dehydrogenase A and ligand 38; **(58)** Lactate dehydrogenase A and ligand 40; **(59)** Lactate dehydrogenase A and ligand 49; **(60)** Lactate dehydrogenase A and ligand 50; **(61)** Lactate dehydrogenase A and ligand 51; **(62)** Lactate dehydrogenase A and ligand 52; **(63)** Lactate dehydrogenase A and ligand 53; **(64)** Lactate dehydrogenase A and ligand 54; **(65)** Lactate dehydrogenase A and ligand 55; **(66)** Lactate dehydrogenase A and ligand 57; **(67)** Lactate dehydrogenase A and ligand 59; **(68)** Lactate dehydrogenase A and ligand 60; **(69)** Lactate dehydrogenase A and ligand 61; **(70)** Lactate dehydrogenase A and ligand 62; **(71)** Lactate dehydrogenase A and ligand 63; **(72)** Lactate dehydrogenase A and ligand 64; **(73)** Lactate dehydrogenase A and ligand 65; **(74)** Lactate dehydrogenase A and ligand 66; **(75)** Lactate dehydrogenase A and ligand 67; **(76)** Lactate

dehydrogenase A and ligand 68; **(77)** Lactate dehydrogenase A and ligand 69; **(78)** GLUT1 and ligand 1; **(79)** GLUT1 and ligand 2; **(80)** GLUT1 and ligand 3; **(81)** GLUT1 and ligand 4; **(82)** GLUT1 and ligand 5; **(83)** GLUT1 and ligand 8; **(84)** GLUT1 and ligand 9; **(85)** GLUT1 and ligand 10; **(86)** GLUT1 and ligand 13; **(87)** GLUT1 and ligand 15; **(88)** GLUT1 and ligand 16; **(89)** GLUT1 and ligand 17; **(90)** GLUT1 and ligand 18; **(91)** GLUT1 and ligand 19; **(92)** GLUT1 and ligand 20; **(93)** GLUT1 and ligand 25; **(94)** GLUT1 and ligand 27; **(95)** GLUT1 and ligand 29; **(96)** GLUT1 and ligand 31; **(97)** GLUT1 and ligand 37; **(98)** GLUT1 and ligand 39; **(99)** GLUT1 and ligand 41; **(100)** GLUT1 and ligand 50; **(101)** GLUT1 and ligand 53; **(102)** GLUT1 and ligand 55; **(103)** GLUT1 and ligand 56; **(104)** GLUT1 and ligand 57; **(105)** GLUT1 and ligand 59; **(106)** GLUT1 and ligand 65; **(107)** GLUT1 and ligand 66; **(108)** Enolase2 and ligand 5; **(109)** Enolase2 and ligand 50; **(110)** Enolase2 and ligand 51; **(111)** Enolase2 and ligand 63; **(112)** Enolase2 and ligand 66; **(113)** Enolase2 and ligand 67; **(114)** Enolase2 and ligand 68

Table 4.2: Type of interaction between lead methylated-flavonoids (ligand) and PFKB3 protein using Ligplot analysis

S.No.	Protein-ligand	H-bonding	Hydrophobic interaction
1	PFKFB3_ligand2	Thr65, Asn59, Val67, Asp400	Gly71, Val70, Arg98, Ala125, Thr48, Lys47, Pro43
2	PFKFB3_ligand3	Arg74, Asp124, Thr48, Ala44, Lys168, Arg189	Phe87, Gly71, Arg98, Val70, Arg132, Asn127, Ala125, Thr126, Lys47, Pro43
3	PFKFB3_ligand4	Arg189, Thr48, Asp124, Arg132	Tyr193, Asn69, Ala125, Thr126, Arg98, Phe87
4	PFKFB3_ligand5	Asp124, Arg189	Lys168, Thr48, Pro43, Lys47, Thr126, Ala125, Arg98, Val70, Arg74, Phe87, Tyr193
5	PFKFB3_ligand9	Lys168, Thr48, Asp124, Gly71, Arg132, Arg189	Asn69, Thr126, Ala125, Asn127, Arg98, Tyr193, Phe87
6	PFKFB3_ligand10	Arg132, Thr126, Ala44, Thr48, Arg74	Arg98, Val70, Asn127, Ala125, Pro43, Lys47, Lys168, Gly71
7	PFKFB3_ligand16	Arg74, Arg189, Thr48, Lys168	Arg132, Ala125, Val70, Arg98, Phe87, Gly71, Thr126, Lys47, Pro43

8	PFKFB3_ligand17	Arg74, Thr126, Lys168, Thr48	Arg98, Phe87, Arg132, Ala125, Pro43, Lys47, Gly71
9	PFKFB3_ligand20	Arg189, Thr48, Lys168, Arg74	Arg75, Lys47, Asp124, Val70, Arg132, Thr126, Asn127, Ala125, Phe87, Arg98, Gly71
10	PFKFB3_ligand31	Arg75, Thr126, Arg98, Arg74	Thr48, Lys168, Arg189, Lys47, Arg132, Ala125, Phe87, Gly71

Table 4.3: Type of interaction between lead methylated-flavonoids (ligand) and HK2 protein using Ligplot analysis

Sl. No.	Protein_ligand	H-bonding	Hydrophobic interaction
1	HK2_ligand2	Thr536, Ser897	Ile677, Asp861, Asp657, Gly535, Asp352, Arg539, Leu541, Asp895, Gly896
2	HK2_ligand3	Lys866, Thr680, Arg539, Asp532	Glu894, Asp861, Ile677, Gly679, Thr536
3	HK2_ligand4	Thr536, Asp657, Ser897	Asp532, Ile677, Gly896, Asp895, Leu541, Asn557, Lys176, Arg539, Asp861, Gly535
4	HK2_ligand7	Asp657	Lys176, Leu541, Asp895, Arg539, Gly896, Gly898, Asp532, Gly535, Ser897, Asp861
5	HK2_ligand8	Arg539, Glu894, Thr680, Asp532	Lys866, Asp861, Gly862, Ile677, Thr863, Gly679, Gly535, Thr536
6	HK2_ligand9	Thr536, Lys176, Ser897	Asp861, Asp532, Asp657, Ile677, Gly535, Arg539, Glu894, Asp895, Gly896
7	HK2_ligand10	His556, Gly284, Asn557, Arg120	Ser285, Leu286, Asp895, Lys176, Val553, Glu554, Met555
8	HK2_ligand16	Arg539, Glu894, Thr536, Thr680, Asp532	Lys866, Asp861, Asp657, Gly679, Gly535, Thr863, Ile677, Gly862
9	HK2_ligand17	Asp861, Lys866, Thr536,	Gly679, Thr863, Ile677, Gly535,

		Thr680, Asp532, Arg539	Asp657
10	HK2_ligand18	Ser897	Lys176, Leu541, Asp895, Gly896, Arg539, Gly898, Asp532, Gly535, Asp657, Asp861, Asn557, Glu894
11	HK2_ligand19	Gly284, Asn557, His556	Tyr588, Arg120, Met555, Lys176, Val553, Asp895, Leu286, Ser285
12	HK2_ligand20	Arg539, Lys866, Asp861, Thr680, Asp532	Gly896, Thr863, Ile677, Gly679, Thr536, Asp895, Asp657, Gly535
13	HK2_ligand31	Asp532	Asp895, Arg539, Asn557, Gly896, Asp861, Thr863, Gly862, Ser897, Gly535, Asp657
14	HK2_ligand65	Arg539, Thr536, Thr680, Lys866	Asp532, Asp861, Glu894, Gly535, Gly679, Gly862, Ile677, Asp657

Table 4.4: Type of interaction between lead methylated-flavonoids (ligand) and PKM2 protein using Ligplot analysis

Sl. No.	Protein-ligand	H-bonding	Hydrophobic interaction
1	PKM2_ligand1	Leu394, Leu353, Leu353, Tyr390	Gln393, Phe26, Leu394, Phe26
2	PKM2_ligand2	Leu353, Tyr390	Leu394, Phe26, Leu394, Ile389, Phe26, Gln393
3	PKM2_ligand3	Gln393, Asn350, Asp354, Asn350, Lys311	Phe26, Tyr390, Phe26, Asp354, Leu353, Lys311, Gln393
4	PKM2_ligand4	Leu353, Tyr390	Leu394, Gln393, Phe26, Phe26, Tyr390, Leu353, Ile389
5	PKM2_ligand5	Gln393	Leu394, Tyr390, Phe26, Phe26, Leu353, Tyr390, Ile389, Leu394, Gln393
6	PKM2_ligand6	Gln393	Leu353, Phe26, Phe26, Tyr390, Ile389, Leu394, Leu353, Gln393
7	PKM2_ligand7	Leu353, Tyr390	Ile389, Leu394, Gln393, Phe26,

			Leu394, Gln393, Phe26, Tyr390
8	PKM2_ligand8	Gln393, Gln393	Phe26, Leu353, Tyr390, Phe26, Leu353, Ile389, Leu394
9	PKM2_ligand9	Tyr390, Leu353	Ile389, Leu394, Ile389, Tyr390, Leu353, Gln393, Phe26, Phe26, Gln393
10	PKM2_ligand10	Gln393, Gln393, Tyr390, Leu353	Phe26, Phe26, Leu353, Leu394
11	PKM2_ligand15	Gln393, Gln393	Phe26, Leu394, Leu353, Ile389, Phe26, Leu353
12	PKM2_ligand16	Glu418, Arg447	Arg399, Phe395, Phe421, His391, Leu392, Met22, Ala21, Ile404, Cys424, Leu18, Lys422
13	PKM2_ligand18	Leu353	Leu353, Ile389, Leu394, Gln393, Phe26, Ile389, Leu394, Phe26
14	PKM2_ligand19	Tyr390	Ile389, Leu394, Leu353, Phe26, Phe26, Leu353, Leu394, Gln393, Gln393, Tyr390
15	PKM2_ligand20	Gln393	Gln393, Phe26, Leu353, Phe26, Tyr390, Met30, Leu394, Leu353, Ile389, Tyr390
16	PKM2_ligand22	Gln393	Leu353, Tyr390, Phe26, Gln393, Tyr390, Leu394, Leu353, Ile389, Phe26
17	PKM2_ligand31	Arg447, Ile404	Leu392, Phe421, His391, Arg399, Phe395, Glu418, Pro403, Ala21, Met22, Leu18
18	PKM2_ligand33	Arg447	Leu18, His391, Phe421, Ala21, Leu392, Phe395, Arg399, Glu396, Arg400, Arg399, Glu418, Ala402, Ile404
19	PKM2_ligand41	Gln393, Tyr390, Gln393	Leu394, Tyr390, Leu353, Ile389, Phe26, Phe26, Leu353, Leu394
20	PKM2_ligand48	----	Arg400, Ile404, Ala402, Pro403, Glu418, Lys422, Phe421, Arg447, Phe395, Glu396, Leu392, His391

21	PKM2_ligand55	----	Leu353, Asp354, Gly355, Leu394, Leu27, Met30, Gln393, Phe26, Gln393, Glu397, Leu394, Leu353, Phe26, Tyr390
22	PKM2_ligand57	----	Gln393, Glu397, Leu27, Ile389, Asn318, Leu394, Leu353, Phe26, Asp354, Tyr390, Glu397, Tyr390, Gln393, Phe26
23	PKM2_ligand65	Glu275, Leu211	His274, Ala214, Glu300, Asn210, Pro117, Phe244, Val209, Ile119, Val216, Arg246

Table 4.5: Type of interaction between lead methylated-flavonoids (ligand) and LDHA protein using Ligplot analysis

Sl. No.	Protein-ligand	H-bonding	Hydrophobic interaction
1	LDHA_ligand2	Asp165, His192, Asp140, Val135	Asn137, Ala97, Thr94, Ala95, Gly96, Arg98, Val30, Thr247, Ala237, Ile251
2	LDHA_ligand4	Asp165, His192, Asp140, Val135, Thr94, Gly96, Thr247	Ala237, Ile251, Asn137, Ala95, Arg98, Gly28, Val30
3	LDHA_ligand5	Thr247	Ile251, His192, Asn137, Gly96, Ala97, Thr94, Val30, Ala29, Gly28, Arg98, Tyr246, Ile241, Gln99, Leu164
4	LDHA_ligand12	Val135	Ser136, Asn137, Val30, Thr94, Ala29, Gly96, Gly28, Arg98, Thr247, Gln99, Ile241, Leu164, His192, Ile251
5	LDHA_ligand16	Ala29, Gln99, Asp140, His192, Asp165	Arg98, Gly28, Gly96, Ala95, Thr94, Asn137, Ser136, Leu164, Thr347, Ile341, Ile350, Arg165, Ala337, Y1D0
6	LDHA_ligand17	Ala29, His192, Asp140, Asp165, Gln99	Gly28, Thr94, Gly96, Ala95, Asn137, Arg168, Ser136, Leu164, Thr247, Ile241, Val30,

			Arg98
7	LDHA_ligand27	Val135	Ala237, Gln99, Ile251, Asn137, Val30, Ser136, Thr94, Gly96, Gly28, Ala29, Arg98, Thr247
8	LDHA_ligand30	Val135	His192, Leu164, Ile251, Asn137, Gln99, Ala237, Thr247, Gly96, Ala29, Gly28, Arg98, Val30, Thr94, Ser136
9	LDHA_ligand32	Asn137	Ile241, Thr247, Ile251, His192, Ala237, Val135, Arg168, Gln99, Arg98, Gly96, Gly28, Ala29, Val30, Ser136, Thr94
10	LDHA_ligand38	Thr247, Ala29, Asn137	Ala237, Gln99, Ile251, Ser136, Val30, Val135, Thr94, Gly28, Arg98, Gly96, Ile241
11	LDHA_ligand40	Asn137, Ala29	Ala237, Thr247, Val135, Ile251, Ser136, Val30, Thr94, Gly96, Arg98, Gly28, Gln99, Ile241
12	LDHA_ligand49	Ala29	Gly28, Ala95, Gly96, Thr94, Val30, Asn137, Val135, Thr247, Arg98
13	LDHA_ligand50	Thr94, Gly96, Val30, Ala29	Arg98, Thr247, Tyr246, Tyr246, Lys56, Gly28, Ala95
14	LDHA_ligand51	Val30, Lys56, Tyr246, Ala29	Thr94, Gly96, Gly28, Glu60, Tyr246, Arg98, Thr247
15	LDHA_ligand52	Ala29, Asp140, His192, Asp165, Gln99	Ala95, Gly28, Arg98, Ala97, Gly96, Y1D0, Thr94, Asn137, Ile251, Thr247, Ile241, Leu164
16	LDHA_ligand53	Gly96, Thr94, Arg98	Phe118, Ile115, Ile119, Val53, Ile53, Ala29, Val30, Gly28, Ala95, Val50, Asp51, Val25, Tyr82
17	LDHA_ligand54	----	Ala237, Arg105, Thr247, Ile251, Val135, Ser136, Thr94, Arg98, Ala29, Gly28, Val30, Gly96, Gln99

18	LDHA_ligand55	Gly96, Thr94, Gly31, Thr247, Gln99	Val30, Asn137, Ile241, Arg98, Ala29, Tyr246, Gly28, Ala95, Asp51, Gly26
19	LDHA_ligand57	Gly28	Ala95, Gly96, Arg98, Thr247, Val30, Asn137, Val135, Ile251, Thr94, Gly26, Asp51
20	LDHA_ligand59	Asn137, Ala29	Ile251, Gln99, Thr247, Gly96, Arg98, Gly28, Val30, Ser136, Thr94
21	LDHA_ligand60	Ala29	Ala95, Gly96, Thr94, Val30, Asn137, Val135, Thr247, Arg98, Gly28
22	LDHA_ligand61	Asp140, His192, Asp165, Arg105, Gln99, Ala29	Ile241, Arg165, Ile251, Thr247, Ala237, Leu164, Arg98, Gly28, Y1D0, Thr94, Gly96, Asn137, Y135
23	LDHA_ligand62	Ala29	Gly96, Thr94, Val30, Ile251, Ser136, Val135, Asn137, Gln99, Ala237, Thr247, Arg98, Gly28
24	LDHA_ligand63	Arg98, Gly28	Gly26, Ala95, Asp51, Ile115, Ile119, Phe118, Val52, Gly96, Ala97
25	LDHA_ligand64	Ala29	Ala95, Asp51, Gly96, Gly28, Arg98, Val30, Thr247, Thr94, Val135, Asn137, Ile251
26	LDHA_ligand65	Thr247, Gly96, Val135, Thr94	Asn137, Ile251, Ala95, Gly28, Arg98, Val30
27	LDHA_ligand66	Tyr82	Val52, Asp51, Ala95, Ile119, Ile115, Phe118
28	LDHA_ligand67	---	Gly26, Asp51, Ala95, Val25, Val50, Ile119, Tyr82, Phe118, Asn114, Ile115, Val52
29	LDHA_ligand68	---	Asn137, Ser160, Val135, Ile251, His192, Thr247, Ala237, Val30, Gly28, Arg98, Gly96, Ala29, Thr94

30	LDHA_ligand69	---	Phe118, Ile119, Tyr82, Val25, Asp51, Val52, Ala95, Ile115

Table 4.6: Type of interaction between lead methylated-flavonoids (ligand) and GLUT1 protein using Ligplot analysis

Sl No.	Protein-ligand	H-bonding	Hydrophobic interaction
1	GLUT1_ligand1	Asn415, Glu380	Asn411, Phe379, Val165, Ile164, Phe26, Thr137, Trp412
2	GLUT1_ligand2	Asn288	Thr30, Asn411, Trp412, Ser80, Trp388, Thr137, Phe26, Val165, Ile164, Ile168, Phe291
3	GLUT1_ligand3	Gln282, Glu380, Asn317	Trp388, Phe379, Val165, Phe291, Ile287, Tyr292, Asn415, Phe72, Thr30, Trp412, Asn411, Phe26
4	GLUT1_ligand4	Asn415, Glu380	Phe26, Trp412, Trp388, Asn411, Thr137, Ile164, Phe379, Val165
5	GLUT1_ligand5	Asn415	Phe26, Asn411, Trp412, Trp388, Ile164, Phe291, Asn288, Phe379, Ile287, Thr30
6	GLUT1_ligand8	Asn411, Asn288, Trp388	Phe291, Ile287, Thr321, Gly384, Gln161, Glu380, Ser324, Pro385, Gln282, Gln283
7	GLUT1_ligand9	Asn411, Asn415, Asn288	Gln283, Gln282, Trp388, Gln161, Pro385, Gly384, Thr321, Glu380, Ile168
8	GLUT1_ligand10	---	Phe26, Trp412, Thr137, Trp388, Gly384, Pro385, Glu380, Val165, Gln283, Asn288, Ile164, Asn415, Asn411
9	GLUT1_ligand13	Trp388, Glu380	Gln283, Phe291, Gln282, Asn288, Phe379, Gly384, Gln161, Thr321, Pro385, Ser324, Asn411
10	GLUT1_ligand15	Asn288, Gln282, Asn415	Thr30, Phe379, Trp388, Thr137,

			Gly408, Asn411, Trp412, Gln283, Phe26, Ile287
11	GLUT1_ligand16	Asn415, Asn288	Phe26, Asn411, Trp388, Gly384, Pro385, Gln161, Thr321, Glu380, Phe379, Val65
12	GLUT1_ligand17	Asn415	Asn288, Ile164, Val165, Glu380, Gln161, Gly384, Thr137, Trp388, Trp412, Asn411, Phe26
13	GLUT1_ligand18	Asn411, Gln161	Gln283, Trp388, Phe389, Pro385, Glu380, Gln282, Phe379, Asn288, Asn415
14	GLUT1_ligand19	Gln283, Asn411	Trp388, Gln282, Gln161, Ser324, Pro385, Glu380, Phe379, Asn288, Asn415
15	GLUT1_ligand20	Asn288, Asn415, Glu380	Gly384, Gln161, Pro385, Trp388, His160, Phe26, Thr137, Asn411, Trp412, Thr30, Ile164, Phe379
16	GLUT1_ligand25	Asn288	Ile168, Phe291, Asn317, Glu380, Gln161, Val165, Ile164, Asn411, Trp388, Ser80, Gly408, Trp412, Thr137, Asn415, Phe26, Thr30
17	GLUT1_ligand27	Asn288, Asn415, Gln282	Phe379, Thr30, Gln283, Thr137, Trp388, Gly408, Trp412, Asn411, Phe26, Ile287
18	GLUT1_ligand29	Gln282, Trp388	Gly384, Ile168, Asn317, Ile164, Glu380, Val165, Ser324, Leu325, Pro385, Gln161
19	GLUT1_ligand31	Asn415, Gln283	Val165, Asn317, Glu380, Ile164, Gln161, Phe26, Trp388, Thr137, Trp412, Asn411
20	GLUT1_ligand37	Gln283, Gln282	Asn411, Asn288, Thr30, Phe291, Phe379, Glu380, Val165, Pro385, Gln161, Phe389, Trp388
21	GLUT1_ligand39	Trp388	Gln282, Asn288, Thr30, Ile287, Phe291, Phe379, Glu380, Gly384, Val165, Pro385, Gln161

22	GLUT1_ligand41	Gln283, Gln282	Asn411, Thr30, Asn288, Phe291, Phe379, Val165, Glu380, Pro385, Gln161, Phe389, Trp388
23	GLUT1_ligand50	Gln283, Asn288, Trp388	Ile168, Phe291, Ile287, Phe379, Val165, Gln161, Glu380, Pro385, His160, Thr137, Gln282, Asn411, Asn415
24	GLUT1_ligand53	Trp388, Gln283	Gln282, Asn415, Asn288, Ile287, Phe26, Phe379, Gln380, Thr321, Gln161, Leu325, Ser324, Pro385
25	GLUT1_ligand55	Asn288, Asn411, Gln282	Gln283, Ile287, Phe379, Trp388, Gln161, His160, Thr137, Ile164, Asn415, Phe26, Trp412, Thr30, Phe72
26	GLUT1_ligand56	Gln283	Asn288, Ile287, Phe291, Phe379, Glu380, Val165, Ile164, Thr321, Val328, Ser324, Leu325, Gln161, Pro385, Asn411, Gln282
27	GLUT1_ligand57	----	Ala405, Val83, Met142, Ile404, Trp388, Gly138, Thr137, Ser80
28	GLUT1_ligand59	Gln283, Gln282	Asn411, Ser324, Trp388, Pro385, Thr321, Gln161, Glu380, Val165, Thr30, Asn288
29	GLUT1_ligand65	Asn415, Gln283, Glu380	Trp412, Asn411, Thr137, Phe26, Ile164, Val165, Phe379
30	GLUT1_ligand66	---	Gln161, Pro385, Glu380, Asn317, Phe291, Ile287, Phe379, Gln282, Trp388

Table 4.7: Type of interaction between lead methylated-flavonoids (ligand) and ENO protein using Ligplot analysis

Sl. No.	Protein-ligand	H-bonding	Hydrophobic interaction
1	ENO_ligand5	---	Arg372, Lys343, Ser373, Glu210, Glu167, Gly155, Gln166, Asp209, His158, Arg15, Ser40, Asp319

2	ENO _ligand50	Thr41	Glu250, Gln298, Ser249, Asp319, Ser40, His158, Ser157
3	ENO _ligand51	Asn17	Asp209, His158, Asn206, Gly160, Lys202, Lys197, Thr205, Lys193, Lys60, Ala39, Arg15
4	ENO _ligand63	Lys343, Asp209	Ser40, Ala39, His158, Ala159, Gly208, Asn154, Gln166, Gln210, Ser373, Gln167, Asp245, Lys394, Arg372, Asp319, Asp318
5	ENO _ligand66	---	Glu167, His371, Glu210, Asn154, Asp209, Gly155, His158, Gln166, Ala39, Ser373, Arg372, Lys343
6	ENO _ligand67	Lys193	Thr205, Asn206, Lys202, Gly160, Ala159, His158, Asn17, Arg15
7	ENO _ligand68	His158	Ser373, Glu167, His371, Glu210, Arg372, Lys343, Gly42, Ser40, Asp319, Glu45, Glu250, Ala39, Gln166

4.1.2 Surface structure of the protein and ligand interaction

The binding of the ligands with active sites of the targeted protein is also known as the molecular modeling technique. The interaction between the proteins and ligands is determined by the position of the orientation of a ligand when it is bound to the protein. The surface structure of the protein and ligand determined through the pymol software after the modified pdbqt files of proteins and ligands was prepared. The surface structure showed the interaction between the proteins and ligands. The phytochemicals have a high affinity of binding to the targeted protein which resulted into a change in the conformation of the targeted proteins. In the high binding affinity of the interaction between the protein and the ligand complex which increased the greater intermolecular force between the ligands and its proteins as well as high-affinity binding resulted in the higher degree of occupancy for the ligand as its protein binding sites. The following is the surface structure of the targeted proteins and the best lead compounds:

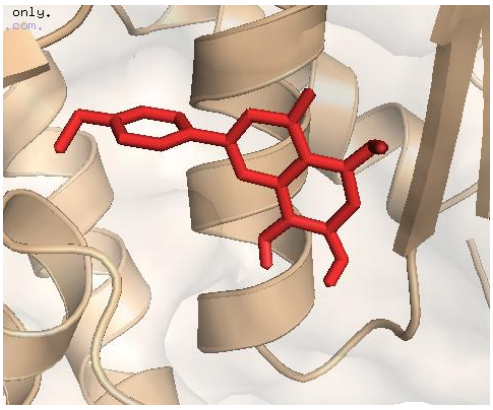

(1)

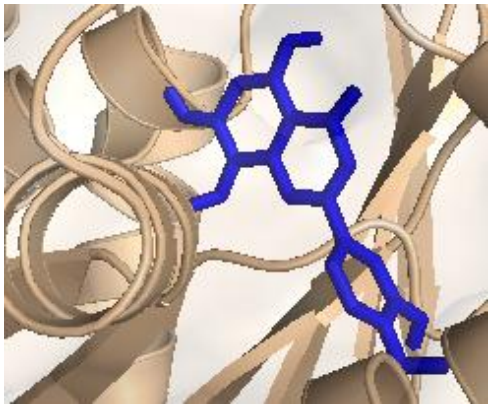

(2)

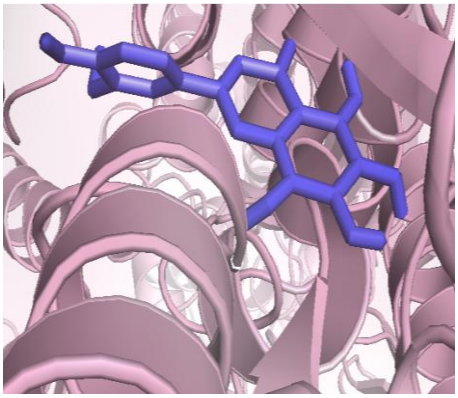

(3)

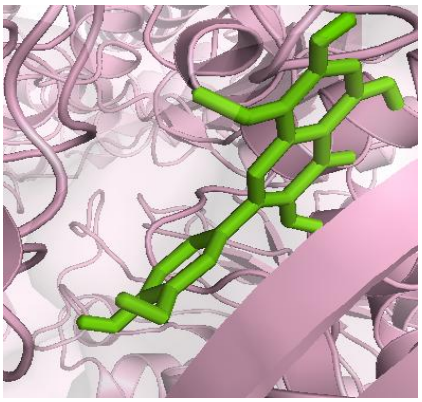

(4)

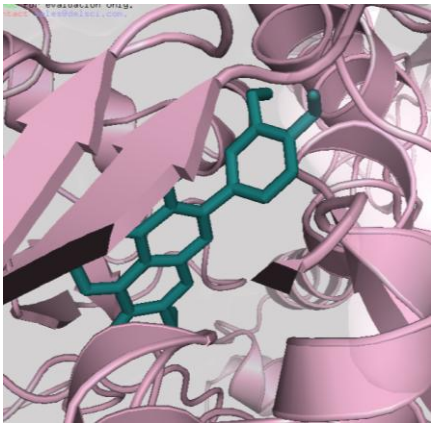

(5)

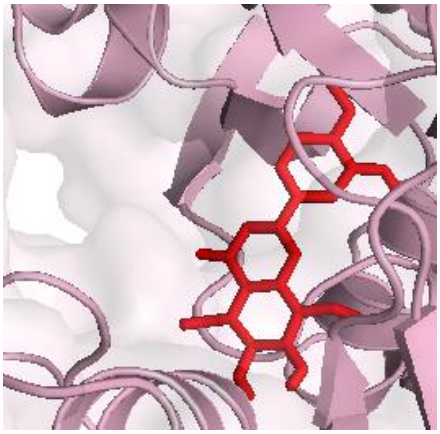

(6)

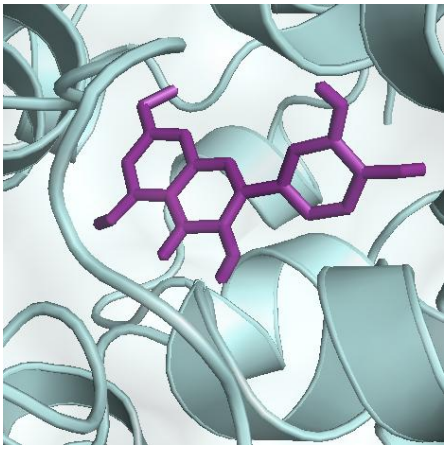

(7)

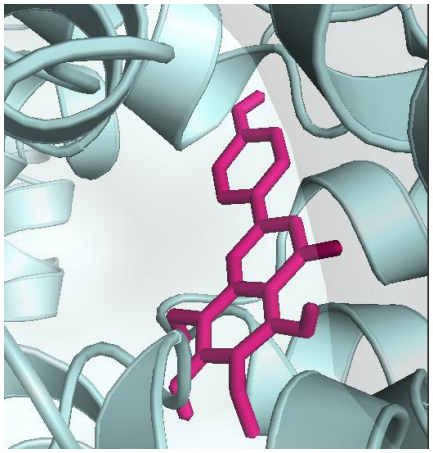

(8)

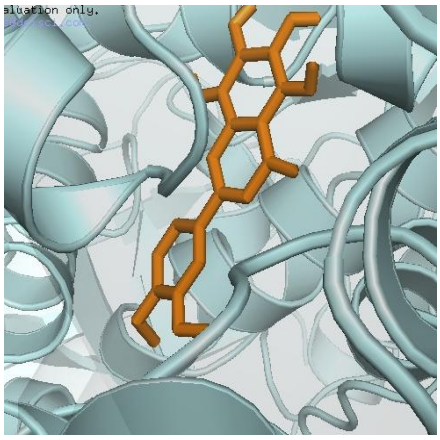

(9)

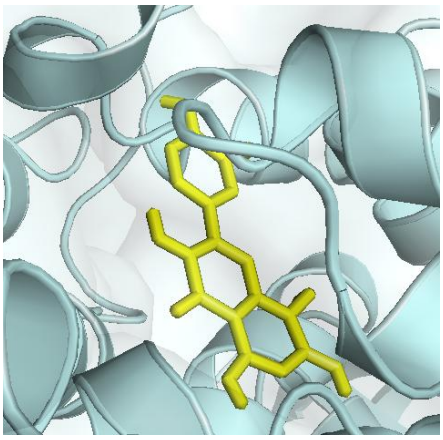

(10)

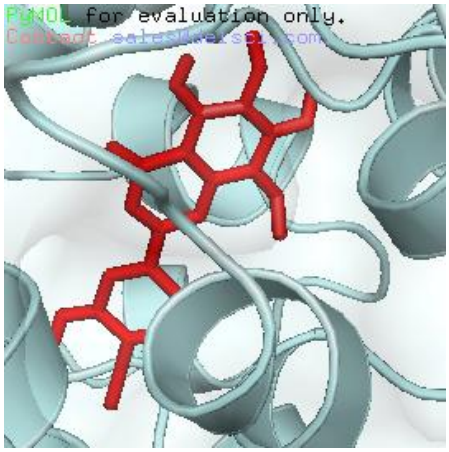

(11)

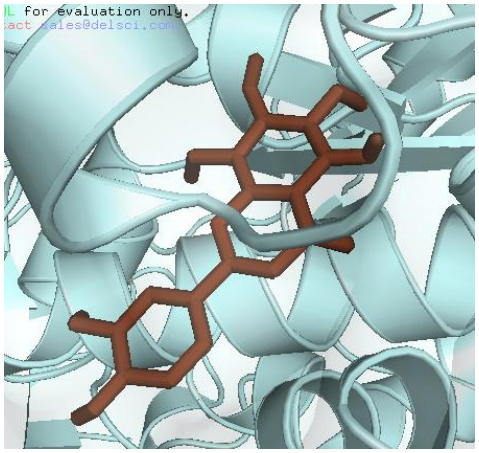

(12)

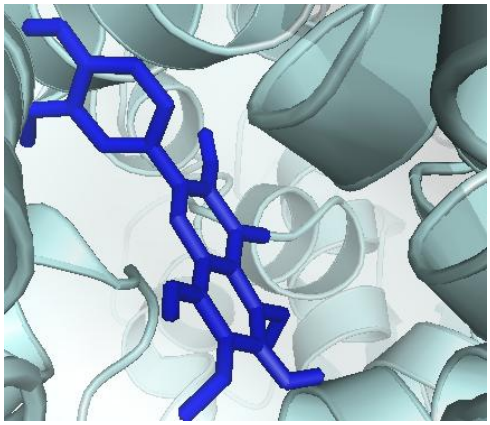

(13)

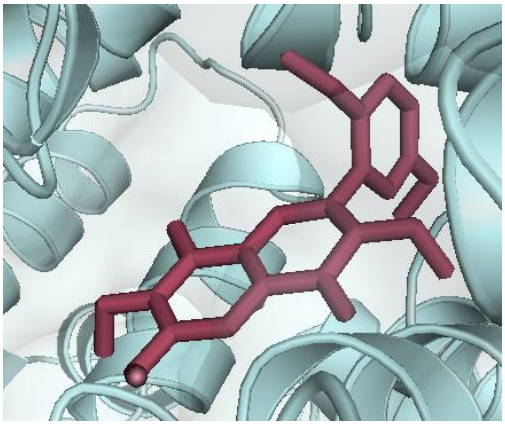

(14)

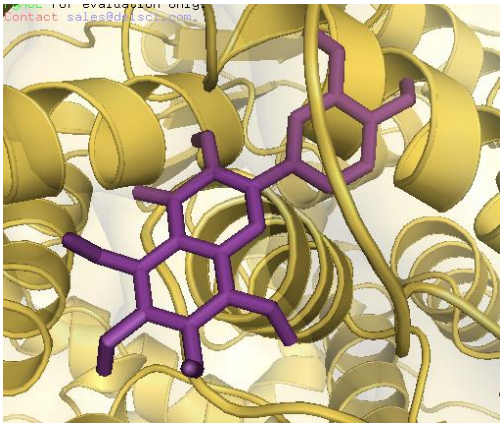

(15)

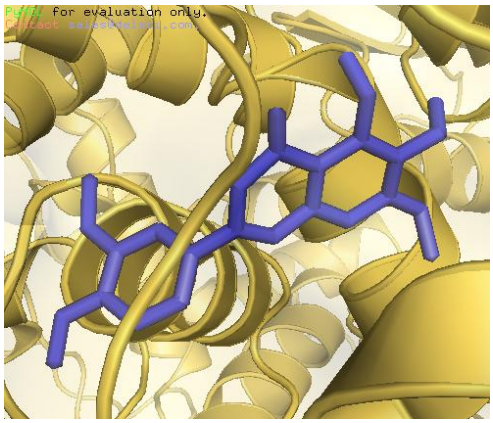

(16)

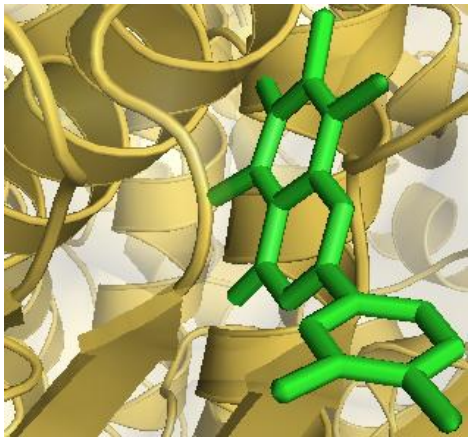

(17)

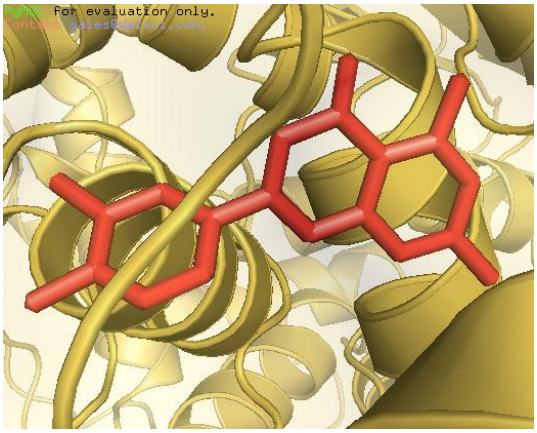

(18)

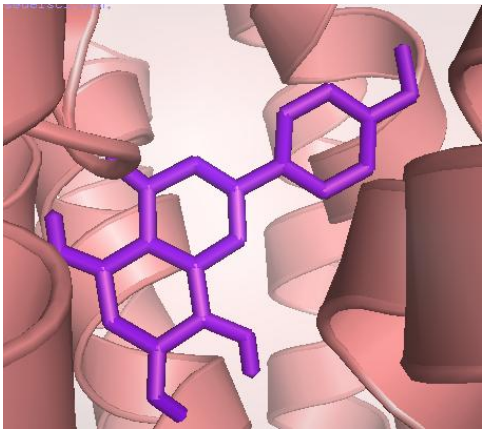

(19)

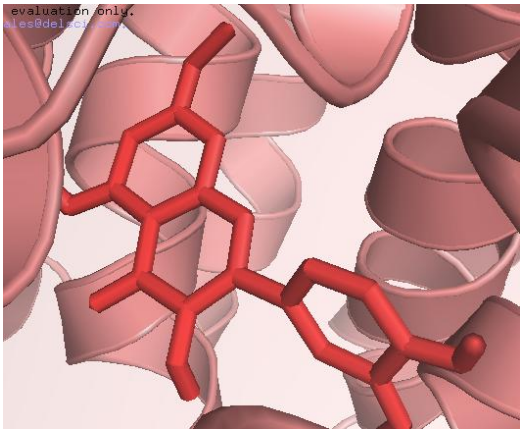

(20)

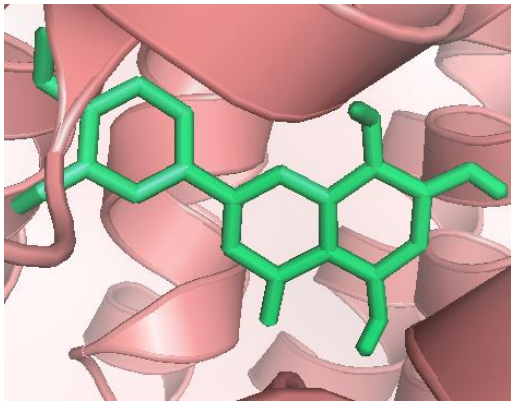

(21)

(22)

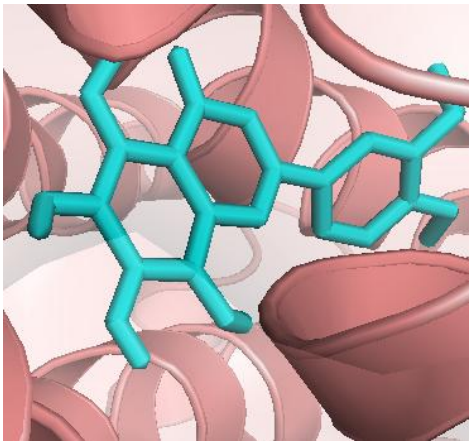

(23)

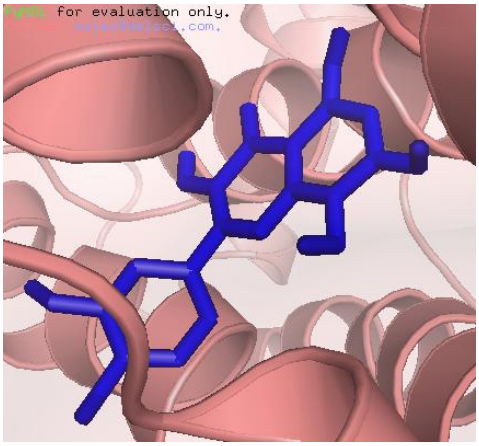

(24)

(25)

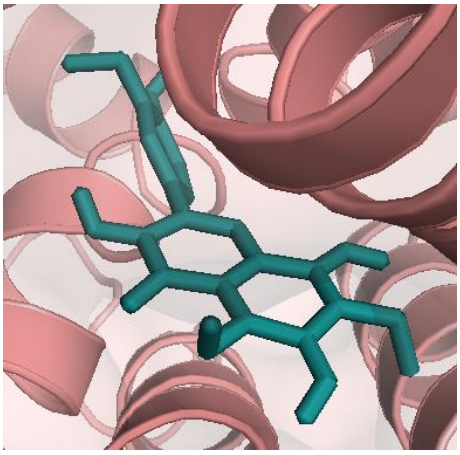

(26)

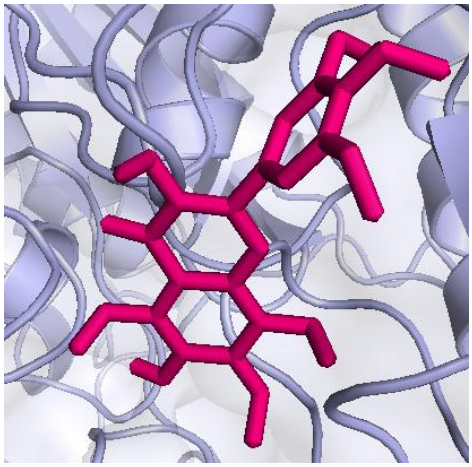

(27)

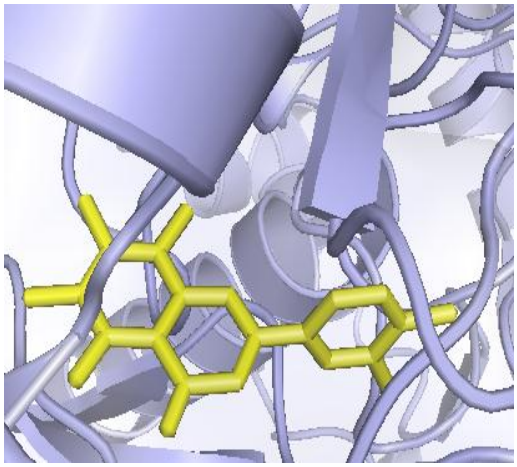

(28)

Figure 4.2(1-28): Binding site and pattern of lead ligands against different target protein

(1) Phosphofructokinase and ligand 2; **(2)** Phosphofructokinase and ligand 4; **(3)** Hexokinase2 and ligand 9; **(4)** Hexokinase2 and ligand 10; **(5)** Hexokinase2 and ligand 16; **(6)** Hexokinase2 and ligand 18; **(7)** Pyruvate kinaseM2 and ligand 3; **(8)** Pyruvate kinase M2 and ligand 7; **(9)** Pyruvate kinaseM2 and ligand 9; **(10)** Pyruvate kinase M2 and ligand 10; **(11)** Pyruvate kinaseM2 and ligand 18; **(12)** Pyruvate kinase M2 and ligand 19; **(13)** Pyruvate kinase M2 and ligand 20; **(14)** Pyruvate kinase M2 and ligand 48; **(15)** Lactate DehydrogenaseA and ligand 49; **(16)** Lactate DehydrogenaseA and ligand 61; **(17)** Lactate DehydrogenaseA and ligand 66; **(18)** Lactate Dehydrogenase2 and ligand 68; **(19)** GLUT1 and ligand 2; **(20)** GLUT1 and ligand 3; **(21)** GLUT1 and ligand 4; **(22)** GLUT1 and ligand 8; **(23)** GLUT1 and ligand 9; **(24)** GLUT1 and ligand 10; **(25)** GLUT1 and ligand 16; **(26)** GLUT1 and ligand 20; **(27)** Enolase2 and ligand 50; **(28)** Enolase2 and ligand 66

4.2 *In vitro* anticancer potential of Compound 003 by using MTT assay

The MTT assay was performed against colon cancer cell lines (HT29). For the evaluation of cytotoxicity, the readings were plotted in graph form. The percentage inhibitions were taken on Y-axis versus control and sample with different concentrations on X-axis. The microplate readings were converted into the percentage inhibition and plotted with control as 100% viable cells. The treatment sample showed dose-dependent moderate antiproliferative efficacy at 100nM, 500nM, 1uM, 50μM and 100μM dose against the given cell lines. At 60μM concentration, the drug inhibits about 53% growth of cells after 72 hours of incubation.

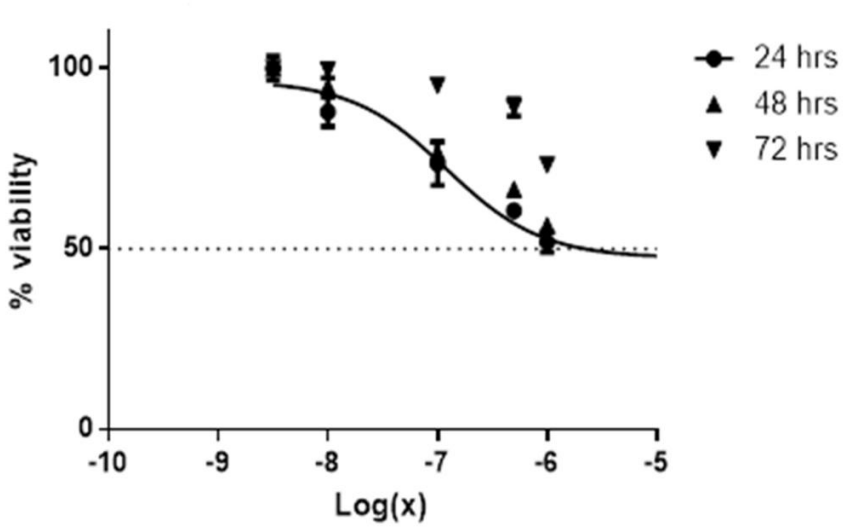

Figure 4.3: MTT assay showing compound 003 treatment against HT29 cell lines

4.3 *In vitro* antioxidant activity assay: DPPH radical scavenging activity

The antioxidant activity of Compound A was measured at different concentrations by using DPPH assay and compared with the standard antioxidant compound. The result showed the percentage inhibition of the sample to be about in the range of 75-85%. The results also showed that with increasing concentration of the sample, the absorbance got decreased and the color of the solution became brighter yellow.

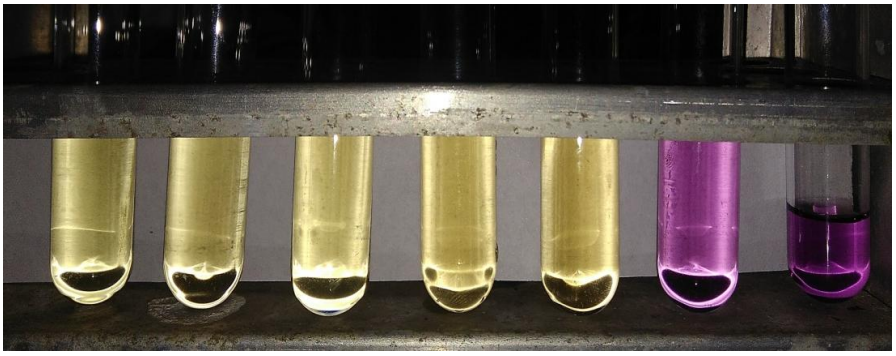

Figure 4.4: DPPH assay showing antioxidant activity

4.4 Antibacterial assay: Disk diffusion method

The antimicrobial activity of the compound A was determined using disk diffusion method. The plates containing penicillin as positive control showed less zone of inhibition whereas the plate containing norfloxacin as positive control showed maximum zone of inhibition. The test sample did not show any antibacterial activity.

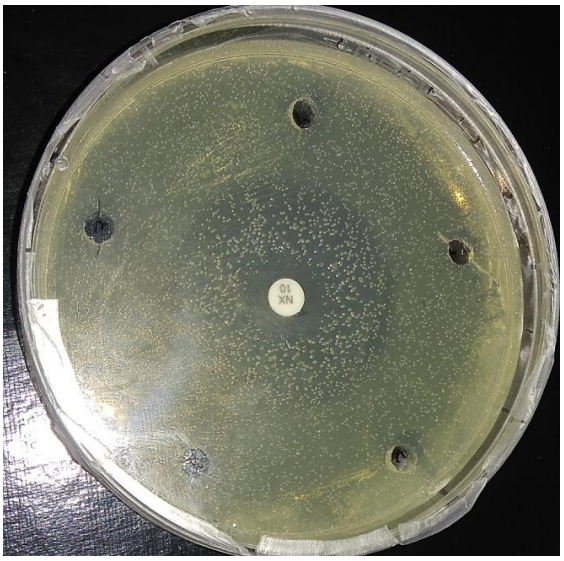

(A)

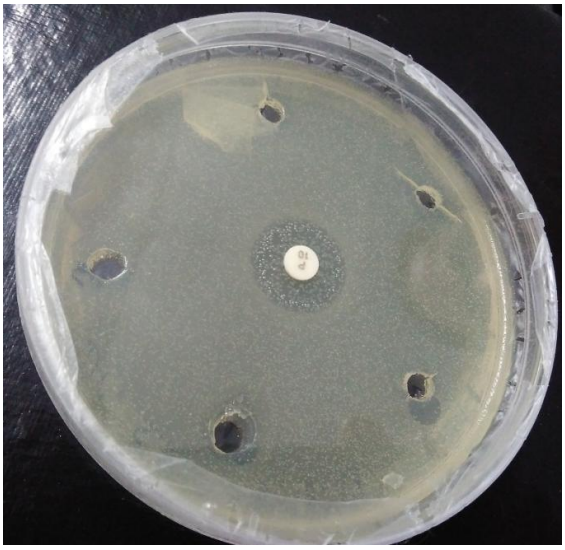

(B)

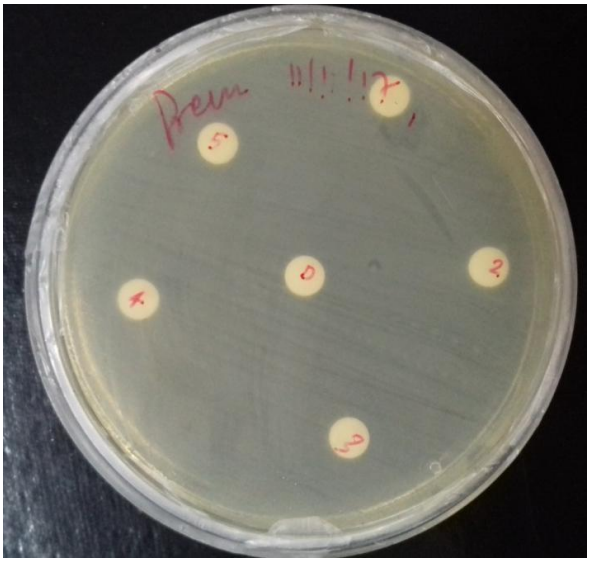

(C)

Figure 4.5: Disk diffusion method **(A)** Plates having norfloxacin as positive control; **(B)** Plates having penicilin as positive control; **(C)** Plates containing drugs and DMSO as negative control

4.5 Discussion

The elevated levels of aerobic glycolysis in cancer cells which causes generation of ATP as the major energy supplier for cells have led to the invention of 'Warburg effect' which is considered to be a prominent cause for malignant transformation through metabolic changes. Our study explores the potential of various phytochemicals (methylated flavonoids) to inhibit the different glycolytic enzymes in cancer cells. The targeted proteins such as glucose transporter 1(GLUT1), hexokinase 2 (HK2), phosphofructokinase2 (PFKFB3), pyruvate kinase M2 (PKM2), lactate dehydrogenase A (LDHA) and enolase (ENO) are the key proteins involved in the glycolysis pathway. The present study revealed that the methylated flavonoids are able to bind to these proteins and inhibit their activity or function.

GLUT family of transporters play the major role of glucose uptake by the cells. The predominance of the GLUT1 isoform in cancer cells is basically related to its nature of irreversibility and high affinity for glucose. There are reports where novel small molecule inhibitors have been studied to target the GLUT1 protein for restricting

glucose uptake by the cells. A novel small molecule, WZB117, has been studied to kill lung and breast cancer cells by inhibiting GLUT1-mediated glucose transport. WZB117 inhibits uptake of the non-metabolizable sugar, 3-o-methylglucose by RBCs and is a competitive inhibitor of GLUT1-mediated zero-trans sugar uptake and exchange transport but is a non-competitive inhibitor of zero-trans exit. This molecule binds at or near the exofacial sugar-binding site of GLUT1 (Ojelabi *et al.* 2016). In the present study, we found that the methylated flavonoids have the potential to inhibit the GLUT1 protein. Results showed that the lead phytochemical 2-(3,4-dihydroxyphenyl)-3,5-dihydroxy-7-methoxy-4H-chromen-4-one inhibits GLUT1 with 228.30% efficacy in comparison to the standard inhibitor. Hexokinase performs chiefly the phosphorylation of glucose to glucose-6-phosphate with the transfer of phosphate from ATP. Amongst all other isoforms of hexokinase, HK2 isoform is found overexpressed in cancer cells because it exists bound to mitochondria in a VDAC-dependent manner which provides access to ATP and entrapment of glucose by cells. Reports have confirmed Benserazide, an FDA-approved decarboxylase inhibitor for adjuvant treatment of Parkinson's disease to suppress tumor growth by inhibiting HK2. According to various studies, the pyrogallol moieties of Benserazide occupied the glucose-binding pocket through H-bond interactions and adopted a similar conformation of the substrate glucose and thus competitively inhibit it (Li *et al*., 2017). In the present study we found that the methylated flavonoids have potential to inhibit HK2 protein. Results showed that the lead phytochemical 5,7-dihydroxy-2-(3-hydroxy-4-methoxyphenyl)-6,8-dimethoxy-4H-chromen-4-one inhibits HK2 with 90.5% efficacy in comparison to the standard inhibitor. PFKFB are a family of homodimeric enzymes catalyzing the conversion of fructose-6-phosphate to fructose-2,6-bisphosphate involving ATP-dependent phosphorylation. The isoform PFKFB3 is chiefly seen to be predominant in cancer cells because of its high PFK2 (phosphorylation) activity and almost no FBPase (de-phoshorylation) activity. Studies have been done to find PFK15 (1-(4-pyridinyl)-3-(2-quinolinyl)-2-propen-1-one), as an inhibitor of PFKFB3, against gastric cancer. Results showed that PFK15 retarded the proliferation leading to cell cycle arrest by blocking signaling pathways. Thus, PFK15 has been established to be a promising anti-cancer drug by targeting aerobic glycolysis (Zhu *et*

al., 2016). In the present study, we found that the methylated flavonoids have the potential to inhibit the PFKFB3 protein. Results showed that the lead phytochemical 2-(3,4-dihydroxyphenyl)-3,5-dihydroxy-7-methoxy-4H-chromen-4-one inhibits PFKFB3 protein with 223.82% efficacy in comparison to the standard inhibitor. The enzyme pyruvate kinase catalyzes the dephosphorylation of phosphoenolpyruvate (PEP) into pyruvate producing ATP in the process. Amongst all the isoforms, PKM2 isoform is predominant in cancer cells because it promotes tumor angiogenesis in cooperation with HIF-1 that transactivates the associated genes. Reports have revealed that the natural products, such as Shikonin and its analog alkannin, belonging to a family of necroptotic inducers, displayed potent and promising selective inhibition of PKM2 by not inhibiting PKM1 and PKL (Wong *et al*., 2013). In the present study, we found that the methylated flavonoids have potential to inhibit the PKM2 protein. Results showed that the lead phytochemical 5,7-dihydroxy-2-(3-hydroxy-4-methoxyphenyl)-6,8-dimethoxy-4H-chromen-4-one inhibits PKM2 with 134.31% efficacy in comparison to the standard inhibitor. Lactate dehydrogenase plays the major role in the reduction of pyruvate into lactate and the oxidation of NADH into NAD^+. The overexpression of LDHA isoform in cancer cells is primarily because of its higher affinity for pyruvate. Studies have shown 3-dihydroxy-6-methyl-7-(phenylmethyl)-4-propylnaphthalene-1-carboxylic acid (FX11), a selective inhibitor (competitive in nature) to inhibit LDHA, through screening a varied number of compounds obtained from gossypol, a natural compound and a known malarial LDH inhibitor. FX11 induced oxidative stress and cell senescence *in vitro*, which led to progression inhibition of human lymphoma and pancreatic cancer xenografts *in vivo* (Miao *et al*., 2013). In the present study, we found that the methylated flavonoids have potential to inhibit LDHA protein. Results showed that the lead phytochemical 2-(3,4-dimethylphenyl)-5,7-dimethyl-4H-chromen-4-one inhibits LDHA with 95.2% efficacy in comparison to the standard inhibitor.

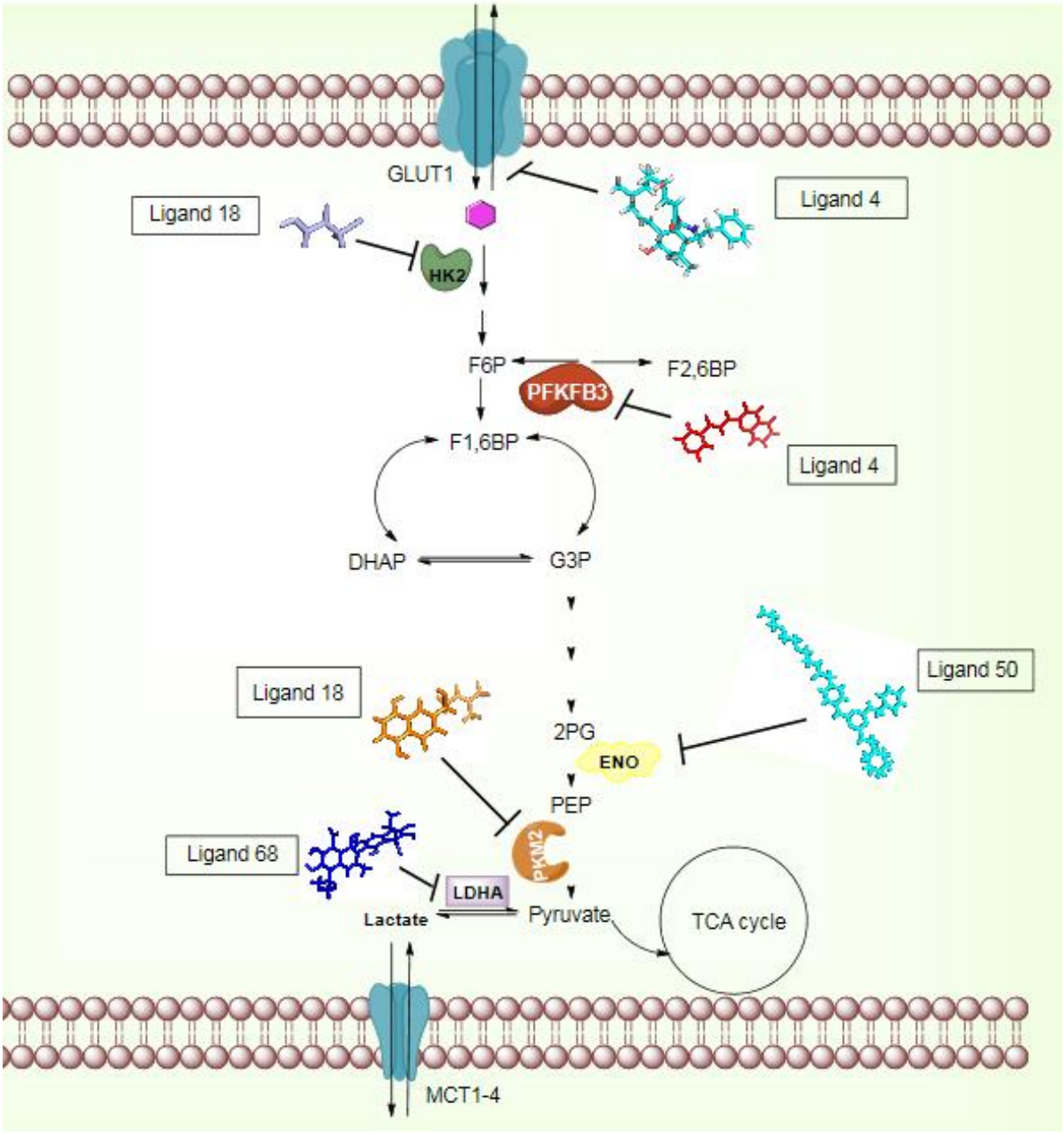

Figure 4.6: Anti-cancer targets in cancer cell carbohydrate metabolic pathway and the lead methylated flavonoid against them

Ligand 4: 2-(3,4-dihydroxyphenyl)-3,5-dihydroxy-7-methoxy-4H-chromen-4-one; **Ligand 18**: 5,7-dihydroxy-2-(3-hydroxy-4-methoxyphenyl)-6,8-dimethoxy-4H-chromen-4-one; **Ligand 50**: 6-hydroxy-3,5,7,8-tetramethoxy-2-(3,4,5-trimethoxyphenyl)-4H-chromen-4-one; **Ligand 68**: 2-(3,4-dimethylphenyl)-5,7-dimethyl-4H-chromen-4-one

Enolase enzyme is chiefly concerned with the conversion of 2-phosphoglycerate to phosphoenolpyruvate. ENO's biochemical, proteomics and immunological characterization and its capability to activate a strong specific humoral and cellular immune response, makes this enzyme a promising anti-tumor target. The discovery of 'ENOblock', a small-molecule inhibitor has been made which is the first non-substrate analog of the enzyme. It directly binds to ENO1 and inhibits its activity and can also inhibit cancer cell metastasis in vivo. Thus it is capable of being used in biological assays (Lung *et al*., 2017). In present sudy, we found that the methylated flavonoids have potential to inhibit enolase protein. Results showed that the lead phytochemical 6-hydroxy-3,5,7,8-tetramethoxy-2-(3,4,5-trimethoxyphenyl)-4H-chromen-4-one inhibits enolase protein with 93.33% efficacy in comparison to the standard inhibitor. The given proteins are involved in the glycolytic pathway whose upregulation has been associated with cancer cells. The continuation of occurrence of high-rate glycolysis has often been associated with the transcription factor HIF-1. Similarly, the other oncogenic signaling pathways such as c-Myc, AMPK and mTOR are also associated with the promotion of expression of most glycolytic enzymes and transporters.

Thus, our study corroborates with the previous studies and the phytochemicals 2-(3,4-dihydroxyphenyl)-3,5-dihydroxy-7-methoxy-4H-chromen-4-one, 5,7-dihydroxy-2-(3-hydroxy-4-methoxyphenyl)-6,8-dimethoxy-4H-chromen-4-one, 2-(3,4-dimethylphenyl)-5,7-dimethyl-4H-chromen-4-one and 6-hydroxy-3,5,7,8-tetramethoxy-2-(3,4,5-trimethoxyphenyl)-4H-chromen-4-one might act as future lead in targeting cancer cell carbohydrate metabolism. These glycolytic enzymes and their function provide vital information for the design and development of new strategies of drug discovery and design with respect to efficacy, reduction of the side effects and treatment strategies. Targeting the major glycolytic enzymes involved in carcinogenesis by natural agents or phytochemicals may lead to an innovative approach that exploits the high glucose flux in cancer cells for cancer therapy. In cancer cells, elevated glucose metabolism and generation of ATP for rapid cancer cell proliferation provides immense potential to target the enzymes through natural compounds for anti-cancer effects.

5. Conclusion:

Since time immemorial natural phytochemicals have been used in the treatment of numerous diseases and disorders. The use of different phytochemicals as potent anti-cancer drugs has also been well established. Cancer cells depend on increased aerobic glycolysis for ATP generation which renders the cell highly proliferative and malignant. These metabolic alterations and increased expression of glycolytic enzymes have provided the advantage of survival for cancer cells. The existing scientific literature study showed that there are various natural agents being used as anti-cancer drug targets by inhibiting glycolytic pathway; while a number of them are still under clinical trials. The present *in silico* study depicted the anti-cancer potential of the methylated flavonoids as novel inhibitors of glucose metabolic pathways in cancer cells. Furthermore, *in vitro* studies can reveal the anti-cancer potential of the phytochemicals.

6. Experimental setup for *in vitro* validation

To validate the anticancer potential of the phytochemicals *in vitro* on the glycolytic pathway, we have a certain designed experimental setup.

Experimental setup 1: GLUT1 inhibition by lead compound

Principle: Decreased uptake of glucose by the cells in the presence of inhibitor will be reflected by the increased concentration of glucose in media (in comparison to experimental setup without inhibitor). This will reveal the GLUT1 activity in the cells.

Experimental setup 2: HK2 inhibition by lead compound

Principle: Decreased phosphorylation of glucose by the cells in the presence of inhibitor is reflected by the increased concentration of glucose in media. (in comparison to the experimental setup without inhibitor). This involves the lysis of the cells which will reveal the HK2 activity of cells in phosphorylating glucose into glucose-6-phosphate. The cell lysate and supernatant will be collected for further estimation.

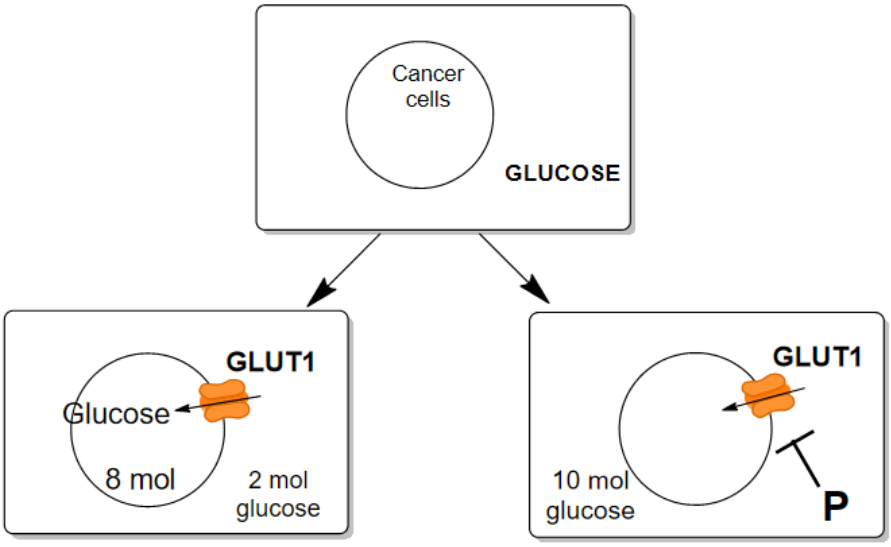

Setup 1: GLUT1 inhibition by lead compound

***P=** Lead phytochemical inhibition

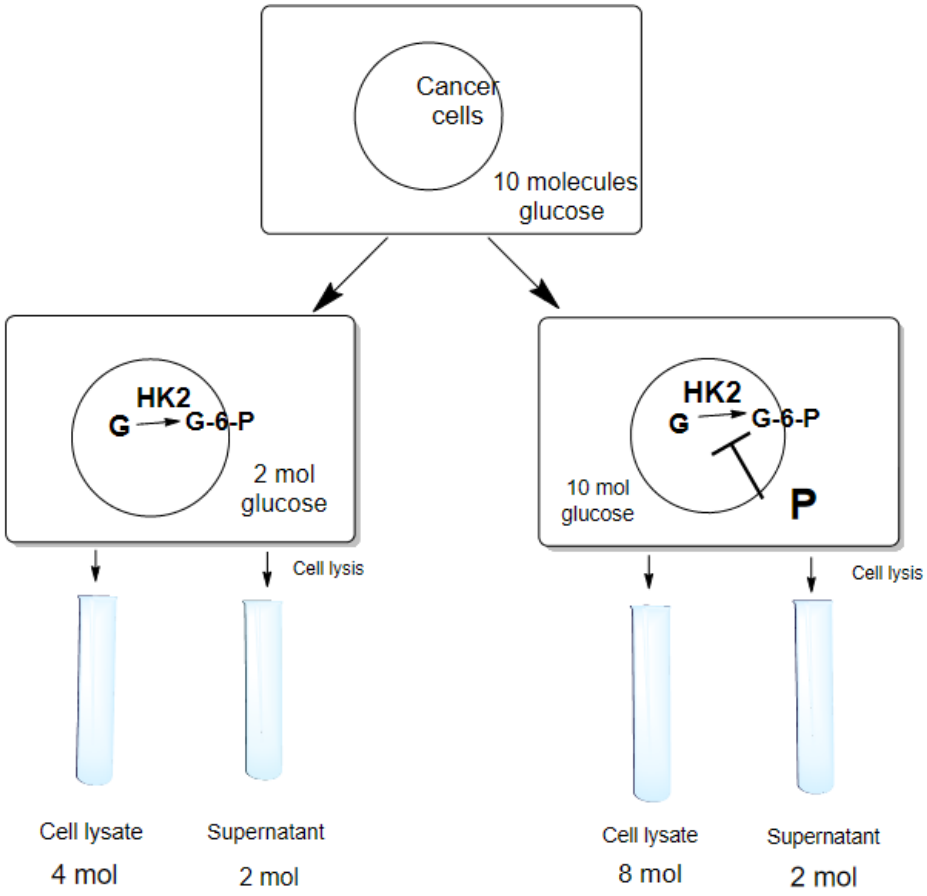

Setup 2: HK2 inhibition by lead compound

G= Glucose, G-6-P= Glucose-6-phosphate, HK2= Hexokinase2

***P=** Lead phytochemical inhibition

Figure 6.1: Experimental setup showing GLUT1 and HK2 inhibition by lead compounds by *in vitro* studies

List of Publication

1. **Swastika Dash**, Prem Prakash Kushwaha and Shashank Kumar. (2017). Targeting Cancer Cell Carbohydrate Metabolism by Phytochemicals Phytochemistry, In Volume 1: *Fundamentals, Methods, and Applic*ations, Eds:Egbuna Chukwuebuka, Ifemeje Jonathan Chinenye, Udedi Stanley Chidi, Shashank Kumar, CRC press, USA. (Communicated)

2. **Swastika Dash**, Prem Prakash Kushwaha, and Shashank Kumar, (2018). Environmental toxicology and cancer: An inevitable link, In *Environmental toxicology and Associated Health Concern*, Eds: Abbas Ali Mahdi, Y. K. Sharma, Murtaza Abid & M.M Abid Ali Khan, Springer Nature, New Delhi, India. (Communicated)

3. **Swastika Dash**, Swagata Das, Prem Prakash Kushwaha and Shashank Kumar. (2018) Environmental toxicology and diabetes, In *Environmental toxicology and Associated Health Concern*, Eds: Abbas Ali Mahdi, Y. K. Sharma, Murtaza Abid & M.M Abid Ali Khan, Springer Nature, New Delhi, India. (Communicated)

4. Prem Prakash Kushwaha, **Swastika Dash**, Atul Kumar Singh and Shashank Kumar. (2018) Cell Membrane Receptor and Quantitative ligand binding, In *Clinical Biochemistry, Cell Culture, and Drug Development*, Ed: Shashank Kumar, Cambridge Scholars Publishing, U.K. (Communicated)

References:

Allison, S.J., Knight, J.R.P., Granchi, C., Rani, R., Minutolo, F., Milner, J., Phillips, R.M. (2014). Identification of LDH-A as a therapeutic target for cancer cell killing via (i) p53/NAD(H)-dependent and (ii) p53-independent pathways. *Oncogenesis* **3(5):** e102

Bauer, A.W., Kirby, W.M., Sherris, J.C. and Turck, M. (1966). Antibiotic susceptibility testing by a standardized single disk method. *The American Journal of Clinical Pathology* **45(4):** 493–496.

Bhanot,, A., Sharma, R., Noolvi, M. N. (2011). Natural sources as potential anti-cancer agents: A review. *International Journal of Phytomedicine* **3(1):** 9-26

Bola, B.M., Chadwick, A.L., Michopoulos, F., Blount, K.G., Telfer, B.A., Williams, K.J., Smith, P.D., Critchlow, S.E., Stratford, I.J. (2014). Inhibition of Monocarboxylate transporter-1 (MCT1) by AZD3965 enhances radiosensitivity by reducing lactate transport. *Molecular Cancer Therapuetics* **13(12):** 2805-2816

Calvaresi, E.C. and Hergenrother, P.J. (2013). Glucose conjugation for the specific targeting and treatment of cancer. *Chemical Science* **4(6)**:2319-2333

Capello, P., Principe, M., Bulfamante, S., Novelli, F. (2017). Alpha-Enolase (*ENO1*), a potential target in novel immunotherapies. *Frontiers in Bioscience*, **22**, 944-959.

Chen, X., Li, L., Guan, Y., Yang, J., Cheng, Y. (2016). Anticancer strategies based on the metabolic profile of tumor cells: therapeutic targeting of the Warburg effect. *Acta Pharmacoligica Sinica* **37(8):**1013–1019.

Dallakyan, S. and Olson, A. J. (2015). Small-molecule library screening by docking with PyRx. *Chemical Biology: Methods and Protocols* **1263:** 243-250

Doherty, J.R. and Cleveland, J.L. (2013). Targeting lactate metabolism for cancer therapeutics. *Journal of Clinical Investigation* **123(9):** 3685-3692

Dong, G., Mao, Q., Xia, W., Xu, Y., Wang, J., Xu, L., Jiang, F. (2016). PKM2 and cancer: The function of PKM2 beyond glycolysis. *Oncology Letters* **11(3):** 1980-1986.

Evans, A., Bates, V., Troy, H., Hewitt, S., Holbeck, S., Chung, Y.L., Phillips, R., Stubbs, M., Griffiths, J., Airley, R. (2008). Glut-1 as a therapeutic target: increased chemoresistance and HIF-1-independent link with cell turnover is revealed through COMPARE analysis and metabolomic studies. *Cancer Pharmacology* **61(3):** 377-93

Fang, A., Zhang, Q., Fan, H., Zhou, Y., Yao, Y., Zhang, Y., Huang, X. (2017). Discovery of human lactate dehydrogenase A (LDHA) inhibitors as anticancer agents to

inhibit the proliferation of MG-63 osteosarcoma cells. *Medicinal Chemistry Comm*unications**,8:** 1720-1726

Gordaliza, M.(2007). Natural products as leads to anticancer drugs. *Clinical Translational Oncol*ogy **9(12):** 767-776.

Granchi, C., Fancelli, D., Minutolo, F. (2014). An update on therapeutic opportunities offered by cancer glycolytic metabolism. *Bioorganic and medicinal chemistry letters* **24(21):** 4915-4925

Gurrapu, S., Jonnalagadda, S.K., Alam, M.A., Nelson, G.L., Sneve, M.G., Drewes, L.R., Mereddy, V.R. (2015). Monocarboxylate Transporter 1 inhibitors as potential anticancer agents. *ACS Medicinal Chemistry Letters* **6(5):**558-561.

Hay,N. (2016). Reprogramming glucose metabolism in cancer: can it be exploited for Cancer therapy. *Nature Reviews Cancer* **16(10):**635-649

Heiden, V., Matthew, G., Christofk, H.R., Schuman, E., Subtelny, A.O., Sharfi, H., Harlow, E.E., Xian, J., Cantley, L.C. (2011). Identification of small molecule inhibitors of pyruvate kinase M2. *Biochemical Pharmacol*ogy **79(8):**1118-24

Iqbal, M.A., Gupta, V., Gopinath, P., Mazurek, S., Bamezai, R. (2014). Pyruvate kinase M2 and cancer: an updated assessment. *FEBS letters* **588(16):**2685-2692

Ji, H., Wang, J., Guo, J., Li, Y., Lian, S., Guo, W., Yang, H., Kong, F., Zhen, L., Guo, L., Liu, Y. (2016). Progress in the biological function of alpha-enolase. *Animal Nutrition* **2(1):** 12-17

Jung, D.W., Kim, W.H., Park, S.H., Lee ,J., Kim, J., Su, D., Ha, H.H., Chang, Y.T., Williams, D.R. (2013). A unique small molecule inhibitor of enolase clarifies its role in fundamental biological processes. *ACS Chemical Biology* **8(6):**1271-82

Kapoor, K., FinerMoore, J.S., Pederson, B.P., Caboni, L., Waight, A., Hillig, R.C., Bringmann, P., Heisler, I., Muller, T., Siebeneicher, H., Stroud, R.M. (2016). Mechanism of inhibition of human glucose transporter GLUT1 is conserved between cytochalasin B and phenylalanine amides. *PNAS* **113(17):** 4711-4716

Kennedy, K.M., Dewhirst, M.W. (2010). Tumor metabolism of lactate: the influence and therapeutic potential for MCT and CD147 regulation. *Future Oncology* **6(1):**127-48

Kochel, K., Tomczyk, M.D., Simoes, R.F., Fraczek, T., Sobon, A., Oliviera, P.J., Walczak, K.Z. (2017). Evaluation of biological properties of 3,3′,4,4′-benzophenonetetracarboxylic dianhydride derivatives and their ability to inhibit hexokinase activity. *Bioorganic Medicinal Chemistry* **27(3):**427-431

Kumar, S. (2016). Novel Wnt and Notch signalling natural inhibitors as double edged sword against cancer war: an approach towards computer based drug design. *Cancer Therapy and Oncology International Journal*. **1(4):**001-002.

Kumar, S., Chashoo, G., Saxena, A.K., Pandey, A.K.(2013). *Parthenium hysterophorus*: A probable source of anticancer, antioxidant and anti-HIV Agents. *BioMed Research International* **2013:**1-11

Kumar, S., Kumar, R., Dwibedi, A., Pandey, A.K. (2014). *In Vitro* antioxidant, antibacterial, and cytotoxic activity and *in vivo* effect of *Syngonium podophyllum* and *Eichhornia crassipes* leaf extracts on isoniazid induced oxidative stress and hepatic markers. *BioMed Research International* **2014:**1-11

Lahlou, M. (2013). The success of natural products in drug discovery. *Pharmacology and Pharmacy* **4(3A):** 17-31

Leonard, G.P., Satani, N., Maxwell, D., Lin, Y., Hammoudi, N., Peng, Z., Pisaneschi, F., Link, T.M., Lee, G.R., Sun, D., Francesco, M.E.D., Czako, B., Asara, J.M., Wang, Y.A., Bornmann, W., DePinho, R.A., Muller, F.L. (2016). SF2312 is a natural phosphonate inhibitor of enolase. *Nature Chemical Biology* **12(12):**1053-1058

Li, W., Zheng, M., Wu, S., Gao, S., Yang, M., Li, Z., Min, Q., Sun, W., Chen, L., Xiang, G., Li, H. (2017). Benserazide, a dopadecarboxylase inhibitor, suppresses tumor growth by targeting hexokinase 2. *Journal of Experimental and Clinical Cancer* **36(1):**58.

Lin, H., Zeng, J., Xie, R., Schulz, M.R., Tedesco, R., Qu, J., Erhard, K.F., Mack, J.F., Raha, K., Rendina, A.R., Szewzuck, L.M., Kratz, P.M., Jurewicz, A.J., Cecconie, T., Martens, S., Martin, J.D., Chen, S.B., Jiang, Y., Nickels, L., Schwartz, B.J., Smallwood, A., Zhao, B., Campobasso, N., Qian, Y., Briand, J., Rominger, C.M., Oleykowski, C., Hardwicke, M.A., Luengo, J.I. (2016). Discovery of a novel 2,6-disubstituted glucosamine series of potent and selective hexokinase 2 inhibitors. *ACS Medicinal Chemistry Letters* ***7*** **(3):** 217–222

Liu, Y., Cao, Y., Zhang, W., Bergmeier, S., Qian, Y., Akbar, H., Colvin, R., Ding, J., Tong, L., Wu, S., Hines, J., Chen, X. (2012). A small-molecule inhibitor of glucose transporter 1 downregulates glycolysis, induces cell-cycle arrest, and inhibits cancer cell growth *in vitro* and *in vivo. Molecular Cancer Therapeutics* ***11(8):*** *1672-82*

Lodish, H. (2000) Oxidation of glucose and fatty acids to carbon dioxide. *Molecular and Cell Biology* 4th edition.

Lu, Q.Y., Zhang, L., Yee, J.K., Go, V.W., Lee, W.N. (2015). Metabolic Consequences of LDHA inhibition by epigallocatechin gallate and oxamate in MIA PaCa-2 pancreatic cancer cells. *Metabolomics* **11(1):**71-80

Lung, J., Chen, K.L., Hung, C.H., Chen, C.C., Hung, M.S., Lin, Y.C., Wu, C.Y., Lee, K.D., Shih, N.Y., Tsai, Y.H. (2017). In silico-based identification of human α-enolase inhibitors to block cancer cell growth metabolically. *Dovepress* **2017(11):**3281-3290

Mathupala, S.P., Ko, Y.H., Pedersen, P.L. (2006). Hexokinase II: Cancer's double-edged sword acting as both facilitator and gatekeeper of malignancy when bound to mitochondria. *Oncogene* **25(34):** 4777-4782.

Miao, P., Sheng, S., Sun, X., Liu, J., Huang, G. (2013). Lactate dehydrogenase A in cancer: a promising target for diagnosis and therapy. *IUBMB Life* **65(11):**904-10

O'Neal, J., Clem, A., Reynolds, L., Dougherty, S., Imbert-Fernandez, Y., Telang, S.; Chesney, J., Clem, B.F. (2016). Inhibition of 6-phosphofructo-2-kinase (PFKFB3) suppresses glucose metabolism and the growth of HER2+ breast cancer. *Breast Cancer Research and Treatment* **160(1):**29-40.

O'Boyle, N. M., Banck, M., James, C. A., Morley, C., Vandermeersch, T., Hutchison, G. R. (2011). Open Babel: An open chemical toolbox. *Journal of Chemical Informmatics* **3(1):**1.

Ojelabi, O., DeZutter, J., Lloyd, K., Carruthers, A. (2016). Novel small molecule, WZB117, competitively inhibit GLUT1-mediated glucose transport to halt cancer growth. *FASEB Journal* **30(Supp.1)**

Pinksofsky, H.B., Dwyer, D.S., Bradley, R.J. (2000). The inhibition of GLUT1 glucose transport and Cytochalasin B binding activity by tricyclic antidepressant. *LifeScence* **66(3):**271-8

Porporato, P.E., Dhup, S., Dadhich, R.K., Copetti, T., Sonveaux, P. (2011). Anticancer targets in the glycolytic metabolism of tumors : A comprehensive review. *Frontiers of Pharmacol*ogy **2(49)**:1-18

Qian, X., Xu, W., Xu, J., Shi, Q., Li, J., Weng, Y., Jiang, Z., Feng, L., Wang, X., Zhou, J., Jin, H. (2017). Enolase 1 stimulates glycolysis to promote chemoresistance in gastric cancer. *Oncotarget.* **8(29):**47691-47708.

Qin, J., Chai, G., Brewer, J.M., Lovelace, L.L., Lebioda, L. (2006). Fluoride inhibition of Enolase: Crystal structure and thermodynamics. *Biochemistry* **45(3):**793-800

Ramos, A.D., Borrellas, A.R., Melero, A.G., Alemany, A.L. (2012). α-Enolase, a multifunctional protein: Its role on pathophysiological situations. *Journal of Biomedicine and Biotechnology* **2012:**1-12

Ribnicky, D.M., Poulev, A., Schmidt, B., Cefalu, W.T., Raskin, I. (2008). Evaluation of botanicals for improving human health. *The American Journal of Clinical* Nutrition **87(2)**:472S-5S

Shibuya, K., Okada, M., Suzuki, S., Seino, S., Takeda, H., Kitanaka, C. (2015). Targeting the facilitative glucose transporter GLUT1 inhibits the self-renewal and tumor-initiating capacity of cancer stem cells. *Oncotarget* **6(2):**651-661.

Song, Y. H., Sun, H., Zhang, A. H., Yan, G. L., Han, Y., Wang, X. J. (2014). Plant-derived natural products as leads to anti-cancer drugs. *Journal of Medicinal Plant and Herbal Therapy Research,* **2(2014):** 6-15.

Wang, H., Wang, L., Zhang, Y., Wang, J., Deng, Y., Lin, D. (2016). Inhibition of glycolytic enzyme hexokinase II (HK2) suppresses lung tumor growth. *Cancer Cell International* **16(9):**1-11

Wong, N., Melo, J.D., Tang, D. (2013). PKM2, a central point of regulation in cancer metabolism. *International Journal of Cell Biology* **2013:**1-11

Yang, Y., Su, D., Zhao, L., Zhang, D., Xu, J., Wan, J., Fan, S., Chen, M. (2014). Different effects of LDH-A inhibition by oxamate in non-small cell lung cancer cells. *Oncotarget* **5(23):**11886-11896

Zhang, Q., Zhang, Y., Zhang, P., Chao, Z., Xia, F., Jiang, C., Zhang, X., Jiang, Z., Liu, H. (2014). Hexokinase II inhibitor, 3-BrPA induced autophagy by stimulating ROS formation in human breast cancer cells. *Genes Cancer* **5(3-4):**100-12

Zhao, Y., Butler, E.B., Tan, M. (2013). Targeting cellular metabolism to improve cancer therapeutics. *Cell Death Disease***, 4(3):**e532.

Zhao, Z., Han, F., Yang, S., Wu, J., Zhan, W. (2015). Oxamate-mediated inhibition of lactate dehydrogenase induces protective autophagy in gastric cancer cells: involvement of the Akt-mTOR signaling pathway. *Cancer Letters* **358(1):**17-26

Zhu, W., Ye, L., Zhang, J., Yu, P., Wang, H., Ye, Z., Tian, J. (2016) PFK15, a small molecule inhibitor of PFKFB3, induces cell cycle arrest, apoptosis and inhibits invasion in gastric cancer*. PLoS One* **11(9)**:e0163768